Russian Fiber Lasers

Number 1

2020

Russian Fiber Lasers

RUSSIAN FIBER LASERS

Journal of the Institute of Automation and Electrometry SB RAS

Volume 1, Number 1, December 2020

JOURNAL FOUNDER
Institute of Automation and Electrometry of the Siberian Branch of the Russian Academy of Sciences (IA&E SB RAS)
Address: Academician Koptyug ave. 1, Novosibirsk, Russia 630090
Registration data and number: 08.08.1994, 1025403647807
Taxpayer Identification Number: 5408100032
Industrial Enterprises Classifier: 540801001
Tel: (383) 330-79-69, 339-93-58.
Fax: (383) 330-88-78
E-mail: iae@iae.nsk.su
Web: http://www.iae.nsk.su

Nanophotonics

Sensitivity enhancement of plasmonic grating in near field

L.L. Frumin, D.A. Shapiro*

Institute of Automation and Electrometry SB RAS, Novosibirsk

**E-mail: shapiro@iae.nsk.su*

As predicted and tested experimentally by Liedberg [1], under proper conditions, the reflectivity of a thin metal film is extremely sensitive to optical variations in the medium on one side of it. Among devices developed recently, the sensors based on the surface plasmons are distinguished (see [2,3]). A plane wave falls to the boundary with an analyte from the glass. Its incident angle is close to the total internal reflection. A metallic layer or a plasmon-supporting sub-wavelength grating at the interface makes the reflection coefficient's dependence on the incidence angle (or the wavelength) sensitive to the refractive index of the analyte.

The purpose of the present paper is to study a way to increase sensitivity. We propose to measure the local field in points where the field enhancement factor $F_1 = |E_x/E_0|^2$ of a grating being maximal. Here E_x is the tangential component of the electric field, E_0 is the amplitude of an incident wave. For this purpose, we consider the subwavelength periodic sequence of metallic cylinders placed above the dielectric half-space ε_1, shown in Fig.1. An analyte with refractive index n_a fills half-space ε_2=n_a^2.

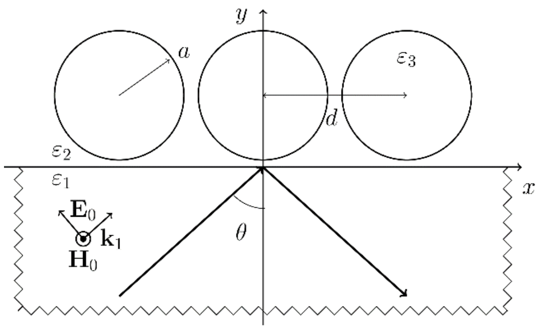

Fig. 1. The sketch of medium 2, above the dielectric subspace 1. The circular cylinders of radius *a* form the grating with period *d*. Inset illustrates the polarization state of *p*-wave.

The approximate analytical formulas could be derived using the coupled-mode approach [4]. Here we calculate the field numerically by the boundary element method [5]. One can see some typical results of numerical modeling in Fig. 2. Figure 2(a) demonstrates the shift of resonance in angular dependence for a gold grating for two close refractive indices. We see a significant shift after changing n_a by 1% only. The location of peak at $\varepsilon_1 = 2.25$ corresponds to angles θ_0 = 0.7297 (n_a = 1) or θ_0 = 0.7342 (n_a = 1.01).

Figure 2(b) occurs more indicative. It displays the shift of angular resonance for a silver grating while the index changes by 0.1%. We take the refractive index from the Polyanskiy database [6]. In both figures, we see the sharp cusp-like resonances near the angle of total reflection. The cusp is a consequence of the Fresnel field angular dependence [7] shown in Fig.3. Its small-angle tail is unusually steep; for an unperturbed dielectric-analyte interface, it has the infinite derivative from left side. This dependence leads to high sensitivity to the analyte index.

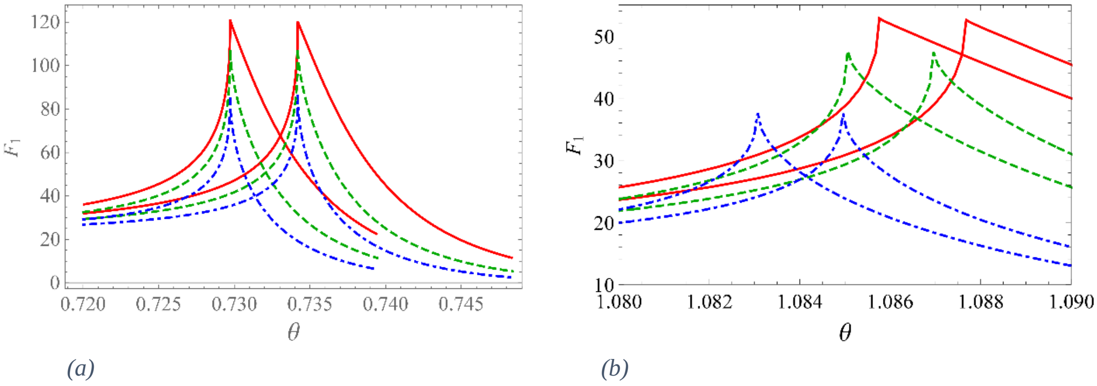

Fig. 2. Angular dependence of the local field in the gap for a gold grating in gas (a): λ= 0.7749 (solid line), 0.8266 (dashed), 0.8856 μm (dot-dashed) $n_a = 1.00$ at the left, $n_a = 1.01$ at the right and silver lattice; for silver grating in water (b): λ= 0.9537 (solid line), 1.033 (dashed), 1.127 μm (dot-dashed) $n_a = 1.3270$. 1.3265. 1.3251, respectively, for the left plots, n_a is greater by $0.001n_a$ for the right curves.

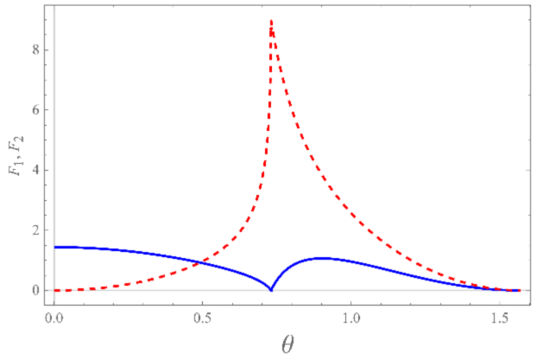

Fig. 3. The Fresnel angular dependence near the plane normalized by the incident field: $F_1 = |E_x/E_0|^2$ (solid), $F_2 = |E_y/E_0|^2$ (dashed line).

We suggest applying a grating of parallel metallic cylinders on the glass substrate to increase the sensitivity of optical refractive index measurements. It is helpful to measure the field between neighbor cylinders. This signal is strong owing to the gap plasmon amplification. Moreover, its angular dependence has a very sharp cusp, which is a consequence of the total internal reflection. Both the factors are essential for further potential exploiting the subwavelength metallic grating in chemo- and bio-sensing techniques.

The authors are grateful to V.P. Drachev and S. V. Perminov for helpful discussions. The work is supported by the Russian Foundation of Basic Research, grant # 20-02-00211.

References

[1] B. Liedberg, C. Nylander, I. Lunström, *Sensors and actuators*. **4**, 299-304 (1983)
[2] Y. Xu et al., *Adv. Opt. Mater.* **7**, 1801433 (2019)
[3] T. Allsop, R. Neal, *Sensors* **19**, 4874 (2019).
[4] E. Efremova, S. Perminov, S. S. Vergeles, arXiv:1905.04784
[5] L. L. Frumin et al., *J. Opt.* **15**, 085002 (2013)
[6] M. N. Polyanskiy, “Refractive index database,” https://refractiveindex.info.
[7] L. D. Landau and E. M. Lifshitz, *Electrodynamics of continuous media* (Pergamon, Oxford, New York, 1984).

Direct and inverse scattering transform algorithm for complex wave fields

A.A. Gelash[1,*], **R.I. Mullyadzhanov**[2,3]**, L.L. Frumin**[1]

[1]*Institute of Automation and Electrometry SB RAS, Novosibirsk*
[2]*Institute of Thermophysics SB RAS, Novosibirsk*
[3]*Novosibirsk State University, Novosibirsk*

[*]*E-mail:* agelash@gmail.com

The discovery of the complete integrability of some nonlinear partial differential equations has stimulated impressive progress in mathematical physics of nonlinear waves. Among these equations are the focusing and defocusing nonlinear Schrodinger (NLSE) equations serving as the fundamental models of nonlinear optics [1]. This breakthrough has taken place due to the development of the Inverse Scattering Transform (IST) method allowing one to solve the initial-value problem in terms of the nonlinear harmonics decomposition representing the scattering data or the IST spectrum [2]. The spectrum can be found using the Direct Scattering Transform (DST), leading to the full knowledge of the nonlinear wave field evolution governed by the integrable differential equation, while the IST procedure allows one to reconstruct the wave field. In some cases, the DST and the IST problems can be solved analytically, but in the general case - which is the subject of this work - only numerically. After several decades of analytical studies of integrable equations, the rapid growth of interest to describe arbitrary shaped, noisy, and even random nonlinear wave fields has promoted the need for accurate numerical methods for the IST/DST. For example, the recent applications of the DST/IST techniques in nonlinear optics studies are ranging from experimental observation of complex interactions of the NLSE breathers [3] and statistically stationary state of spontaneous modulation instability [4] to the development of novel optical telecommunication methods [5,6]. In this work, we take advantage of two efficient numerical techniques: the DST algorithm based on the Magnus expansion [7] and IST algorithm based on the Toeplitz inner bordering scheme [8]. Using a combination of these methods, we demonstrate efficient direct and the inverse scattering transform for various examples of complex optical pulses. Our approach allows to find the whole IST spectrum of an arbitrary wave field and then reproduce each of the spectrum components separately in order to study their nonlinear role in the signal formation. Finally, we discuss the mitigation of the numerical instabilities of the DST and IST in the presents of a large number of solitons in the wave field, see [9], using the application of arbitrary precision arithmetic.

The work was supported by the Russian Science Foundation (Grant No. 20-71-00022).

References

[1] S. Novikov, S.V. Manakov et al, Theory of Solitons: The Inverse Scattering Method (1984)
[2] Y.S. Kivshar and G. Agrawal, Optical solitons: from fibers to photonic crystals (2003)
[3] G. Xu, A. Gelash, A. Chabchoub et al, *Phys. Rev. Lett*. **122(8)**, 084101 (2019)
[4] A.E. Kraych, D. Agafontsev, S. Randoux et al, *Phys. Rev. Lett*. **123**, 093902 (2019)
[5] H. Bülow, *Journal of Lightwave Technology*. **33(7)**, 1433-1439 (2015)
[6] L.L. Frumin, A.A. Gelash, S.K. Turitsyn, *Phys. Rev. Lett.* **118(22)**, 223901 (2017)
[7] R. Mullyadzhanov and A. Gelash, *Opt. Lett.* **44**, 5298 (2019)
[8] O. Belai, L. Frumin, E. Podivilov and D. Shapiro, *J. Opt. Soc. Am. B.* **24**, 1451 (2007)
[9] A. Gelash and R. Mullyadzhanov, *Phys. Rev. E.* **101**, 052206 (2020).

Plastic Deformation as Nature of Femtosecond Laser Writing of Waveguides in YAG crystals

S.S. Fedotov[1], **L.N. Butvina**[2], **A.G. Okhrimchuk**[1,2,*]

[1]*Mendeleev University of Chemical Technology of Russia, Moscow*
[2]*Prokhorov General Physics Institute of Russian Academy of Sciences, Dianov Fiber Optics Research Center, Moscow,*
[*]*E-mail: okhrim@fo.gpi.ru*

Direct femtosecond laser writing in the bulk of transparent glasses and crystals has proved itself as a quick and flexible method of forming waveguides and waveguide circuits in a 3D format. This technique allows to structure refractive index with micron- and sub-micron resolutions. Admittedly the mechanism and nature of the refractive index change in glass is basically clear. As opposed to glass the mechanism of refractive index change in crystals, which is suitable for low loss waveguide writing, is not clarified yet. Forming of voids and phase transformation are examples of the extreme impact of ultrashort laser pulses on a crystal, and such mode obviously isn’t suitable for writing of low loss waveguides [1,2]. Meanwhile, knowledge of the state of the matter obtained as a result of moderate modification in crystals is important for discovering ways improving uniformity of the modification tracks composing waveguide, as this knowledge opens the way to reduce propagation loss.

Here we focused on the study of longitudinal nonuniformity of tracks and the statistics of transmitted pulse energy in the course of track writing in the YAG:Nd single crystal and silica glass, and these findings allowed us to draw a conclusion about nature of modification in broad ranges of sample translation speeds and laser pulse energies, starting from modification threshold, that is, for energy range, where most smooth tracks are formed, which are suitable for writing of waveguides with low propagation loss.

We measured the relative standard deviation of the laser pulse transmittance (RSDT) under laser writing conditions, and longitudinal inhomogeneity of the written tracks R. We presented the results as plots against the number of laser pulses that overlap with each other in the modification region $P=D/(f*V)$, where D is the diameter of the laser beam waist, f is the laser pulse repetition rate, V is the translation speed of the beam waist (the scanning direction is perpendicular to the laser beam) (Fig.1). Longitudinal inhomogeneity of a track R in the YAG:Nd was investigated with Fourier analysis of their phase images obtained by the quantitative phase microscopy (QPm) (Fig.1c). We have revealed the surges in the plots of RSDT and the longitudinal inhomogeneity at P=11-15 for the crystal, and further monotonic growth of these parameters with overlap increase. No surges of RSDT are observed for silica glass (Fig.1b). Instead of this, RSDT decreases at large overlaps.

We believe that the modification of the YAG:Nd crystal under the impact of femtosecond pulses is a plastic deformation in a microvolume. The plastic deformation is accompanied by generation of vacancies, their fusion into vacancy disks, and the subsequent generation of dislocations on them. The decrease in the refractive index in the modification region is the result of the crystal density decrease during the plastic tension under impact of the internal pressure arising in the region of the electron plasma. The decrease in crystal density is associated with the generation of vacancy disks and agglomeration of dislocations. We have identified three modes of plastic deformation relevant to direct laser writing. The first mode is characterized by an easy glide of dislocation (P<9), the second is the hardening mode (P>15), at which dislocation of different sleep systems are generated, and the third mode is an intermediate one with self-organization in dislocation system (P=9-15), which appeared as modulation of refractive index with period of 1.2 μm [3]. The mode of plastic deformation is defined by two independent parameters, that are laser pulse energy E_p and overlap of exposed areas by laser pulse sequences P.

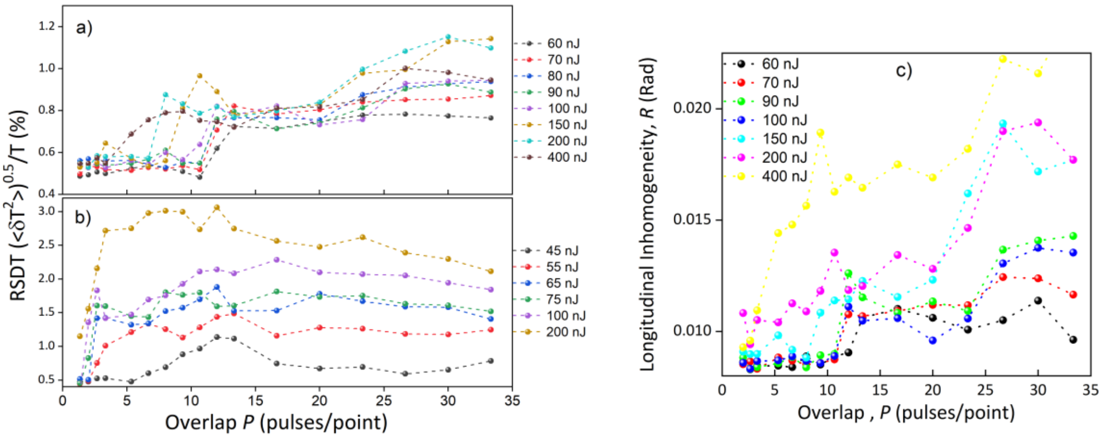

Fig.1. Plots of RSDT for YAG (a) and silica glass (b), and track roughness in YAG (c) upon overlap.

We presume that the surges in the dependences of the longitudinal inhomogeneity and RSDT on the overlap in the crystal are connected with the change from the plastic deformation mode with easy glide of dislocations to the hardening mode. The qualitatively different dependence of RSDT for YAG and silica glass is explained by the fundamentally different nature of plastic deformation in crystals and glass. In crystals, it is the generation and slipping of dislocations that have long-range fields. In glass, rearrangement of the short-range order is only possible; therefore, the hardening in glass is not observed.

Plastic deformation mode with easy glide of dislocations has to be provided for direct laser writing of waveguides with low scattering loss. In order to get this mode, it is necessary to set the laser pulse overlap in the range of 3-7. We expect that the proposed model of laser writing can be expanded on other crystals and open a new approach in the study of direct femtosecond laser writing in crystals.

Funding Russian Science Foundation under Grant #18-19-00733.

References

[1] E. G. Gamaly, S. Juodkazis, et al., Phys. Rev. B - Condens. Matter Mater. Phys. **73**, 1–15 (2006).
[2] A.G. Okhrimchuk, et al., Opt. Mater. Express **7**, 3408 (2017).
[3] D. Kuhlmann-Wilsdorf, Mater. Sci. Engineering A **113**, 1–41 (1989).

Role of ion diffusion in direct femtosecond laser writing in tellurite glass

G.K. Alagashev[1,*], **M.P. Smayev**[1], **A.A. Gulin**[2], **A.G. Okhrimchuk**[1,3]

[1]*Mendeleev University of Chemical Technology of Russia*
[2]*N.N. Semenov Federal Research Center for Chemical Physics RAS*
[3]*Prokhorov General Physics Institute of the Russian Academy of Sciences, Dianov Fiber Optics Research Center*

[*]*E-mail: alagashevgrigory@gmail.com*

Waveguide devices based on soft glass with a large nonlinear refractive index are promising for integral nonlinear photonics and mid-IR photonics, in particular, for generating a mid-IR supercontinuum [1]. Direct femtosecond laser writing makes it possible to create such devices. However, designing waveguides with specified characteristics in such glasses and calculation of the waveguide parameters are difficult due to the complex refractive index profile. The latter circumstance is apparently related to the fact that the change in the refractive index is caused not only by a change in the density of the glass (as, for example, when recording waveguides in a quartz glass), but also by the mutual diffusion of chemical elements from and into zone of impact by the laser beam (the laser plasma zone) [2].

In this work we investigated laser writing in the volume of glass with the composition of $70TeO_2$-$22WO_3$-$8Bi_2O_3$. Femtosecond laser beam focused by a lens with NA=0.85 at the repetition frequencies in the range of 50 – 1000 kHz. In order to facilitate the numerical simulation of the process and understanding the modification mechanism, the writing was made without scanning the sample with respect to the laser beam waist, and with a different number of pulses and at different repetition rates. The spatial distribution in the refractive index change in the modification region was measured using quantitative phase microscopy (QPm). Figure 1 shows the plot of the maximum variation in the transmitted light phase, caused by the change in the refractive index in the modification region, against number of laser pulses.

The spatial distribution of the metal oxides in the modification region was investigated by of time-of-flight secondary ion mass spectrometry (ToF-SIMS). A significant change in the concentrations of Bi_2O_3, WO_3, and TeO_2 in the region of the laser action and in its vicinity was found. In particular the yield of bismuth oxide ions decreases in the region of the waist of the laser beam. However the spatial resolution of the method turned out to be insufficient to associate the distribution of concentration changes with the phase profile. Therefore numerical calculations of the thermal diffusion of ions were undertaken. Diffusion was modeled using coupled heat and diffusion equations:

$$\rho C_p(T)\frac{\partial T}{\partial t} + \nabla\cdot\left(-k(T)\nabla T\right) = F(t) \qquad (1)$$

$$\frac{\partial C}{\partial t} + \nabla\cdot\left(-D(T)\nabla C - CD_T(T)\nabla T\right) = 0 \qquad (2)$$

The temperature dependences for the heat capacity (C_p) and thermal conductivity (k) of glass in the range of 300 – 950 K were previously measured for glass with a similar composition. The temperature dependence of the diffusion coefficients is taken to satisfy the Arrhenius law:

$$D(T) = D_0 \exp(-E_a/RT) \tag{3}$$

where R is the universal gas constant, E_a is the diffusion activation energy. Thermal diffusion coefficient reads as:

$$D_T(T) = D(T)Q/RT^2 \tag{4}$$

where Q is the heat of transfer [3]. The impact of laser pulses was simulated through the heating $F(t)$, with a spatial distribution in the form of a generalized normal distribution. We suppose that the change in refractive index is proportional to the change in the relative concentration of glass components. The shape of the experimental dependence of the phase on the number of pulses was approximated by the calculated dependence of the concentration change on the number of laser pulses under varying parameters E_a and Q. Good agreement between theory and experiment was obtained for pulses with the highest energy E_p = 90 nJ (Fig. 1). For energies of 50 and 70 nJ and for less than 10 pulses the model predicts significantly lower values of the concentration change than it is necessary to explain the phase change. The calculations performed indicate that the redistribution of chemical elements due to diffusion makes a significant contribution to the change in the refractive index, but at the same time, it is necessary to take into account other factors (for example the change in density due to deformation) in order to explain the change in the refractive index at low heating.

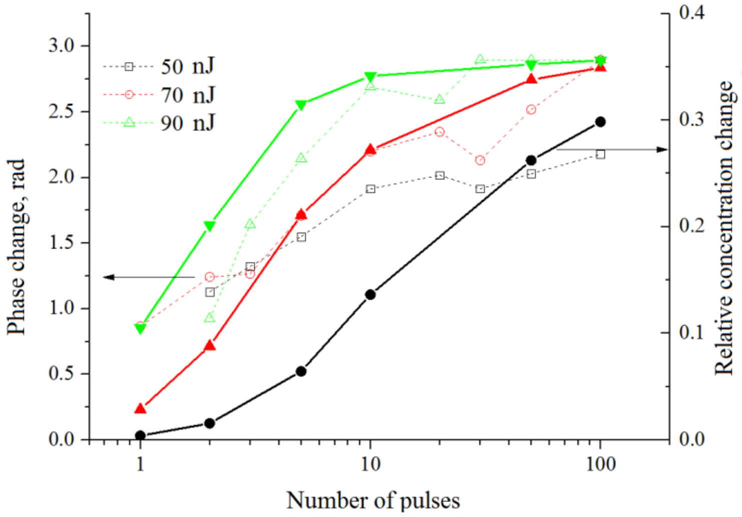

Fig.1 Comparison of the measured variation of the optical phase of radiation transmitted through the modified regions (dashed line) and the simulated ion concentration (solid lines) at a pulse repetition rate of 1 MHz. Q = 104 J/mol, $E_a = 7{\cdot}10^4$ J/mol, D_0 = 10 m^2/s, $C(0) = 2.5{\cdot}10^3$ mol/m^3.

The research was supported by the Russian Science Foundation, grant # 18-19-00733.

References

[1] A.G. Okhrimchuk, A.D. Pryamikov, et al, *J. Light. Technol*. **38**, 1492–1500 (2020).
[2] T. Gretzinger, T. T. Fernandez, et al, *Opt. Lett.* **45**, 3369 (2020)
[3] P. Shewmon, *Diffusion in Solids* (1963).

New gain media, schemes and generation regimes of fiber lasers

Ultrafast Fiber Amplifiers Beyond the Gain Narrowing Limit

P. Sidorenko and F.W. Wise*

School of Applied and Engineering Physics
Cornell University
**E-mail: frank.wise@cornell.edu*

Two major challenges that arise in the development of ultrafast fiber amplifiers are management of the high nonlinear phase shifts encountered in stretcher-less amplification systems and (2) generation of bandwidths much broader than the gain spectrum that can be compressed to clean, sub-100-fs pulses. We will describe a new regime for amplification of ultrashort pulses in fiber that is distinguished by the use of a dynamically-evolving gain spectrum as a degree of freedom [1]. As a pulse experiences nonlinear spectral broadening, absorption and amplification actively reshape the pulse and the gain spectrum itself. We refer to this regime as gain-managed amplification. The dynamic co-evolution of the field and excited-state populations supports pulses that can broaden spectrally by almost two orders of magnitude, and well beyond the gain bandwidth, while remaining cleanly compressible to their sub-50-fs transform limit. Theory and experiments suggest that a nonlinear attractor underlies the management of the nonlinearity by the gain. Initial instruments based on this process have generated microjoule-level and 40-fs pulses [2], and 20-fs pulses appear to be possible.

Gain-managed amplification can be exploited in oscillators as well as in amplifiers. The pulse energy from mode-locked fiber oscillators based on concatenated Mamyshev regenerators (so-called Mamyshev oscillators) have risen dramatically in the past few years [3-5]. Environmentally-stable instruments that generate ~200-nJ and 40-fs pulses have been demonstrated [6]. The peak power thus reaches several megawatts, which is the highest reported for a femtosecond fiber oscillator. We now understand that gain-managed amplification underlies the generation of stable pulses at such high power in an oscillator.

Initial applications of amplifiers and lasers based on gain-managed amplification will be mentioned, along with future prospects for enhanced performance.

References

[1] P. Sidorenko, W. Fu, and F. W. Wise, *Optica* **6**, 1328 (2019).
[2] P. Sidorenko and F. Wise, *Opt. Lett.* **45**, 4084 (2020).
[3] K. Regelskis, J. Želudevičius, et al, *Opt. Lett.* **40**, 5255 (2015).
[4] I. Samartsev, A. Bordenyuk, and V. Gapontsev, "Environmentally stable seed source for high power ultrafast laser," in A. L. Glebov and P. O. Leisher, eds. (2017), p. 100850S.
[5] Z. Liu, Z. M. Ziegler, L. G. Wright, and F. W. Wise, *Optica* **4**, 649 (2017).
[6] P. Sidorenko, W. Fu, L. G. Wright, and F. W. Wise, "*Opt. Lett.* **43**, 2672 (2018).

High Power Narrow-Linewidth Fiber Lasers

**Pu Zhou*, Wenchang Lai, Wei Liu, Can Li,
Rongtao Su, Hu Xiao, Jinyong Leng, Pengfei Ma****

College of Advanced Interdisciplinary Studies, National University of Defense Technology, Changsha 410073, China

**E-mail:* zhoupu203@163.com

***E-mail:* shandapengfei@126.com

High power narrow-linewidth fiber lasers have been under intensive investigation due to their potential applications in beam combination (coherent and spectral), gravitational wave detection (GVD), nonlinear frequency conversion and so on. In this talk, we will present the progress of high power narrow-linewidth fiber lasers in our lab [1-9] in the past few years and the very recent result.

Single frequency fiber laser is a special kind of narrow-linewidth fiber lasers with unique property in coherence length. One of the main scheme for power scaling of single-frequency fiber laser is to employ master oscillator power amplifier (MOPA) scheme. In the earlier stage, power scaling is mainly limited by the Stimulated Brillouin Scattering (SBS) effect, where up to 300 Watt level has been demonstrated by using large-mode-area fiber and therein shorter fiber length [1], the threshold of SBS can also be increased by introducing strain gradient and thermal gradient in the system [2]. Because of the newly discovered transverse modal instability (TMI) effect, further power scaling is limited by both SBS and TMI effects. Recently, by using polarization-maintaining tapered Yb-doped fiber (T-YDF) and shorter seed wavelength, SBS and TMI can be well suppressed simultaneously, a 550 W single frequency fiber MOPA has been achieved with a slope efficiency of 80% [3].

The typical spectral linewidth for narrow-linewidth fiber laser is usually narrower than 0.3 nm (about 100 GHz for 1 μm laser). The output power can be significantly increased because much highly SBS threshold compared with single frequency fiber laser. There are several key issues for narrow-linewidth fiber lasers in addition to power scaling, that is, linewidth narrowing, TMI and even Stimulated Raman Scattering (SRS) effect suppressing. A kilowatt-level linearly-polarized fiber laser with a linewidth of about 1.8 GHz has been achieved [4]. The power can be increased to 2 kilowatt-level by broadening the linewidth [5]. By using tandem-pumping scheme, which will result in less heat generation and thus higher MI threshold, near 4 kilowatt-level output power has been achieved [6], but the SRS effect should be considered since much longer active fiber is required for efficient pump absorption in tandem pumped ones [7].

From the other aspect of review, Raman gain can be used for power scaling single frequency or narrow linewidth fiber amplifier with special wavelength. For example, over 1 kW narrow-linewidth 1120 nm fiber laser was obtained with slope efficiency of ~ 77% and near-diffraction-limited beam quality has been reported [8]. Single frequency fiber laser with 1120 nm wavelength was also achieved with a Raman fiber amplifier [9].

Recently, we have successfully demonstrated a diode-pumped narrow linewidth fiber amplifier. White noise modulation is employed to suppress the SBS, high-loss for HOM inside the fiber is employed to suppress the TMI, and up to 4.09 kW output power has been achieved. The output spectrum and beam quality measured at full power operation is shown in Figure 1. The SRS effect is suppressed by a factor of near 50 dB, and the linewidth is about 0.28 nm. The beam quality factor M^2 is about 1.05. To the best of our knowledge, this is the highest output power from a narrow linewidth fiber amplifier.

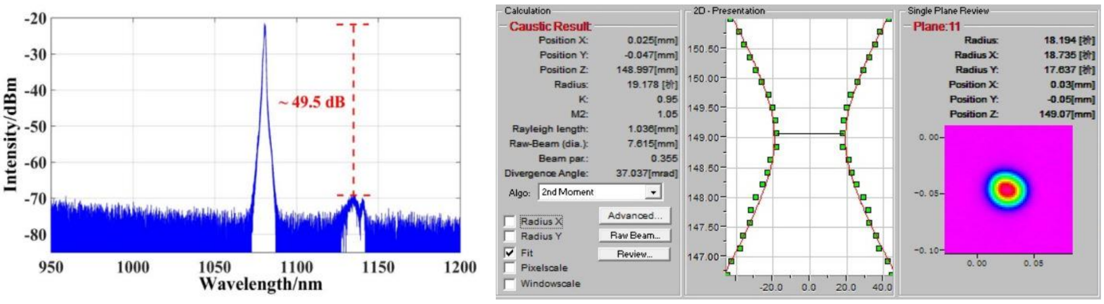

Fig. 1. Spectrum and beam quality measurement result at full power operation.

In the futher work, further narrowing the linewidth with new technique [10], increasing the output power by optimazing pump scheme [11] and expanding the operating wavelength [12]will be investigated in detail.

Acknowledgment

This work reviews in this paper is sponsored National Natural Science Foundation of China (NSFC) (No. 61705264), Hunan Provincial Innovation Construct Project (No. 2019RS3017), Innovative Research Team in Natural Science Foundation of Hunan province, China (No. 2019JJ10005) and Research Plan in Key Areas of Guangdong province, China (No.2018B090904001). The authors would like to express sincere thanks to Long Huang, Yu Miao, Daren Meng, Jiaxin Song, Rumao Tao, Yakun Liu, Hanwei Zhang, Man Jiang, Jian Wu, Yanxing Ma, et al. for their contribution to the work that support this talk.

References

[1] P. Ma, P. Zhou, Y. Ma, et al. *Appl.Opt*. **52**, 4854 (2013).
[2] L. Huang, H. Wu, R. Li, et al. *Opt. Lett.* **42**, 1-4 (2017)
[3] W. Lai, P. Ma, W. Liu, et al. *Opt.Express*, **28**, 20908-20919 (2020)
[4] D.Meng, W.Lai, X.He, et al. *Laser Phys*. **29**, 035103 (2019)
[5] P.Ma, R.Tao, R.Su, et al. *Opt.Express*, **24**, 4187-4195 (2016)
[6] P.Ma, H.Xiao, D.Meng, et al. *High Power Laser Science and Engineering*, **6**, e57 (2018)
[7] P.Zhou, H.Xiao, J.Leng, et al. *Journal of the Optical Society of America B*, **34**, A29-A36 (2017)
[8] Y.Miao, P.Ma, W.Liu, et al. IEEE *Access* **6**, 71988-71993 (2018)
[9] P.Ma, Y.Miao, W.Liu, et al. *Opt. Lett.* **45**, 1974-1977 (2020)
[10] W. Lai, P. Ma, W. Liu, et al. IEEE *Access* **8**, 71988-71993 (2020)
[11] W. Liu, P. Ma, Y. Miao, et al. IEEE *J. Sel. Top. Quantum Electron*, 24, 3100408 (2018)
[12] Y.Liu, R.Su, P.Ma, et al. *Appl.Opt*. 56, 4213 (2017)

Fiber Brewster Gratings and their applications in ultrafast fiber lasers

Chengbo Mou[1,*], Zinan Huang[1], Qianqian Huang[1], Zhijun Yan[2], Kaiming Zhou[3], Lin Zhang[3], Antreas Theodosiou[4], Kyriacos Kalli[4]

[1]Key Laboratory of Specialty Fiber Optics and Optical Access Networks, Shanghai Institute for Advanced Communication and Data Science, Joint International Research Laboratory of Specialty Fiber Optics and Advanced Communication, Shanghai University, P. R. China
[2]School of Optical and Electronic Information, National Engineering Laboratory for Next Generation Internet Access System, Huazhong University of Science and Technologies, P. R. China
[3]Aston Institute of Photonic Technologies (AIPT), Aston University, Birmingham, United Kingdom
[4]Photonics and Optical Sensors Research Laboratory, Cyprus University of Technology, Cyprus
[*]E-mail: mouc1@shu.edu.cn

The rapidly developing fiber laser, with its own performance and production advantages, such as excellent beam quality, high electrical and optical efficiency, fundamental compatibility with optical systems, compact structure, and low maintenance, has gradually replaced the solid-state laser in scientific research and industrial applications. A simple, effective, and reliable passive mode-locking technique for implementing an ultrafast fiber laser remains a subject of intense interest to researchers in the laser field. For this purpose, mode-locked elements based on semiconductor nonlinear optical absorption have driven the development of novel nanomaterial saturable absorber (SA) in the past few decades. However, the high cost, complicated preparation process and low damage threshold restrict the further improvement of this kind of SA. There is another ideal way to generate ultrashort pulses is to utilize techniques based on the intrinsic Kerr nonlinearity of optical fibers. Among them, the nonlinear polarization rotation method with intra-cavity polarizing elements has been extensively used due to its high power tolerance and large modulation depth.

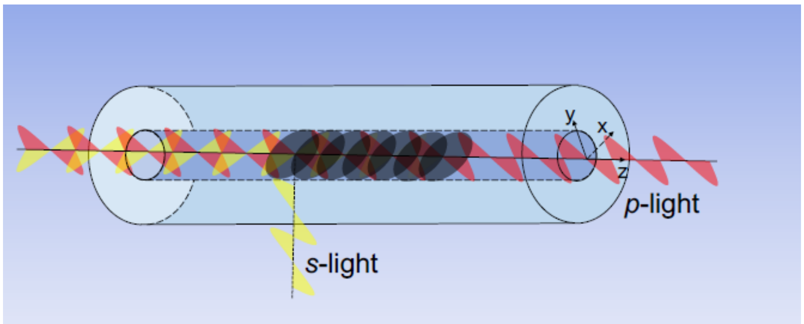

Fig. 1 The schematic of fiber Brewster grating in-fiber polarizer.

Back in 2005, 45° tilted fiber grating was first reported as an effective in-fiber polarizer [1] which is able to tap out the *s*-light and propagate the *p*-light based on the Brewster's law (Fig. 1). Compared with other types of in-fiber polarizers, the fiber Brewster grating own many unique advantages such as high polarizing efficiency, broadband responsivity, flexible wavelength adjustability, mechanical robustness and it can be adapted to most types of fiber. Then we successfully fabricated a UV-inscribed fiber Brewster grating with phase scanning technique and employ it as a polarizer to implement an all-fiber ultrafast laser (Fig. 2) [2]. In succession, we have used this kind of fiber Brewster gratings to achieve mode-locked erbium-doped fiber lasers with various operation regimes in C+L wavebands, such as different pulse shaping mechanisms (conventional solitons, stretched pulses, dissipative solitons, noise-like pulses, etc), wavelength tunable/switchable and harmonic mode-locking. Furthermore, it also can be utilized in 1 μm and 2 μm mode-locked fiber lasers.

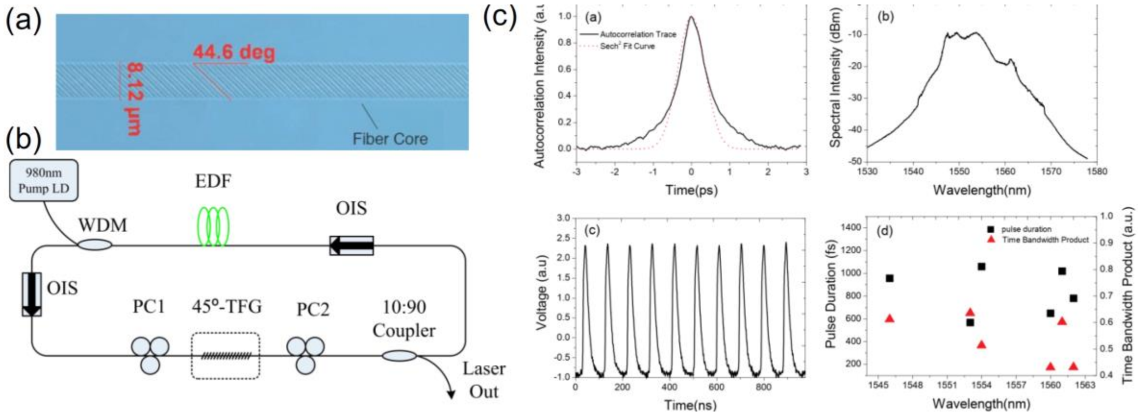

Fig. 2(a) The microscope image of the UV-inscribed fiber Brewster; the schematic (b) and measured characteristics (c) of the first all-fiber soliton mode-lockd laser based on UV-inscribed fiber Brewster grating [2].

Recently, we also have carried out research on femtosecond laser direct writing fiber Brewster grating in view of some shortcomings of UV inscription. To date, we have demonstrated that femtosecond laser inscribed fiber Brewster grating can effectively mode lock an erbium-doped fiber laser [3] and a thulium-doped fiber laser [4] in soliton regimes. In addition, the dissipation soliton and noise-like pulse output have been achieved in net-normal dispersion cavity. The femtosecond laser direct writing inscription avoids the use of expensive phase masks and photosensitivity enhancement process, which provides enormous flexibility for the design of in-fiber polarizing devices. In addition, it is not necessary to strip the fiber coating to thus maintain the mechanical strength of the grating, which is conducive to the integration and reliability of fiber lasers. Efforts are underway to further improve the performances to achieve high energy mode-locked all-fiber lasers.

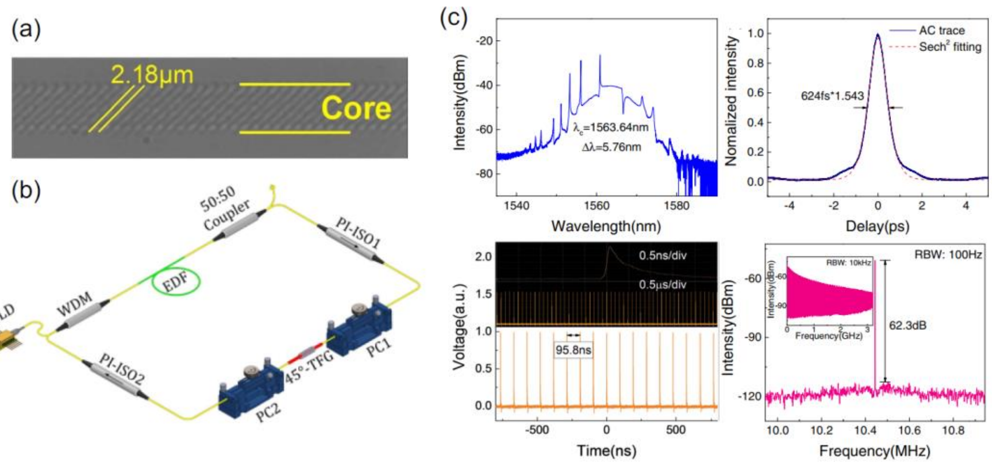

Fig. 3(a) The microscope image of the femtosecond-laser-inscribed fiber Brewster; the schematic (b) and measured characteristics (c) of the all-fiber soliton mode-locked laser based on femtosecond-laser-inscribed fiber Brewster grating [3].

The authors would like to acknowledge support from National Natural Science Foundation of China (61975107), Natural Science Foundation of Shanghai(20ZR1471500), and Ministry of Education '111' project (D20031).

References

[1] K. Zhou, G. Simpson, et al, *Opt. Lett*. **30**, 1285-1287 (2005).
[2] C. Mou, H. Wang, B. et al, *Opt. Express* **18**, 18906-18911 (2010).
[3] Z. Huang, Q. Huang, et al, *Opt. Lett*. **44**, 5177-5180 (2019).
[4] N. Kanagaraj, A. Theodosiou, et al, *Laser Physics Letters* **16**, 095104 (2019).

Novel geometries and layouts of double-clad fibers for fiber lasers

P. Peterka[1,*], P. Koška[1], A. A. Jasim[1], M. Grábner[1], J. Aubrecht[1], M. Kamrádek[1,2], O. Podrazký[1], I. Bartoň[1], F. Todorov[1], Nithyanandan Kanagaraj[1,3], I. Kašík[1] and P. Honzátko[1]

[1]*Institute of Photonics and Electronics of the Czech Academy of Sciences*
[2]*Faculty of Nuclear Sciences and Physical Engineering, Czech Technical University in Prague*
[3]*now in Optoelectronic Research Centre, University of Southampton, United Kingdom*
[*]*E-mail: peterka@ufe.cz*

High-power operation of fiber lasers was mainly enabled by the invention of cladding-pumping in a double-clad fiber structure. Pump absorption is enhanced by broken circular symmetry of inner cladding cross-sections and by mode-scrambling of the pump modes resulting from unconventional fiber coiling, e. g., twisted fiber on standard spool [1, 2], spiral shape coil [3] or kidney shape coil with concave and convex sections of the coil shape [4], see Fig. 1 and 2. However, theoretical studies were mostly limited to the assumption of a straight fiber until recently, when the rigorous model accounting for double-clad fiber bending and twisting was described [1, 2, 5]. Here we review the results of numerical modeling of pump absorption in various types of double-clad fibers, e. g., with cross-section shape of hexagon, stadium, and circle; two-fiber bundle (so-called GT Wave fiber structure, see Fig. 3) as well as panda fibers. We analyzed both the cases: of diode pumping where the ratio of core area to inner cladding area is usually small, and the case of tandem pumping by high-brightness fiber laser sources, where the respective ratio is usually larger. We show also our results in processing of fiber preforms by CO_2 laser in order to get almost arbitrary cross sectional shape of the inner cladding [6]. Examples of such fiber cross sections are shown in Fig. 1. Unlike the common grinding method, CO_2 laser shaping allows to achieve almost any cross section shape, namely it allows combination of concave and convex sections.

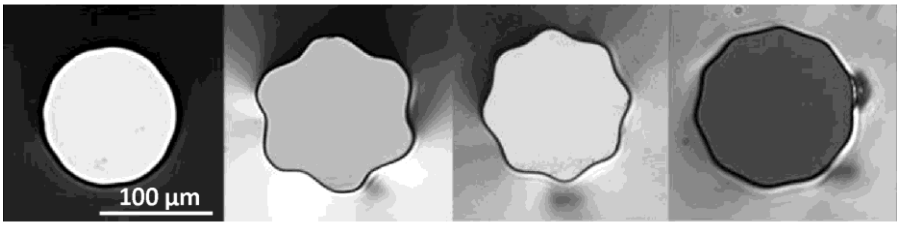

Fig. 1. Examples of noncircular fiber cross sections whose silica preforms were shaped by CO_2 laser. From left: hexagonal shapes with shallow and deeper groves, octagonal and decagonal cross sections.

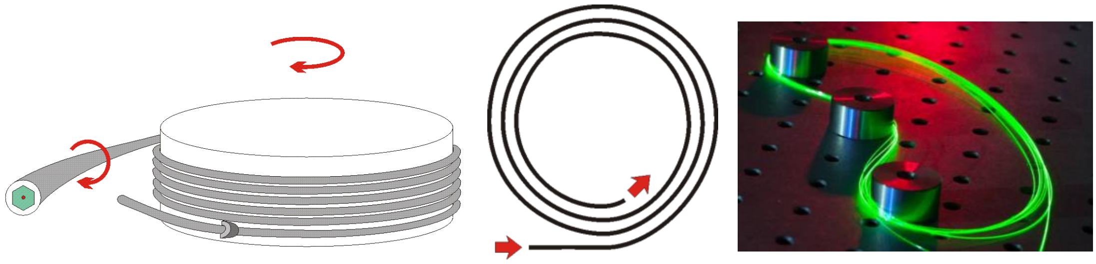

(a) **(b)** **(c)**

Fig. 2. Examples of fiber layout for improvement of pump absorption efficiency: (a) twisted fiber on a standard circular spool, (b) spiral spool and (c) kidney-shaped spool. The spiral spool offers slowly vary-

ing effective absorption cross section through change of the coiling diameter. Used with permission from ref. [7] (©[2019] IEEE)

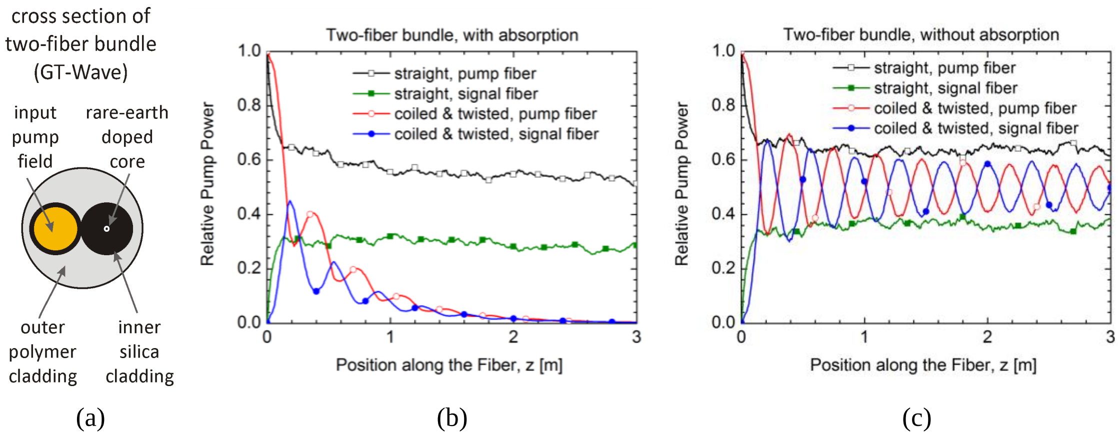

Fig. 3. (a) Cross section of the two-fiber bundle double-clad waveguide structure; the yellow part schematically represents the input pump distribution. The pump power distribution between both fibers in GT-Wave two-fiber bundle was numerically calculated either for the case of straight arrangement orfor coiled and twisted fiber bundle. Two cases of signal fiber are considered, (a) without rare-earth dopants and (b) with Yb-doped core. Used with permission from ref. [1] (©[2016] IEEE)

Our model used for pump absorption efficiency optimization (against other published models which do not take into account fiber twist) has a significant application potential in the design of fiber lasers and amplifiers because double-clad fibers of shorter lengths can be used [1, 2]. This minimizes the deleterious effect of background losses and nonlinear effects. In addition, our model finally explained highly efficient pump coupling in GT-Wave fiber structure where the pump fiber is only touching the fiber with the active core, see Fig. 3(a). While only negligible absorption occurs in straight GT-Wave structure, see green line in Fig. 3(b), it is the twist of the fiber bundle that enables efficient pump absorption, see the blue line in Fig. 3(b) [1].

The new geometries and layouts shall finally result in a highly efficient laser of small footprint without the need of water cooling and holds great potential for applications with low power consumption, tightly limited space and weight requirements. The proposed design will also minimize the risk of damage of the fiber during laser operation, which is a key point in fiber based laser architecture. Portions of the work have already been presented in papers [1, 2, 7].

This work was financially supported by the Czech Science Foundation under project No. 19−03141S.

References

[1] P. Koska, P. Peterka, and V. Doya, *IEEE J. Sel. Top. Quantum Electron.* **22**, 4401508 (2016).
[2] P. Koska, et al., *Opt. Express* **24**, 102-107 (2016).
[3] C. A. Codemard, A. Malinowski, and M. N. Zervas, in Proc. SPIE Photonics West, Fiber Lasers XIV: Technology and Systems, San Francisco, USA, 2017, p. 1008315.
[4] H. Zellmer, et al., in Proc. *Opt. Amplifiers and Their Appl.*, Victoria, Canada, 1997, p. FAW18.
[5] P. Koska and P. Peterka, *Opt. Quantum Electron.* **47**, 3181-3191 (2015).
[6] A. A. Jasim, et al., *Opt. Express* **28**, 13601-13615 (2020).
[7] P. Peterka, et al., in IEEE Proc. *21st International Conference on Transparent Optical Networks (ICTON)*, Angers, France, 2019, p. Th.B6.1.

Artificial Rayleigh fibers and its laser's application

**S.M. Popov[1,*], O.V. Butov[2], A.P. Bazakutsa[2],
M.Yu. Vyatkin[1], A.A. Fotiadi[3,4], Yu.K. Chamorovskiy[1]**

[1]*Kotelnikov Institute of Radioengineering and Electronics (Fryazino Branch) of RAS, Fryazino, Russia*
[2]*Kotelnikov Institute of Radioengineering and Electronics of RAS, Moscow, Russia*
[3]*Ulyanovsk State University, Ulyanovsk, Russia*
[4]*University of Mons, Mons, Belgium*

**E-mail: sergei@popov.eu.org*

At the moment, optical fibers (OF) are used in various branches of science and technology. In addition, optical fibers common using in information systems (communication lines and fiber sensors). The use of optical fiber in laser systems is also developing. Usually, OFs are doped with such rare-earth ions as erbium, ytterbium, bismuth, thulium, etc. are used to obtain lasing. Recently, a new direction so-called random fiber lasers [1–3] are actively developing. This direction of photonics has become a subject of great interest for researchers around the world due to the fact that random fiber lasers are able to generate light with unique performance characteristics without imposing strict requirements on the optical cavity. In this case, amplification is achieved as due to the Raman scattering effects [2] as stimulated Brillouin scattering (SBS) [3]. The feedback in the optical fibers is achieved due to weak stationary ("frozen into the glass grid") scattering centers uniformly distributed over the fiber length (Rayleigh scattering). This leads to the fact that cavity of random lasers are constructed using long (1–100 km) OFs. Current trends in random fiber lasers are associated with the transition to lasers with cavities [4] based on short artificial Rayleigh optical fibers (OFs containing an array of fiber Bragg gratings - FBGs) [5].

We have developed an OF with FBG. The inscription of which is performed during the OF drawing process [5]. The formation of an FBG array in such an optical fiber is performed using pulsed radiation from an excimer UV laser passing through a phase mask. The number of FBGs of such OF can reach 10,000 ones per 100 meters. The increase in the return signal in comparison with the Rayleigh scattering level reaches 50 dB at the wavelength of λ = 1550 nm. The typical width of the reflection spectrum of the FBG array is 0.3 nm. The width of the reflection spectrum of the array reaches 4 nm using a chirped phase mask. It is also possible to expand of the reflection spectrum up to 4 nm by means of the tapering of the optical fiber with the FBG array. It is possible to inscribe FBG array both in an optical fiber drawn from a photosensitive preform and in a conventional single-mode telecommunication optical fiber of the SMF-28 type. In the latter case, the inscription contrast reaches 25 dB at the wavelength of λ = 1550, which significantly increases the Rayleigh scattering level and expands the possibilities of using such an optical fiber in a coherent reflectometry system [6-7].

We obtained narrow-band lasing with a lasing line width of less than 10 kHz at the wavelength of 1552 nm [8] using an OF with an FBG array 100 meters long. Additionally, a short section (~ 1 m) of an Er-doped with erbium ions was added to the cavity of a random laser, which was used as a dynamic mode filter [9]. The tapered optical fiber with an FBG array can be used as a resonator [10] to obtain tunable lasing in a band of up to 4 nm.

It is also possible to inscribe FBG arrays during the drawing process of the OF doped with erbium ions [11–12]. It makes possible to create OFs that combine both increased reflectivity and the possibility of forming dynamic gratings, which are extremely important for spectral selection of laser radiation. In fig. 1 (a) shows the frequency reflectogram (OFDR) trace of an OF doped with erbium ions. The inscription contrast reaches 30 dB at the wavelength of 1547.6 nm with a reflection spectrum width of up to 0.3 nm. The lasing radio-frequency spectrum measured by the self-heterodyne method is shown on Fig. 1 (b). The lasing efficiency reaches 2.5% at a pump power of 300 mW at the wavelength of 976 nm. The cavity length is 5 m.

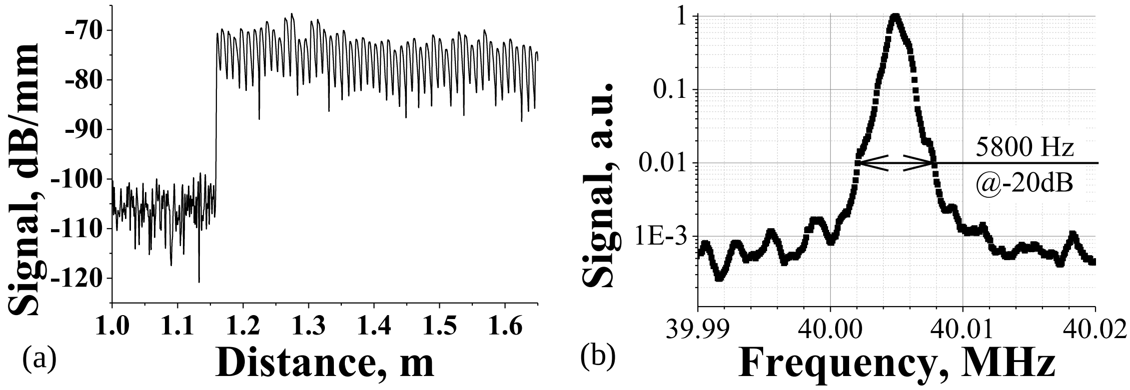

Fig. 1. Frequency reflectogram (OFDR) trace (a) of erbium ions doped OF with an FBG array, and (b) lasing radio-frequency spectrum, measured by the self-heterodyne method.

The design of the laser ensures the predominance of the reflectivity created by the dynamic grating of the inverted population over the stationary centers of reflection. It makes it possible to effectively carry out nonlinear filtering directly in the OF cavity [12]. In this case, the width of the laser line is narrowed to a frequency range of less than 1 kHz.

The authors are grateful to the staff of the IRE RAS for manufacturing the preform (Prof. K.M. Golant, V.A. Aksenov) and drawing the experimental fiber (I.L. Vorobyev, V.V. Voloshin, A.O. Kolosovskii). The work was carried out within the framework of the state task and partially supported by the Russian Foundation for Basic Research (RFBR) and NSFC grant 20-57-53013. The work of A.A.F is supported by Russian Science Foundation grant 18-12-00457 and RFBR grant 18-42-732001 r_mk.

References

[1] A.A. Fotiadi, R.V. Kiyan, *Opt. Lett.* **23**, 1805-1807 (1998)
[2] S. Turitsyn, S. Babin, A. El-Taher, et al., *Nature Photon* **4**, 231–235 (2010)
[3] A. Fotiadi, *Nature Photon* **4**, 204–205 (2010)
[4] M.I. Skvortsov, S.R. Abdullina, et al., *Quantum Electron* **47,** 696–700 (2017)
[5] I.A. Zaitsev, O.V. Butov, et al., *Journal of Comm. Tech and Electr.* **61**, 639–645 (2016)
[6] S.M. Popov, O.V. Butov, et al.,, *Quantum Electron* **49**, 1127–1131 (2019)
[7] D.R. Kharasov, D.M. Bengalskii, et al.,, *Quantum Electron* **50**, 510–513 (2020)
[8] S.M. Popov, Oleg V. Butov, et al., *Results in Physics* **9**, 806-808. (2018)
[9] I.A. Lobach, R.V. Drobyshev, et al., *Optics Letters* **42**, 4207-4210 (2017)
[10] S.M. Popov, O.V. Butov, et al., *Results in Physics* **9**, 625-627 (2018)
[11] S.M. Popov, O.V. Butov, et al., *Results in Physics* **16**, 102868 (2020)
[12] S.M. Popov, O.V. Butov, et al., *Proc. SPIE* **11357**, 113571Q (1 April 2020)

Amplification of pulsed radiation at a wavelength of 2.27 μm in a Tm^{3+}- doped tellurite fiber

S.A. Filatova[1,*], V.A. Kamynin[1], V.V. Koltashev[2], B.I. Galagan[1], S.E. Sverchkov[1], V.V. Dorofeev[3], S.E. Motorin[3], V.B. Tsvetkov[1], B.I. Denker[1]

[1]*Prokhorov General Physics Institute of the Russian Academy of Sciences*
[2]*Prokhorov General Physics Institute of the Russian Academy of Sciences, Dianov Fiber Optics Research Center*
[3]*Devyatykh Institute of Chemistry of High-Purity Substances of the Russian Academy of Sciences*
[*]*E-mail: filsim2910@gmail.com*

Compact laser sources operating in the spectral range of 2.2 - 3 μm are of interest both for scientific and applied problems. Such sources can be used in spectroscopy, gas detection (CO, CH_4), laser ranging, material processing, medicine and etc. [1, 2]. Researches of tellurite glasses show that fibers based on them, doped with rare earth elements, in contrast to standard silica fibers, are a promising medium for lasers and amplifiers emitting in this spectral range [3, 4].

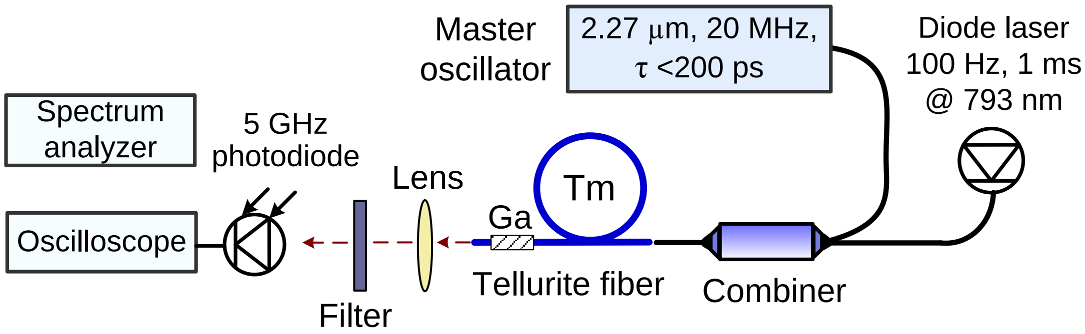

Fig. 1. Experimental setup.

Fig. 1 shows the scheme of experimental setup for amplifying of pulsed radiation at a wavelength of 2.27 μm in tellurite fiber doped with thulium ions (Tm^{3+}). A laser system consisting of a holmium-doped (Ho^{3+}) fiber laser and amplifier, a nonlinear fiber, and a spectrally selective element was used as a master oscillator (MO). The Ho^{3+}- doped fiber laser generated pulsed radiation at a wavelength of 2.07 μm with a pulse duration of about 1 ps and a repetition rate of 20 MHz. The amplified pulsed radiation was transformed in a 5 m long nonlinear fiber with a GeO_2 concentration in the core of more than 30 mol. %. Thus, broadband radiation with a peak at a wavelength of 2.28 μm was obtained. A fiber Bragg grating with a high reflection at a wavelength of 2.27 μm was used to obtain spectrally-selected pulsed radiation. Fig. 2(a) shows the spectrum of reflected part of the broadband radiation. Then, the pulsed radiation was introduced through a fiber combiner into a 1.5 m long Tm^{3+}-doped tellurite fiber. The estimated signal power at the combiner input was 30 μW. The concentration of Tm^{3+} ions in the tellurite fiber was 5×10^{19} cm^{-3}, and the diameters of the cores and cladding were 35/100/280 μm. The Tm^{3+} amplifier was pumped by a laser diode with a radiation wavelength of 793 nm and a power of 4 W. The diode radiation was modulated to prevent the destruction of tellurite fiber ends due to overheating. Modulation parameters are shown in Fig. 1.

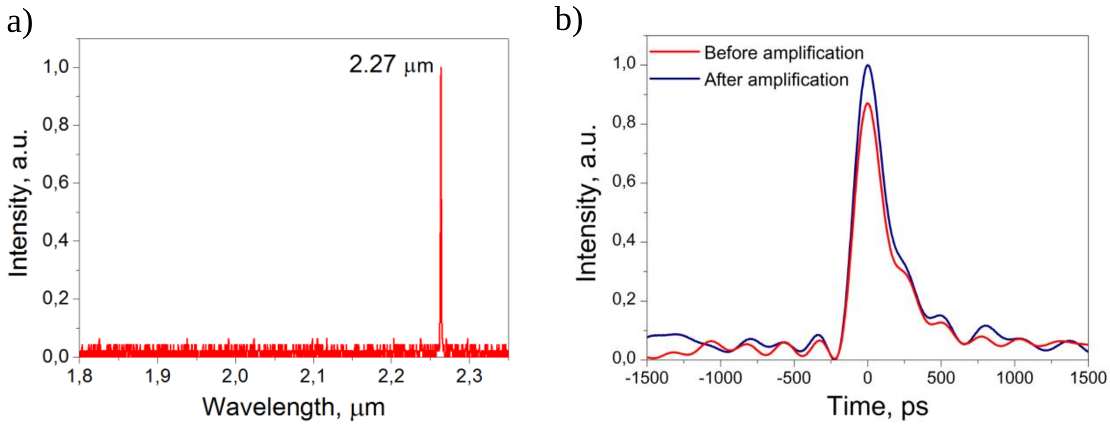

Fig. 2. (a) Reflected part of the broadband spectrum, (b) the pulse oscillograms before and after amplification in Tm^{3+}-doped tellurite fiber.

Fig. 2(b) shows the pulse oscillograms before and after amplification, measured using a 5 GHz photodiode (PD). A bandpass filter (2 – 2.5 μm) was used to cut-off the pump radiation, as well as lens for the pulsed radiation focusing at a wavelength of 2.27 μm. The spectral composition of the amplified pulsed radiation did not differ from that shown in Fig. 2(a).

Thus, we have demonstrated the amplification of spectrally selected pulsed radiation at a wavelength of 2.27 μm in a tellurite fiber doped with Tm^{3+} ions. The overall gain can be estimated as 0.8 dB/m.

References

[1] J. Ma, Z. Qin et al., *Applied Physics Reviews* **6.2**, 021317 (2019)
[2] D.C. Sordillo, L.A. Sordillo et al., *Photonic Therapeutics and Diagnostics XII*, Proc. SPIE **9689**, 96894J (2016)
[3] B.I. Denker, V.V. Dorofeev et al., *Laser Physics Letters*, **16(1)**, 015101 (2018)
[4] S.V. Muravyev, E.A. Anashkina et al., *Scientific reports*, **8(1)**, 1-13 (2018)

Linearly-polarized Ho-doped fiber laser with wavelength self-sweeping near 2.09 µm

A.D. Vladimirskaya[1,2,*], **I.A. Lobach**[1], **S.I. Kablukov**[1]

[1]*Institute of Automation and Electrometry SB RAS, Novosibirsk, Russia*
[2]*Novosibirsk State Technical University, Novosibirsk, Russia*
[*]*E-mail: anastasiavladimirskaya97@gmail.com*

The sources with lasing near 2 µm are of particular interest due to presence of strong absorption lines of water and carbon dioxide in this spectral range. Spectral analysis of the molecules can be used in bioatmospheric analysis as well as in medicine. In particular, the *Helicobacter Pylori* bacteria can be detected by analyzing carbon dioxide isotopes in human expired air [1]. The method is based on measurement of relative difference between concentration ratio of 12- and 13-isotopes of carbon dioxides in the test sample and standard one for the isotopes. For this purpose, a spectrometer based on a tunable laser with lasing near 2 µm can be applied. There are many methods for laser's frequency tuning, such as application of diffraction gratings, Bragg gratings or interferometers. However, the wavelength tuning can be obtained without tunable elements in fiber lasers with self-induced frequency sweeping ("self-sweeping" for short) [2]. The lasing near 2 µm can be achieved in fiber lasers based on Thulium- as well as Holmium-doped active fibers. Such a self-sweeping Ho-doped fiber laser with lasing near 2100 nm has been demonstrated in [3]. However, stability of lasing was violated due to thermal and mechanical impact. It makes difficult to use this lasing source for continuous measurements. Probably, the lasing instability has been caused because of using non-polarized active fiber. In this paper, we present the Ho-doped fiber laser with self-sweeping near 2.09 µm which suits better for described practical tasks.

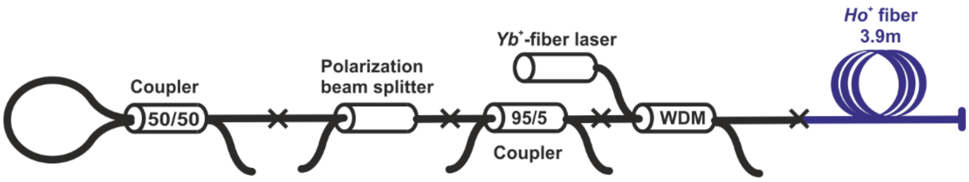

Fig.1. Schematics of the Ho-doped self-sweeping fiber laser.

The experimental scheme of the laser is presented in Fig.1. We have used polarization maintaining (PM) active fiber and components in this work to prevent the effect of mechanical deformations on the output lasing. The active medium of the fiber laser is 3.9 m long Ho-doped silica fiber (IXBlue IXF-HDF-PM-8-125). The fiber has a core diameter of 8 µm, and absorption of 8.9 dB/m at 1125 nm wavelength. An Yb-doped fiber laser with maximum output power of 4.8 W at wavelength of 1125 nm is used as the pump. This pump is significantly different from a thulium fiber laser with lasing in range of 2020-2030 nm which was used in paper [3]. The laser cavity is formed by a high-reflective fiber loop mirror (FLM), based on a 50/50 coupler at 2000 nm wavelength at one side and a right-angle cleaved active fiber end at the other side. The Ho-doped fiber is pumped through 1310/1960 wavelength division multiplexer (WDM). Mismatch of the WDM and the pump wavelengths affects the lasing efficiency. A polarization beam splitter is used as a polarizer in the laser. 5 percent ports of 95/5 intracavity coupler are used for measurements of the laser parameters.

The laser operates in a reverse self-sweeping regime near wavelength of 2.09 µm in a range of pump powers from 0.75 to 1.05 W. The sweeping range and rate is about 5 nm and 1.1 nm/s correspondingly (Fig. 2a). The generated power at cleaved output end is about 150 mW. The intensity dynamics is quasi-CW, which differs from the results of [3], where the output generation is self-sustained pulsations, which are usually observed in the self-sweeping regime. It is also worth noting that the laser operation mode lasted for a long time (more than 1 hour), it also differs from results of work [3], where duration of the operation was limited to a few minutes. We believe that the developed self-sweeping source can be used for spectroscopy of 12- and 13-isotopes of carbon dioxides (Fig.2b).

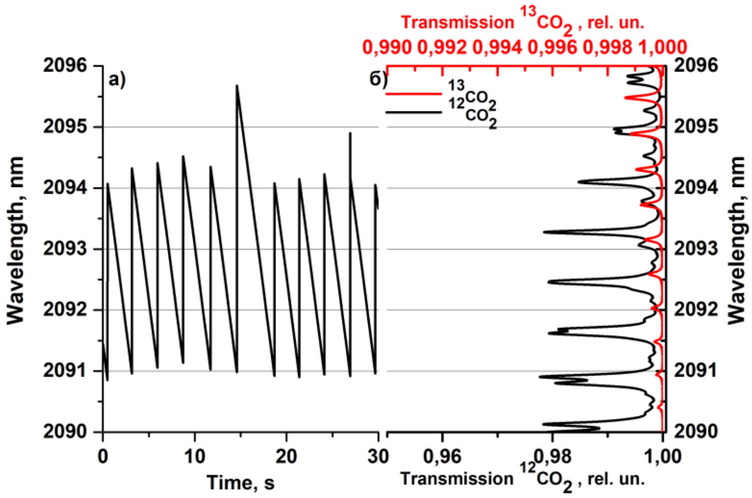

Fig.2. Spectral dynamics of the laser (a) and transmission spectra of 12- and 13-isotopes of carbon dioxides (b).

The authors are grateful to Ph.D. V.A. Kamynin for the providing ytterbium fiber pump laser. The reported study was funded by RFBR according to the research project № 20-32-70058

References

[1] D.Y. Graham, P.D. Klein, et al, *The Lancet*, 1174-7 (1987).
[2] I.A. Lobach, S.I. Kablukov, et al, *Opt. Express* **19**, 17632-17640 (2011).
[3] J. Aubrecht, P. Peterka, et al, *Opt. Express* **25** 4120–5 (2017).

Output power saturation of ytterbium-erbium doped fiber laser

A.A. Surin[1,*], N.V. Kovalenko[1,2]

[1] *IPG IRE-Polus, Fryazino*
[2] *Moscow Institute of Physics and Technology, Moscow*
* *E-mail:* aSurin@ntoire-polus.ru

One of the effects limiting the output power in lasers based on erbium and ytterbium-erbium doped active media is saturation, which was theoretically predicted in the works [1,2]. In both works, the effect is explained by the existence of a "bottleneck" that restricts the transmission of excitation to the working level. In [1] it is said that the bottleneck is the transition between the levels of erbium $^4I_{11/2} \rightarrow {}^4I_{13/2}$.

This paper presents for the experimental observations of this effect in an ytterbium-erbium doped fiber laser, and a convenient formula for estimating saturation power is theoretically derived.

Figure 1 shows the scheme of the experiment. Three lasers consisting of ytterbium-erbium doped active fiber supporting polarization, fiber brag gratings, and fiber polarizers were studied. The parameters of the used active fibers are shown in Table 1. The lasers were pumped at 1065 and 1070 nm by single-mode radiation into the core of the active fiber.

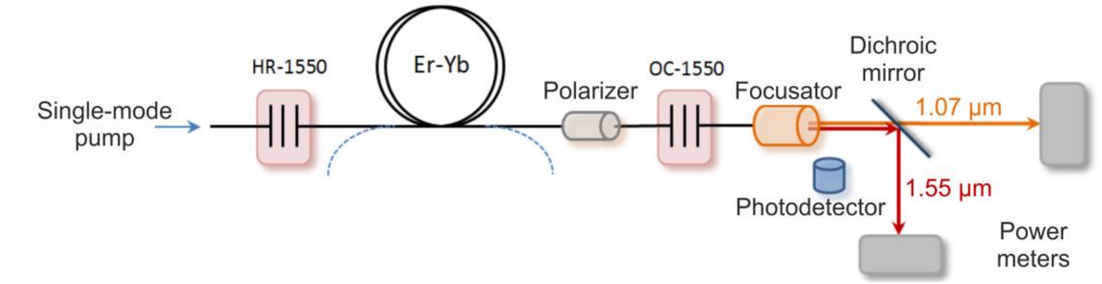

Fig.1. Scheme of the experiment.

Figure 2 shows the watt-watt characteristic of a laser with 5 m length active fiber. The signal power of 1550 nm at low pump power increases with a differential efficiency of 27% and reaches saturation at ~15W. The saturation effect is observed for each laser. The corresponding values are shown in table 2.

The output power of the laser system is limited, since the number of erbium ions involved in generation is limited, and there is a finite time in which the ion can receive energy and transfer part of it to the external environment in the form of electromagnetic radiation.

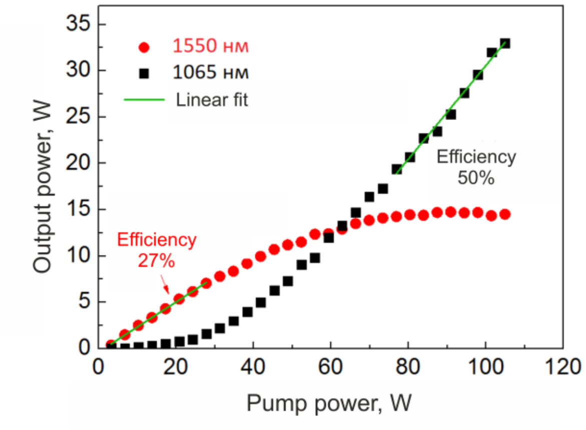

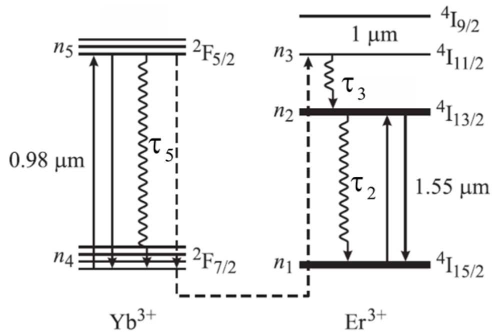

Fig.2. The dependence of the received output power at 1550nm and the unabsorbed pump at 1065nm on the pump power (left) and the scheme of energy levels in the ytterbium-erbium active medium (right).

Based on the assumption that the generation bottleneck is the transition $^4I_{11/2}\rightarrow{}^4I_{13/2}$ (Fig.2) a formula for the saturation power can be obtained P_{sat}:

$$P_{sat} = \frac{hc}{\lambda_s}\frac{N_{Er}}{\tau_3}\left(1+\frac{\sigma^e_{Yb}}{\sigma^a_{Yb}}\left(1+\frac{\sigma^a_{Er}}{\sigma^e_{Er}}\right)\right)^{-1}$$

Where N_{Er} - number of erbium ions in the medium, τ_3 - lifetime at the level $^4I_{11/2}$, λ_s - the wavelength of the signal, $\sigma^a_{Er}, \sigma^e_{Er}, \sigma^a_{Yb}, \sigma^e_{Yb}$ - absorption and luminescence cross sections of the working levels of erbium and ytterbium, respectively, h – Planck's constant, c – speed of light.

Based on experimental data and the proposed formula, we estimated the lifetime of the level $^4I_{11/2}$ (Tab.1). It can be seen that the saturation powers P_{sat} differ significantly for lasers with different amounts of erbium ions and pump wavelengths, however, the restored lifetimes τ_3 have approximately the same values. In the world literature, this time for phosphate glass media is in the range 1-3 μs [1,3].

Table.1. Active fiber parameters and experimental results

Active fiber length, m	Active fiber core diameter, μm	Erbium ions concentration, ppm	Pump wavelength, nm	P_{sat}, W	τ_3, μs
4	9,1	230	1070	1,7	1,53
6	9,1	230	1070	2,5	1,56
5	18	300	1065	15	1,38

The authors express their gratitude to the management of the IPG IRE-Polyus for supporting these studies.

Literature

[1] R.S. Quimby, *Applied Optics*, **30** (18), 2546-2552 (1991)

[2] E. Yahel, A. Hardy, *Journal of lightwave technology*, **21**(9), 2044-2052 (2003)

[3] N.E. Alekseev, V.P. Gaponcev, M.E. Jabotinskii, Laser phosphate glasses, M.:Nauka (1980)

Photoinduced defects in Er/Al-doped optical fiber

A.P. Bazakutsa*, **A.A. Rybaltovsky, O.V. Butov**

Kotelnikov Institute of Radioengineering and Electronics of RAS, Moscow

**E-mail: a.bazakutsa@gmail.com*

Recently, questions of the technology of manufacturing single-frequency fiber lasers have become increasingly important. One of the promising areas is the development and manufacture of distributed feedback (DFB) fiber lasers, designed on the basis of silica fibers with a highly Er doped core [1]. The resonator of such a laser is formed with an extended fiber Bragg grating (FBG) inscribed along its entire length with a phase shift in its structure [2]. In this case, the grating is inscribed directly in the core of the active fiber. FBG is usually made by UV laser irradiation. To increase the efficiency of inscription, the fiber can be previously loaded with molecular hydrogen. In our work [3], we have shown the negative effect of UV irradiation on the gain properties of the active fiber, while the presence of hydrogen in the glass network is an additional negative factor. However, it was found that the photoinduced gain degradation could be partially restored by exposing the fiber to 976 nm pump radiation.

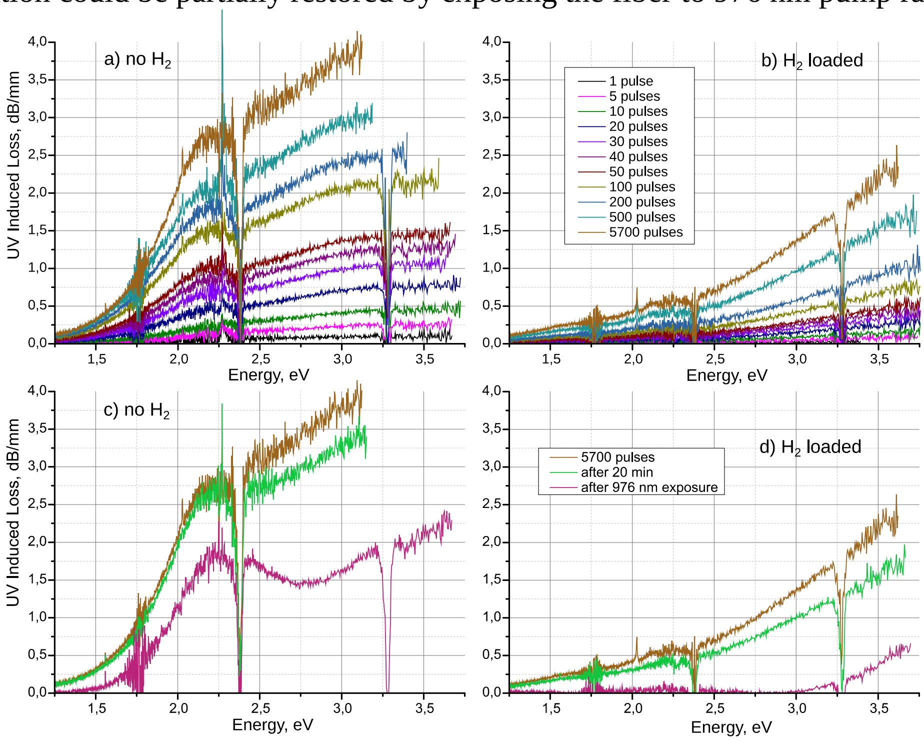

Fig. 1. Induced absorption spectra of the fiber samples in the UV and visible spectral range for pristine (a) and H_2-loaded (b) fiber depending on the number of UV laser pulses. Evolution of spectral shape in 20 minutes at room temperature after the UV irradiation and consequent 976 nm exposure of the sample without H_2 (c) and H_2-loaded fiber (d).

In this work, we investigated the changes in the absorption spectra of an active erbium doped fiber codoped with aluminum under the influence of UV irradiation. The studies were carried out in the UV and visible range, where the most characteristic spectral bands of the main defects in this type of glass are observed. From the change in the absorption spectra, a conclusion was drawn about the dynamics of defects formation and their subsequent decay. The dynamics of changes in absorption spectra as a result of UV irradiation and subsequent exposure at 976 nm is shown in Fig. 1. For convenience of comparison, we approximated the obtained absorption spectra by three Gaussian functions corresponding to resonant absorption energies of 2.3, 3.2, 4.1 eV. The first two correspond to the absorption bands of aluminum oxygen – hole centers (Al-OHC), the third - to aluminum E 'centers (AlE'). The changes in the intensity of the Gaussian peaks obtained as a result of the approximation are shown in Fig. 2.

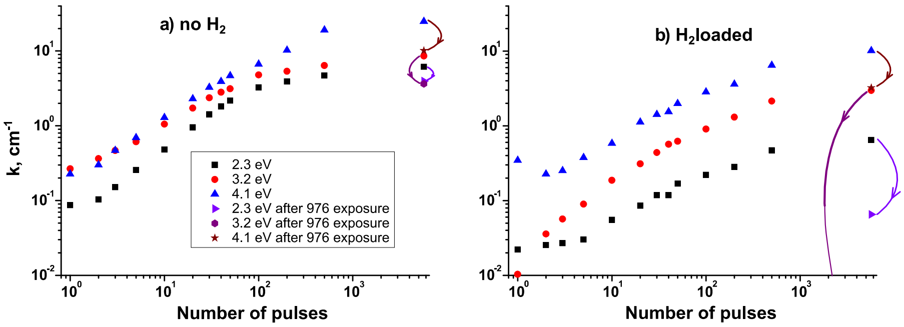

Fig. 2 Intensity of the Gaussian peaks of the induced absorption spectra for a fiber without hydrogen (a) and hydrogen-loaded (b). The arrows show the effect of the 976 nm exposure.

Figure 2 is plotted on a logarithmic scale on both axes for better visualization of the results. We see that the dependence of the absorption peak intensity on the exposed UV dose has a power-law activation nature with saturation at the maximum exposed dose, typical for photoionization processes. The arrows on the right side of the graphs show the decrease in the intensity of the corresponding absorption peaks under the influence of 976 nm exposure. It should be noted that the intensity of the 3.2 eV peak in the H_2 loaded sample decreases almost to zero. The 976 nm pump photon energy is only 1.27 eV. In this case, the minimum excitation energy of Al-OHC is ~ 2 eV. It is known that low-intensity green luminescence with a maximum at a wavelength of 483 nm was observed in the spectrum of Er-doped fibers under 976 nm [4]. This luminescence, which corresponds to the $^4F_{7/2} \rightarrow {}^4I_{15/2}$ transitions, despite its low intensity, has a sufficient quantum energy (~ 2.5 eV) to excite Al-OHC centers, leading with a high probability to their photoinduced decay, or, in the presence of hydrogen molecules to their conversion to hydroxyl centers H − O − Al≡.

References

[1] A.M. Smirnov, A.P. Bazakutsa et al, *ACS Photonics* **5**, 5038-5046 (2018)
[2] P. Varming, J. Hubner and M. Sejka, *IOOC'95 Tech. Digest* **5**, PD1-3 (1995)
[3] A.P. Bazakutsa, A.A. Rybaltovsky and O.V. Butov, *JOSA B* **36**, 2579-2586 (2019)
[4] A.V. Kir'yanov, Yu.O. Barmenkov and A.D. Guzman-Chavez, *Lasers Physics* **18**, 1251-1256 (2008)

Pulsed fiber and hybrid lasers, high-energy and ultra-short pulses

Stabilization of a fiber femtosecond frequency comb to an optical frequency standard based on a single ytterbium ion

N.A. Koliada[1,*], V.S. Pivtsov[1,2], A.S. Dychkov[1], S.A. Farnosov[1], S.A. Kuznetsov[1], A.A. Filonov[1], D.Yu. Primakov[1]

[1]*Institute of Laser Physics SB RAS*
[2]*Novosibirsk State Technical University*
[*]*E-mail: n.koliada@mail.ru*

A femtosecond frequency comb is one of the main parts of a femtosecond optical clock (FOC) [1 - 2]. FOCs allow studying fundamental physical processes and measuring the frequency of transitions of atoms and molecules. Systems based on FOCs are being developed to increase the accuracy of satellite navigation. Modern FOC includes three main parts – an optical frequency standard, a femtosecond frequency comb (whose frequencies are stabilized to the reference standard) and an electronic stabilization system. The femtosecond comb generates equidistant frequencies. Each frequency of this comb is expressed by the sum $f_n = f_o + n{\cdot}f_{rep}$, where f_o is the offset frequency of the comb, f_{rep} is the pulse repetition rate (intermode frequency), n is an integer [3]. If stabilize two of these three frequencies, one can obtain a comb of stabilized optical and radio frequency. Each component will have a relative stability of the reference optical standard.

In this work, we experimentally investigated the possibility of precision stabilization of the femtosecond optical frequency comb (generated by a femtosecond erbium fiber laser) to an optical frequency standard based on a single ytterbium ion [4]. The comb offset frequency f_o was detected using a two-arm f-2f interferometer [5] and stabilized using an extracavity fiber coupled acousto-optic frequency modulator (AOFM). Using an optical mixer, the beat frequency f_b was obtained between the frequency of the output optical radiation of the Yb + standard (at a wavelength of 871 nm) and the nearest frequency-doubled component of the femtosecond comb (at a wavelength of 1742 nm). The obtained beat signal was stabilized using an intracavity electro-optical modulator based on a KTP crystal [6]. In this way, all components of the femtosecond frequency comb were stabilized. An advantage of the proposed method is that the stabilization of high-frequency disturbances of two signals using an intracavity EOM and an extracavity AOFM practically does not affect each other. With this approach, the modulation frequency of ~ 200 kHz for f_b with the EOM and the modulation frequency of ~ 30 kHz for f_o with the AOFM have become possible. The stabilization frequency of the AOFM is limited by the AOFM configuration and the PLL system and can be increased.

Instability of the output radio frequency of a fiber comb was investigated. To implement the measurement, a Ti: Sa-based femtosecond frequency comb (developed earlier at the Institute of Laser Physics of the SB RAS) was additionally used. Each frequency comb was stabilized to the frequencies of two different laser systems that are part of the optical standards (based on a single ytterbium ion). The intermode beat signal at a frequency of ~ 3 GHz was detected at the outputs of both frequency combs. Using a radio frequency mixer, a difference signal was obtained at a frequency of ~ 10 MHz. The resulting difference signal was recorded using a Microsemi TSC-5120A phase noise test set. This device compares phases of the reference signal and the signal under test. A signal from a passive hydrogen standard («Vremya-CH» JS COMPANY) with a frequency of 10 MHz was used as a reference signal. The Allan deviation was calculated for the obtained data, which characterizes the total relative instability of the signals at the output of two femtosecond combs. The obtained values are close to the instability of the laser systems of the optical standards.

The work was carried out using the equipment of the Center for Collective Use "Femtosecond Laser Complex" at the ILPh SB RAS. The research was carried out with the financial support of the program of fundamental scientific research of the SB RAS No. II.11.1.

References

[1] S.N. Bagayev, V.I. Denisov et al, *Laser Phys.* **14**, 1367 -1374 (2004)
[2] S.A. Diddams, Th. Udem et al, *Science* **293**, 825 - 828 (2001)
[3] H.R. Telle, G. Steinmeyer et al, *Appl. Phys. B* **69**, 327-332 (1999)
[4] S.V. Chepurov, A.A. Lugovoy et al, *Quantum Electronics* **49**, 412-417 (2019)
[5] M.C. Stumpf, S. Pekarek et al, *Appl. Phys. B* **99,** 401-408 (2010)
[6] N.A. Koliada, B.N. Nyushkov et al, *Quantum Electronics* **46**, 1110-1112 (2016)

Propagation simulation of ultra-short high-power pulse in birefringent single mode optical fiber

V.A. Burdin
Povozhskiy State University of Telecommunications and Informatics
E-mail: burdin@psati.ru

Femtosecond lasers are now increasingly being used in various industries. The variety of their applications requires different forms, duration and power of optical pulses. Often development of lasers with necessary parameters of pulses and means of pulse delivery to the place of application requires the development of special optical fibers. However typical designs of quartz fibres can also be used quite often for these purposes. Moreover, optical polarization-maintaining fibers are especially in demand. Concept, based on solving the coupled nonlinear Schrödinger equations, which often lead to Manakov's equations, are well established to describe optical propagation processes pulses in birefringent optical fibers taking into account nonlinearity, dispersion and mode coupling. As a rule, this system is solved by splitting into physical processes. The method has some advantages, providing acceptable error at relatively low requirements for computing resources. Also, the chromatic dispersion of the third order and Raman scattering effect must be taken into account, when modeling propagation of ultrashort optical pulses of duration less than 10 ps in optical fibers. At the same time, the equations of the system are introduced additional terms. As a result, the nonlinear operator includes derivatives of functions from complex time envelope, when solving a given system of equations by the method of splitting by physical processes. This is the main problem of implementing the split method by physical processes to solve a system of coupled nonlinear Schrödinger equations with components to take into account the Raman effect.

In papers [1], [2] it is proposed a nonlinear operator to lead to a system of Madelung equations and execute it by solving this system of differential equations on each step. It is shown that this approach provides stable solutions in contrast to direct calculation of a nonlinear operator with derivatives from complex time envelope calculated directly by numerical methods or using the Fourier transform. At the same time, the following options for calculating derivatives using the Fourier transform were considered:

$$|A|^2 F^{-1}\left[j\omega F\left(A\right)\right] \text{ and } F^{-1}\left[j\omega F\left(|A|^2\right)\right].$$

Here F and F^{-1} – a forward and inverse Fourier transform operator, respectively; A – complex envelope; ω – angular frequency; j – imaginary unit. In paper [3] it is proposed to calculate the intensity derivative as follows:

$$\mathrm{Re}\left\{F^{-1}\left[j\omega F\left(|A|^2\right)\right]\right\}.$$

This option was used in this work, but here nonlinear coefficient component before the first derivative of complex time envelope was not taken into account unlike paper [3]. Previously, applied algorithm for implementing the split method by physical processes to solve the Schrödinger system of coupled nonlinear equations, describing high-power optical pulse propagation process in single mode birefringent optical fiber, was tested on an example with known experimental data.

In particular, the propagation of the optical pulse with a duration of 12 fs and a peak power of 175 kW in birefringent a butterfly type single mode fiber at a wavelength of 798 nm is simulated. Results of response calculations on optical fiber output matched well enough with experimental data in both time and spectral domains. At the same time, unlike paper [1], the proposed algorithm eliminated the need solving an additional system of differential equations at each step of solution, and the number of Fourier transforms, which needed for direct calculation of the nonlinear operator of the splitting method by physical processes, have been halved. Subsequently, the simulation was carried out for longer optical fiber samples depending on beat length of polarization-maintaining fiber and optical power distribution between modes at input. Example of the simulation results, obtained for propagation of optical pulse with a duration of 12 fs in the optical fiber, is shown in figure 1. Presented in the work simulation results demonstrate significant dependency of pulse distortion in birefringent fiber from beat length and input conditions.

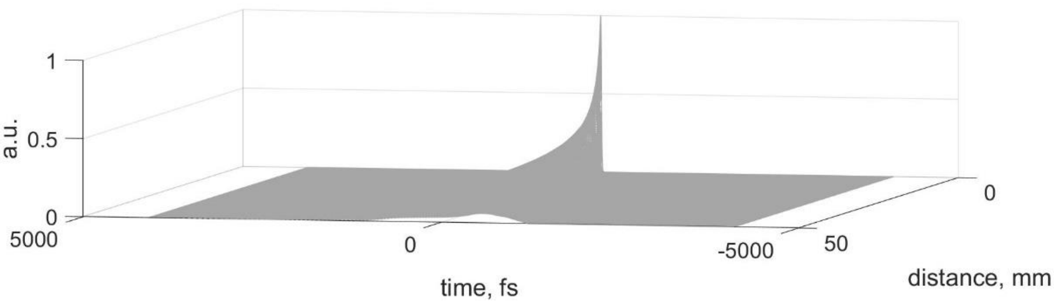

Fig. 1. Evolution of high-power femtosecond pulse over birefringent single mode optical fiber.

Reference

[1] R. Deiterding, R. Glowinski et al, *J. Lightwave Technology* **31(12)**, 2008-2017 (2013)
[2] B. R. Deiterding, S.W. Poole, arXiv:1504.01331 [math.NA] (2015)
[3] R. Deiterding, S.W. Poole, Splitting Methods in Communication, Imaging, Science, and Engineering. Scientific Computation. Springer, Cham (2016)
[4] V.A. Burdin, A.V. Bourdine, *Prikladnaya photonika* **6(1-2)**, 93-108 (2019)

Real-time pulse dynamics in bidirectional mode-locked fibre lasers

I. Kudelin[1], **S. Sugavanam**[1], **M. Chernysheva**[2,*]

[1] *Aston Institute of Photonic Technologies, Aston University*

[2] *Leibniz Institute of Photonic Technology*

[*] *E-mail: Maria.Chernysheva@leibniz-ipht.de*

Real-time observation of the emergence of coherent structures from noise via instabilities is of particular interest across disciplines ranging from biology to astrophysics. In the context of photonics, ultrafast fibre lasers provide an ideal test-bed for an experimental observation of dynamical instabilities and generation of coherent structures of ultrashort pulses.

The availability of real-time measurement techniques like spatio-temporal dynamics, time lenses [1], Dispersive Fourier Transform (DFT) [2] and others have enabled the observation of self-organisation of such coherent features [3] and their complexes [4], soliton interactions and soliton explosions [5]. Such real-time approaches also enable observation of build-up dynamics of various ultrashort pulses, *e.g.* employing DFT technique [3,6], which confirm the origination of ultrashort pulses from intensity fluctuations on the noise floor, shaped further via modulation instabilities [3] or Q-switched dynamics [7]. All this works substantially increase the knowledge of soliton behaviour and dynamics in nonlinear systems.

Bidirectional ultrafast fibre lasers present an attractive solution, enabling the generation of two mutually coherent ultrashort pulse trains in a simple and turnkey system [8]. Still, the lack of a comprehensive numerical model describing steady-state bidirectional generation, and even less ultrafast soliton breakdowns and collisions, is obstructing the achievement of the performance compared with unidirectional lasers.

In the current presentation, real-time build-up dynamics of counter-propagating solitons in ultrafast ring Er-doped fibre laser, recorded via the dispersive Fourier transform methodology, will be discussed [9]. Even though the counter-propagating pulses experience independent build-up dynamics from modulation instability, undergoing breathing dynamics, diverging sub-ordinate pulse structures formation and annihilation, and Q-swtuch instabilities, etc. to a stable bidirectional pulse train. Yet, the interaction of pulses in the cavity presents the key underlying phenomenon driving formation evolution distinct from unidirectional pulse build-up. These observations open up a great avenue towards versatile manipulation of the nonlinear soliton dynamics. Our findings will provide physical foundations for bidirectional ultrafast fibre laser design to carry forward their applications, including dual-comb spectroscopy and gyroscopy.

References

[1] J. Azaña, *Opt. Commun*. **217**, 205–209 (2003)
[2] K. Goda, B. Jalali, *Nat. Photonics* **7**,102 (2013)
[3] J. Peng,.et al. Commun. Phys.**1**, 20 (2018)
[4] X. Liu, X. Yao, Y. Cui, *Phys. Rev. Lett.* **121**, 023905 (2018)
[5] C. Lapre et al. *Sci. Reports* **9**, 1–12 (2019)
[6] P. Ryczkowski, et al. *Nat. Photonics* **12**, 221 (2018)
[7] X. Wang, et al. *Opt. Express* **27**,2747–2753 (2019)
[8] M. Chernysheva, S. Sugavanam, S. Turitsyn, *APL Photonics* **5**, 016104 (2020)
[9] I. Kudelin, S. Srikanth, M. Chernysheva, *Photonics Res.* **8** (6), 776-780 (2020)

On the coherence of dissipative soliton resonance square pulses

F. Sanchez[1,*], **M. Kemel**[1], **A. Nady**[1,2], **G. Semaan**[1], **M. Salhi**[1] **and A. Komarov**[3]

[1]*Laboratoire de Photonique d'Angers, Faculté des Sciences, 2 Bd Lavoisier, 49045 Angers Cedex*
[2]*Department of Physics, Faculty of Sciences, Beni-Suef University, 62511 Beni-Suef, Egypt*
[3]*Institute of Automation and Electrometry, SB RAS, Novosibirsk, Russia*

[*]*E-mail: francois.sanchez@univ-angers.fr*

Square-pulses in passively mode-locked fiber lasers are generally considered to be the manifestation of the dissipative soliton resonance (DSR). The DSR is a particular solution of the nonlinear propagation equation and it does not suffer from any wave-breaking as it was first predicted in [1,2]. Consequently both the energy and the width of the pulses increase linearly with the pumping power while the peak power remains clamped to a fixed value. In addition, the optical spectrum remains invariant versus the pumping power. Numerous experimental papers reported such kind of behavior and concluded that the observed pulses were real DSR pulses [3-5].

Another important characteristic of DSR pulses is that they exhibit square shape with a perfect temporal coherence. This characteristic is not easy to check because of the pulse duration in square-pulse regime which ranges from few to hundreds of nanoseconds [3-5]. In fact, the coherence measurement in square-pulse regime has been done only with ultra-short pulses in the ps range [3]. In such case it was demonstrated that the pulses were effectively coherent thus confirming that they were real DSR pulses.

In this communication we investigate the coherence of square-pulses in a passively mode-locked double-clad fiber laser and verify whether they operate in DSR regime or not. We demonstrate that although almost all the characteristics of DSR pulses are verified (energy and width scaling with pump power, peak power clamping, optical spectrum), the square-pulses are not temporally coherent thus demonstrating that square-pulses are not necessarily DSR pulses. Our conclusion is based on several series of experiment with distinct optical cavities operating in square-pulse regime in the nanosecond range. The experimental setups consist of two different methods of measurement. The first one is based on a Mach-Zehnder interferometer with a fixed delay which allows to scan a small part of a long square pulse. The second method is based on the Dispersive Fourier Transform (DFT) technique which allows to directly conclude on the pulse coherence.

References

[1] A. Komarov, H. Leblond and F. Sanchez, *Phys. Rev.* **A 71**, 053809 (2005).
[2] W. Chang, A. Ankiewicz et al, *Phys. Rev.* **A 78**, 023830 (2008).
[3] X. Wu, D. Y. Tang et al, *Opt. Express* **17**, 5580 (2009).
[4] K. Krzempek, *Opt. Express* **23**, 030651 (2015).
[5] G. Semaan, F. Ben Braham et al, *Opt. Lett.* **20**, 4767 (2016).

Features of passive mode-locking in a heavily-doped ytterbium fiber laser

A. M. Smirnov[1,2,*] **and O. V. Butov**[1]

[1]*Kotelnikov Institute of Radioengineering and Electronics of RAS, Moscow*
[2]*Faculty of Physics of Lomonosov Moscow State University, Moscow*
[*] *E-mail:*alsmir1988@mail.ru

We have investigated features of the all-fiber heavily doped ytterbium laser operating in passive mode-locked regime with a repetition rate of ultrashort pulses of 456 MHz without the use of additional nonlinear optical elements. The generation dynamics of the heavily-doped ytterbium fiber laser assembled according to the classical Fabry-Perot scheme with two mirrors under continuous direct core pumping at the 976 nm wavelength was studied. The formation of ultrashort pulses as a result of passive mode-locking was shown [1]. Passive mode-locking is explained by saturation of the absorption, while the role of the saturable absorber was played by the active fiber itself with a high content of ytterbium ions. The principle of the created laser operation is similar to lasers operating in the passive mode-locking regime with the use of saturable absorbers [2,3].

The laser was created using a fiber with a high ytterbium oxide content, with a relatively low concentration of large cluster, which made it possible to avoid a high level of "gray" losses in the active fiber [4] (plasma chemical method). The absorption coefficient at the wavelength of 976 nm was about 2.4 dB / mm (Fig. 1). The ytterbium content in the glass corresponding to the measured absorption coefficient was 0.84 mol.% Yb_2O_3 [5]. The difference in the refractive index of the core and shell was 0.009, the core diameter was about 4 microns. The laser was assembled according to the classical Fabry-Perot scheme with an output (0.9) and high reflective (0.999) mirrors in the form of fiber Bragg gratings (FBG) with a maximum reflection at a wavelength of 1067.7 nm. A polarization controller (PC) was used to control birefringence in the laser cavity.

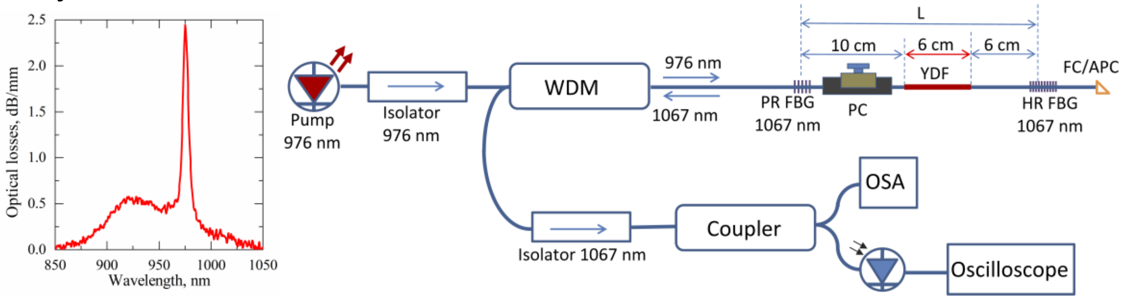

Fig. 1. Absorption spectrum of ytterbium doped fiber (left). Scheme of an experimental setup of an ytterbium fiber laser (right). OSA-optical spectrum analyzer, WDM-multiplexer, PC-polarization controller, L-resonator length

It is shown that depending on the pump power, the laser operates in three different regimes of passive mode-locking. At a low pump power (≈25-50 mW) a stable passive mode-locking regime (CW ML) was achieved, which is characterized by the stable in time ultrashort pulses amplitude (Fig.2a,b). The repetition rate of the ultrashort pulses for a 21.9 cm laser cavity was 456 MHz. The period of the pulses in the train coincides with the time of the cavity pass, which is consistent with the generally accepted theory of passive mode-locking [6]: $\Delta t=2nL/c$ (where L is the length of the cavity, n is the refractive index, and *c* is the speed of light). The observed passive mode-locking in the scheme under consideration can be explained by nonlinear absorption in the active fiber itself, which works similarly to saturable absorbers. The effect occurs on a weakly pumped section of the fiber, in which the population inversion and consequently the absorption level depends on the intensity of the stimulated emission in the cavity.

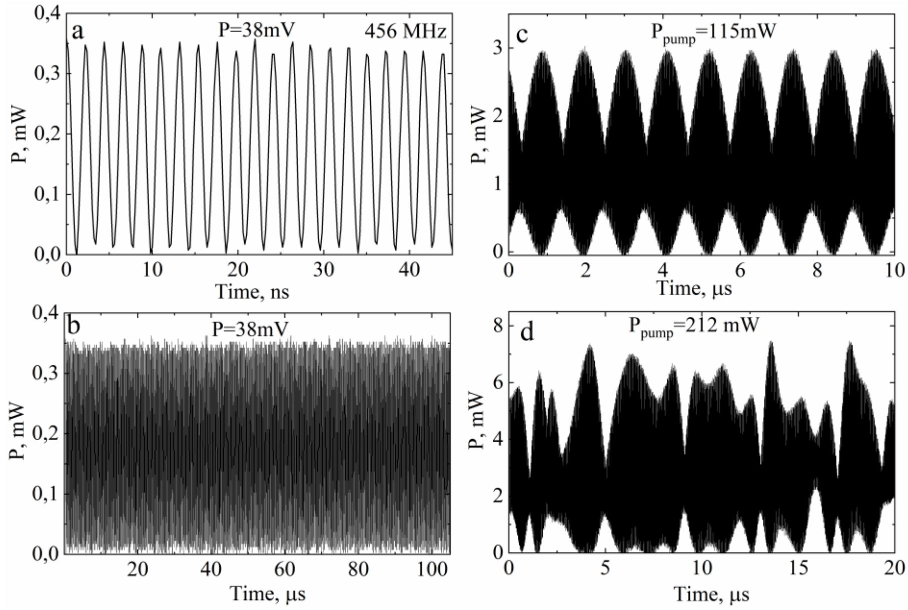

Fig. 2. Ytterbium laser generation power as a function of time at a pump power of 38 mW (stable passive mode-locking regime) at 40 nanosecond (a) and 100 microsecond scale (b), at a pump power of 115 mW (c) (beat mode) and at a pump power of 212 mW (d) (transient chaotic beat mode).

With pump power increase to ≈50-200 mW low-frequency beats occurred in the form of amplitude modulation of the generation intensity envelope (Fig.2c). The detected beats were explained by the dynamics of the elliptically polarized pulse train formation with rotating polarization components for group-velocity-locked vector solitons, which are also called polarization rotation vector solitons (PRVSs) [7]. With a further increase in the pump power (≈200-310 mW), transient chaotic beats (TC ML) appeared (Fig. 2d).

References

[1] A.M. Smirnov, O.V.Butov, *Optics Letters* **44**, 5065-5068 (2019)
[2] U. Keller, *Nature* **424**, 831-838 (2003)
[3] A. J. DeMaria, D. A. Stetser, H. Heynau, *Appl. Phys. Lett*. **8**, 174-176 (1966)
[4] K. Golant, *Proceedings of XXI International Congress on Glass*, L13 (2007)
[5] A.A. Rybaltovsky, O.V. Butov, *et al*, *Tech. Phys. Lett.* **42**, 498–500 (2016)
[6] P.G. Kryukov, *Quantum Electronics* **31**, 95-119 (2001)
[7] B.C. Collings, S.T. Cundiff, *et al*, *JOSA B* **17**, 354-365 (2000)
[8] I. Hartl, X.D. Li, C. Chudoba *Opt. Lett.* **26**, 608-610 (2001)
[9] O. Boyraz, J. Kim et al, *J. Lightwave Technology* **18**, 2167-2175 (2000)

Dissipative solitons with controllable duration of sub-pulses

A. V. Ivanenko[1,*], B. N. Nyushkov[1,2], S. V. Smirnov[1], D. B. Lutsenko[1], M. G. Dyatlov[1], S. M. Kobtsev[1]

[1]*Novosibirsk State University*
[2]*Novosibirsk State Technical University*
[*]*E-mail: ivanenko.aleksey@gmail.com*

Dissipative solitons featuring unique spatio-temporal structure of their electromagnetic field are generated in many mode-locked fibre lasers, and especially in fibre lasers with relatively long cavities [1–3]. The attention drawn to such clustered femtosecond or picosecond pulses (sometimes referred to as double-scale or noise-like pulses) stems from their ability to carry record-high energies and average powers directly from fibre-optical master oscillators [4–5] without any subsequent amplification, as well as to exhibit fairly high efficiency of non-linear optical conversion [6–8]. However, controlling parameters of such pulses — shape and duration of their envelope, parameters of sub-pulse filling — is a complicated task because of non-trivial stochastic structure of the intra-pulse electro-magnetic field. Earlier, works [9, 10] demonstrated the possibility of controlling the degree of coherence of such pulsed wave clusters and the effect of their coherence degree on the efficiency of non-linear optical conversion.

This work for the first time presents a study of how the width of an intra-cavity spectral filter affects the structure of double-scale pulses. It is shown that in an actively mode-locked laser, broader spectral filtering leads to shorter duration of sub-structures inside double-scale pulses without at the same time affecting the pulse envelope duration. For the first time demonstrated is control over the average sub-pulse duration (between 1.4 ps and 170 fs) *via* spectral selection.

The influence of spectral filtration was studied in an ultra-long all-fibre laser actively mode-locked by synchronous pumping at the frequency equal to that of the cavity round trip. The studied configuration of the fibre laser is schematically given in Fig. 1.

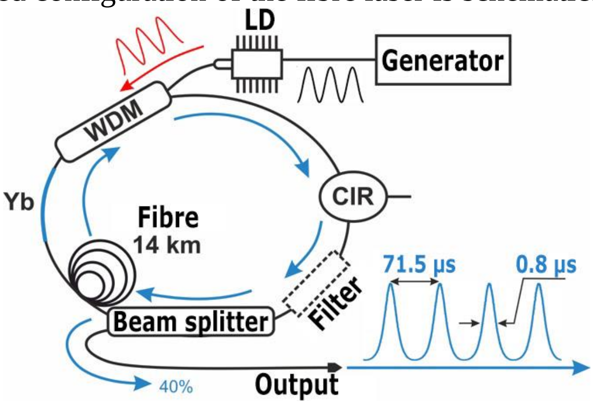

Fig. 1. Fibre laser configuration. LD – laser diode pump, WDM – wavelength division multiplexor for combining the pump and generation waves, Yb – active fibre doped with ytterbium ions.

When the modulation frequency of the pumping laser diode was set to the fundamental cavity round trip frequency the laser generated pulses with the envelope duration of 800 ns.

The studied laser allowed exchanging optical filters. The effect of spectral filtration was estimated from the duration of the central peak of the output auto-correlation function (ACF) corresponding to the average sub-pulse duration. The peak in the centre of the ACF results from beating between various spectral components (superposition of unrelated or weakly related in phase oscillations) present in generation and forming the stochastic sub-pulse filling [11]. Thus, the duration of this central peak is inversely proportional to the width of the generated spectrum and spectral filtration leads to narrower spectrum implying longer sub-pulses.

Depending of the width of the installed filter or its absence, the ACF duration varied from 1.4 ps to 170 fs (Fig. 2). At the same time, the overall duration of the pulse envelope always remained at 800 ns.

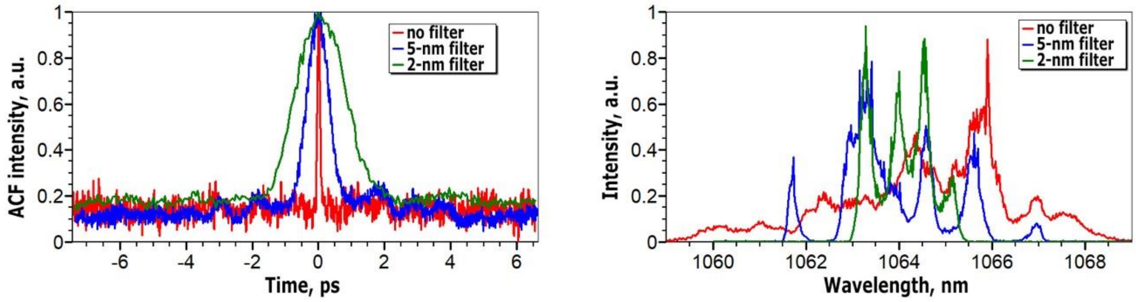

Fig. 2. The central parts of auto-correlation functions and combined optical spectra of double-scale pulses measured at different widths of intra-cavity band-pass filter (central wavelength of the pulse spectrum without filtering is 1030 nm).

The measured results agree well with the model proposed in [11]. As the filter width is broadened by a factor of 2.5 (from 2 nm to 5 nm), that model predicts a reduction of the typical oscillation time (duration of sub-pulses) by the same factor of 2.5, from 1.7 ps down to 680 fs. In our experiment the corresponding figure was 700 fs. The experimental results are in good agreement with the theoretical predictions.

The proposed method creates new possibilities of control over double-scale pulses and their application in various fields of science and technology.

This work was supported by the Russian Foundation for Basic Research (18-32-20021) and by the Ministry of Sciences and Higher Education of the Russian Federation (FSUS-2020-0036).

References

[1] Smirnov S., et al., *Optics express* **20.24**, 27447–27453 (2012).
[2] Kobtsev S., et al., *Optics Express* **17.23**, 20707–20713 (2009).
[3] Pan, Ci-Ling, et al, *InTech*, 2016.
[4] Ivanenko A. et al., *Optics express* **24**.6, 6650–6655 (2016).
[5] Fedotov, Y. S., et al., *Optics express* **22.25,** 31379–31386 (2014).
[6] Smirnov S. et al., *Optics Express* **22.1**, 1058–1064 (2014).
[7] Kobtsev S, et al., *Optics express* **22.17**, 20770–20775 (2014).
[8] Xia H., et al., *Applied optics* **54.32,** 9379–9384 (2015).
[9] S. Kobtsev, et al., *Laser Phys. Lett*., **v. 15, No. 4**, 045102 (2018).
[10] S. Kobtsev, et al., *Proc. SPIE*, **v. 10902**, 109021F (2019).
[11] S. Kobtsev, et al., Chapter 4 in book “Fiber Laser” (ed. M. C. Paul), p. 69–88, InTech, 2016, ISBN: 978-953-51-4615-5.

Investigation of the temperature influence on the mode locked regime of the fiber resonator with dispersion Fourier transformation method

K. Serebrennikov*, I. Petenev, A. Kokhanovskiy

Novosibirsk state university, Novosibirsk
**E-mail: kospi198@gmail.com*

Mode-locked fiber lasers based on the effect of nonlinear polarization rotation (NPR) are widely used in scientific laboratories as sources of ultrashort pulses [1]. A relatively simple implementation of a fiber laser resonator makes it possible to obtain a source of optical pulses with a duration of the femtosecond range. Unfortunately, the stability of the pulsed radiation of NPR-lasers is strongly influenced by the environment, which limits their use outside scientific laboratories.

A new wave of interest in NPR-lasers from the scientific community is associated with the development of machine learning algorithms that make it possible to effectively control the elements of a laser cavity to stabilize and optimize the parameters of pulsed radiation [2]. The key element of the laser system under the control of the machine learning algorithm is the feedback system, which determines the effect of the control elements on the parameters of the optical pulses.

To measure the stability of the operation of a fiber laser commonly devices are used that average the parameters of the output pulses, which leads to the loss of information of inter-pulse fluctuations. The ability to measure fluctuations of parameters from pulse to pulse will allow the development of laser-adaptive systems with an increased level of stability. The most attractive technique for solving this problem is dispersive Fourier transformation (DFT) of optical pulses, makes it possible to measure the optical spectrum of a single pulse [3].

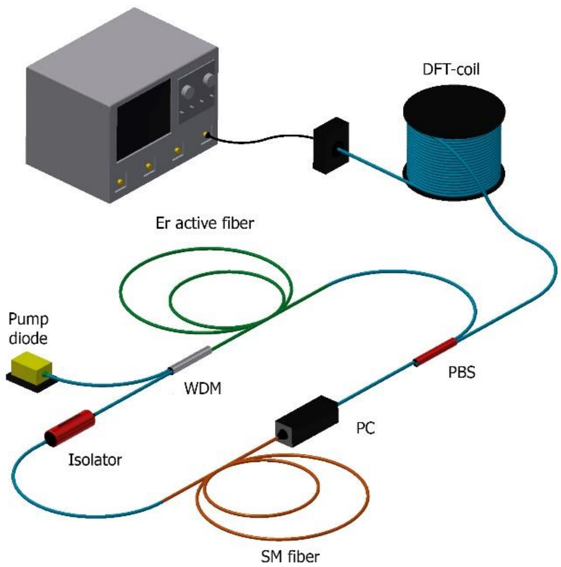

Fig.1. Experimental setup.

In this work, a fiber laser was investigated (Figure 1). An Er - doped fiber (80 cm) was used as an amplifying medium. Pumping is carried out by a laser diode at a wavelength of 980 nm via WDM.

The fiber laser cavity was placed on a heating plate that controlled the temperature of the laser cavity. In the mode of stable pulsed generation at a temperature of 30 ºC, DFT - spectra of optical pulses were measured successively with an increase in the cavity temperature to 41 ºC. (Figure 2) shows the most remarkable pulsed regimes that were established during heating.

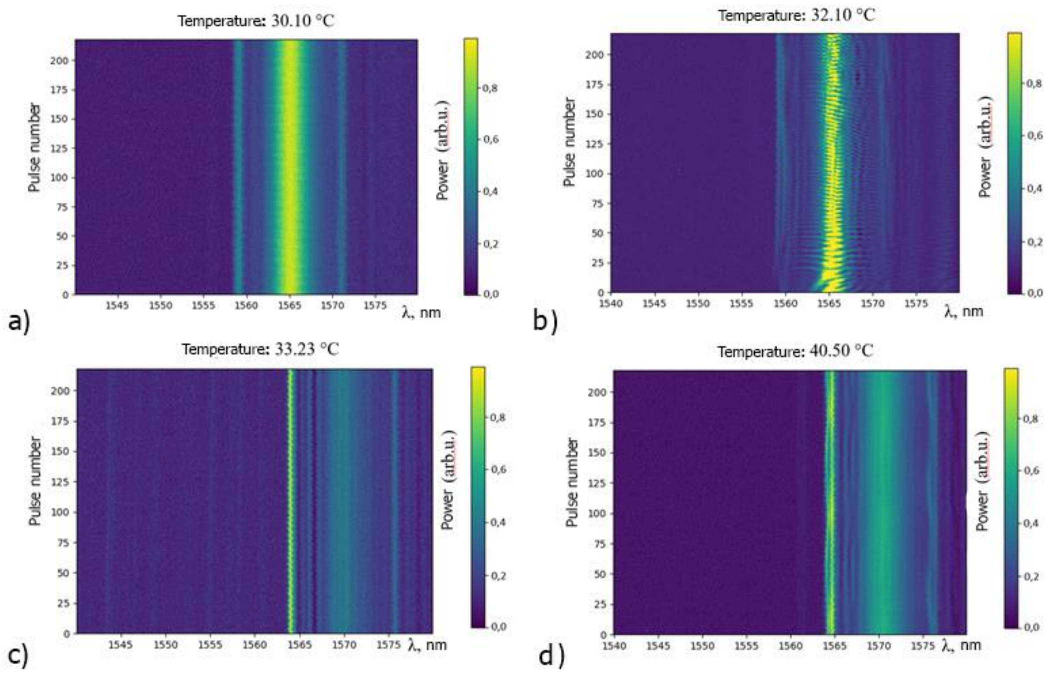

Fig.2. DFT - spectra of pulses versus the temperature of the laser cavity.

To determine the degree of fluctuation of the optical spectrum, the standard deviation of the error between the difference in the optical spectrum of the i-th and first pulses was calculated. The smallest standard deviation for the pulsed mode at 30.10 °C – 30e-3, the largest for the pulsed generation at a temperature of 40.50 °C – 112e-3 (Figure 2 a) and d)). In addition to fluctuations in the optical spectrum, the DFT technique allows one to determine the energy fluctuation from pulse to pulse. When the cavity was heated, the pulse energy varied in the range 1.2 - 2.6 pJ, and the pulse energy spread was from 0.1 - 0.4 pJ.

The results obtained demonstrate that the technique of measuring the dispersive Fourier transform of optical pulses makes it possible to determine the interpulse fluctuations of the energy and optical spectrum under temperature changes in the laser cavity.

This work was supported by the Russian Science Foundation (project No. (17-72-30006)).

REFERENCES

[1] G.P. Agrawal, Nonlinear fiber optics, 4th ed. Academic press, 2007, 539 c.
[2] U.Andral, et al, JOSA B, 33(5), 825 – 833 (2016)
[3] K.Goda, et al, Nat. Photonics, 7, 102 - 112 (2013)

Nonlinear conversion of fiber laser radiation: SRS, SBS, parametric generation, harmonics generation, generation of THz radiation

Wavelength-agile fiber amplifiers for quantum technology

Y. Feng

Shanghai Institute of Optics and Fine Mechanics, CAS, Shanghai, China

E-mail: feng@siom.ac.cn

The progress of quantum science in laboratory has led to advanced technologies which will impact our everyday life. The development of quantum technologies such as computing, communication, sensing and imaging has become greatly attractive even for private sectors. Lasers are key tools in quantum science and technology. For example, high power single frequency lasers at various wavelengths, usually not easy to obtain, are required in laser cooling of atoms, optical standards, precision measurement etc.

In this talk, we discuss the advantage of fiber amplifiers for quantum technology application, which includes power scalability, robustness, and high beam quality, etc. We report our progress in developing high power low noise single frequency Yb, Er, and Raman fiber amplifiers for various quantum applications, usually including frequency doubling to visible and ultraviolet regime. High power single-frequency single-mode linearly-polarized Yb fiber amplifiers were developed for optical lattice generation, cooling of Hg atoms, and cesium Rydberg atoms [1-3]. High power single-frequency single-mode linearly-polarized Raman fiber amplifiers at various wavelengths were developed for different applications in atomic physics study [4-5]. And high power single-frequency single-mode linearly-polarized Er fiber amplifiers at 1560 nm was developed for atom interferometer with Rb atoms after frequency doubling to 780 nm [6]. Technical challenges in wavelength tuning, power scaling stimulated Brillouin scattering suppression, amplified spontaneous emission suppression, and second harmonic generation will be presented.

References

[1] L. Zhang, S. Cui et al, *Opt. Express* **21**, 5456-5462 (2013)
[2] J. Hu, L. Zhang et al, *Opt. Express* **21**, 30958-30963 (2013)
[3] J. Qian, L. Zhang et al, *Appl. Opt.* **57**, 8733 (2018)
[4] X. Yang, L. Zhang et al, *Opt. Lett.* **42**, 4351-4354 (2017)
[5] L. Zhang, H. Jiang et al, *J. Light. Technol.* **34**, 4907–4911 (2016)
[6] J. Dong, X. Zeng et al, *Opt. Express* **27**, 35362 (2019)

Stabilizing Brillouin Fiber Lasers

A.A. Fotiadi[1,2,3,*], V.V. Spirin[4], J.L. Bueno-Escobedo[4], P. Mégret[2], D.A. Korobko[1], I.O. Zolotovskii[1]

[1]*Ulyanovsk State University, Ulyanovsk, Russian Federation*
[2]*University of Mons, Mons, Belgium*
[3]*Ioffe Physico-Technical Institute of the RAS, St. Petersburg, Russian Federation*
[4]Scientific *Research and Advanced Studies Center of Ensenada (CICESE), México*

[*]*E-mail: Andrei.Fotiadi@gmail.com*

Low-noise lasers are a revolutionary tool in precision spectroscopy, displacement measurements, and the development of advanced optical atomic clocks. Further applications include lidars, coherent communications, frequency synthesis, and precision sensors of strain, motion, and temperature. While all applications benefit from lower frequency noise and robust laser design, some of them also require a simple laser configuration generating two locked frequencies. Recently, we have demonstrated a kHz-linewidth laser just combining a standard DFB laser diode and a few passive telecommunication components [1]. The principle of operation employs the mechanism of self-injection locking that could significantly improve the DFB laser performance. While a typical linewidth of free-running DFB semiconductor lasers ranges from a few to tens MHz, self-injection locking of the DFB laser through an external fiber ring cavity causes a drastic reduction of the laser linewidth down to a few kHz making it attractive for a new range of applications.

In such a laser configuration, the same external fiber cavity can be used for self-injection locking of the DFB laser and as Brillouin scattering media to generate the Stokes shifted optical wave. It is worth noting that other teams have already used the fiber ring cavity to generate Brillouin wave from an external laser diode [2]. However, they always face the problem of coupling between the DFB laser and the ring fiber cavity that is, in general, technically complicated and cost-consuming tasks. In our approach, the implementation of the self-injection locking mechanism in the Brillouin fiber laser configuration allows to maintain natural coupling between the DFB laser and the external fiber cavity enabling dual-frequency laser operation. However, a stable generation of two frequencies by the self-injection locked DFB laser has not been achieved yet, making it unavailable for many prosperous applications [3].

Several approaches have been performed to stabilize the laser operation in the self-injection locking regime. The main drawback of this technique is its high sensitivity to fluctuations of the configuration parameters and surroundings. Once getting locked to the cavity resonance, the laser starts to generate the cavity resonant frequency. Then any slow change of the ring mode frequency (due to environment temperature fluctuations, for example) near the stability point causes the same change of the laser frequency. However, a more extended drift of the cavity mode frequency (>10 MHz) causes mode-hopping making laser operation temporally unstable. As a result, a stable laser operation is commonly observed for a few seconds. With precise stabilization of the laser diode current and temperature used in conjugation with the thermal stabilization of the whole fiber configuration the periods of laser stability could be extended to tens of minutes and even more. However, such stabilization method is technically complicated and cost-consuming. The use of polarization maintaining fibers improves to some extent the laser stability preventing polarization mode-hopping [4].

Alternatively, stabilization of semiconductor DFB laser in self-injection locking regime could be achieved by implementing an active optoelectronic feedback controlled by a low-cost USB-DAQ card [5]. In this approach, the narrowing of DFB laser linewidth is still provided by self-injection locking, whereas the active feedback is used only to maintain the laser operation in this regime. Therefore, in terms of feedback circuit bandwidth, complexity, and allocated memory, this solution is much less consuming than optoelectronic systems commonly used with fiber lasers.

Here, we introduce a simple dual-frequency laser [Fig.1, a] leveraging a ring fiber cavity that exploits one ring cavity mode for self-injection locking of a standard semiconductor DFB laser to generate light at pump frequency and another cavity mode to generate Stokes light via stimulated Brillouin scattering. In contrast to the previous laser configurations [3], the system is supplied with a low-bandwidth active optoelectronic feedback helping to maintain the regime of self-injection locking that in its turn takes charge of stable operation of two mutually locked pump and Stokes frequencies [Fig.1, b]. This configuration reduces the natural Lorentzian linewidth of the light emitted by the laser at pump and Stokes frequencies down to 400 Hz and 300 Hz, respectively, and features a stable 300-Hz-width RF spectrum of beating between two laser outputs [Fig.1, c]. Specifically, the laser cavity is spliced from standard SMF-28 components, has no thermal control of the fiber configuration, and employs a DFB laser diode powered by a standard driver. In future, translating the proposed laser design to integrated photonics will dramatically reduce cost and footprint for many applications such as ultra-high capacity fiber and data center networks, atomic clocks, and microwave photonics.

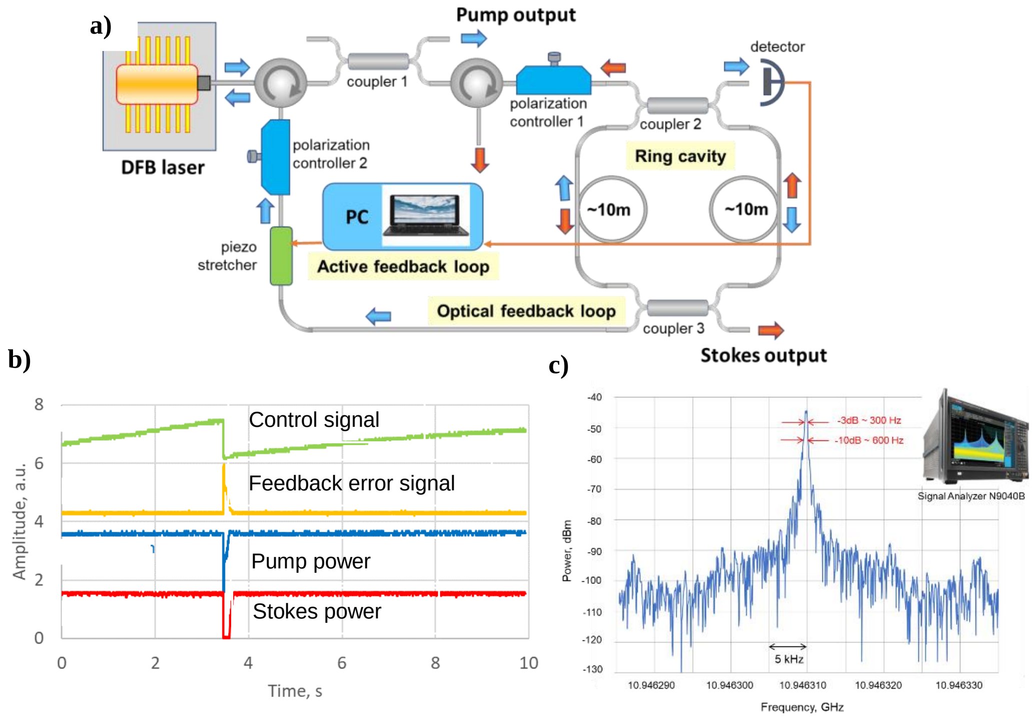

Fig. 1. Dual-frequency laser: experimental setup (a), output powers and operation of optical and electronic feedbacks against a knock on the fiber cavity (b), RF spectrum of beating between two frequencies.

The work is supported by the Russian Science Foundation (grant № 18-12-00457).

References

[1] C. A. López-Mercado et al., *Optics Communications* **359**, 195-199 (2016).
[2] L. Rossi et al., *Opt. Express* **27**, 29448-29459 (2019).
[3] V. V. Spirin et al., *Laser Physics Letters* **10**, 015102 (2013).
[4] J. L. Bueno Escobedo et al., *Results in Physics* **12**, 1840-1842 (2019).
[5] V. V. Spirin et al., *Opt. Express* **28**, 478-484 (2020).

Spatiotemporal Mode-Locking in a Fiber Laser

Vladimir L. Kalashnikov[1,*] **and Stefan Wabnitz**[1,2]

[1]*Dipartimento di Ingegneria dell'Informazione, Elettronica e Telecomunicazioni, Sapienza Universit`a di Roma, via Eudossiana 18, 00184 Rome, Italy*

[2]*Novosibirsk State University, Pirogova 1, Novosibirsk 630090, Russia*

[*]*E-mail: vladimir.kalashnikov@uniroma1.it*

The endeavor of multidimensional soliton generation in nonlinear optics (so-called "light bullets") and liquid crystals, Bose-Einstein condensates, etc., has a long history[1-4]. Such coherent and strongly localized structures could provide unprecedented energy (or mass) condensation, bridging across micro- and macro-scaled phenomena. The study of multidimensional solitons introduces a new branch of "mesoscopic" physics, permitting the study of a broad area of nonlinear phenomena far from thermodynamic equilibrium.

We introduce a spatiotemporal mode-locking mechanism in a fiber (or waveguide) laser, based on nonlinear mode-cleaning enhanced by graded dissipation. Our analysis is based on the generalized dissipative Gross-Pitaevskii equation, which has a broad impact on nonlinear physics, including nonlinear optics and Bose-Einstein condensates. We demonstrate that careful control of dissipative and non-dissipative physical mechanisms results in the self-emergence of stable (2+1)-dimensional dissipative solitons. Achieving such a regime does not require any additional mode-locking mechanisms, and allows for stable energy (or "mass") harvesting by coherent localized structures, such as ultrashort laser pulses or Bose-Einstein condensates.

We anticipate that the nonlinear coupling of spatial modes in either graded-index or photonic-crystal fibers, supported by the presence of graded dissipation, could implement the concept of the distributed Kerr-lens mode-locking[5] in a fiber laser in the regime of multimode self-cleaning. That would provide a means to achieve highly-efficient and stable energy harvesting in an all-fiber laser, without the need of using any additional mode-locking mechanisms. In a broader context, we envisage that photonic devices could provide an efficient tool for metaphorical or analog modeling of strongly localized coherent (or partially coherent) structures, which spontaneously emerge in nonlinear nonequilibrium dissipative systems. In particular, these systems represent a classical analog of a Bose-Einstein condensate in the weakly-dissipative limit.

Acknowledgments

This work has received funding from the European Union Horizon 2020 research and innovation program under the Marie Sklodowska-Curie grant No. 713694 (MULTIPLY), the ERC Advanced Grant No. 740355 (STEMS), and the Russian Ministry of Science and Education Grant No. 14.Y26.31.0017.

References

[1] B. A. Malomed, *Eur. Phys. J. Special Topics* **225**, 2507–2532 (2016)
[2] Y. V. Kartashov et al, *Nature Reviews* **1**,185–197 (2019)
[3] K. Krupa et al, *APL Photonics* **4**,110901 (2019)
[4] V. N. Serkin, T. L. Belyaeva, *Optik* **176** ,38–48 (2019)
[5] J. Zhang et al, *Advanced Solid State Lasers Conference, OSA Technical Digest*, ATh4A.7 (2015)

Mode decomposition of laser beam propagated in a multimode fiber in the Kerr self-cleaning regime

M.D. Gervaziev[1,2,*], D.S. Kharenko[1,2], I. Zhdanov[1,2], V.A. Gonta[1,2], E.V. Podivilov[1,2], S.A. Babin[1,2], S. Wabnitz[1,3]

[1]*Novosibirsk State University*
[2]*Institute of Automation and Electrometry of the Siberian Branch of the RAS*
[3]*DIET, Sapienza University of Rome, Italy*
[*]*E-mail: gervaziev.m@gmail.com*

For a long time multimode (MM) fibers have remained unclaimed due to poor beam quality. Usually, the beam quality is inversely proportional to the number of excited modes. However, an intensive research of nonlinear effects of high-power laser beam propagation in MM graded-index (GRIN) fiber has led to the discovery of some unexpected phenomena, such as Kerr self-cleaning of the beam [1] and generation of a supercontinuum width high peak power pulses [2]. The self-cleaning mechanism is that most of the beam energy flows into the fundamental mode. This process is accompanied by redistribution of energy towards higher-order modes. An increase in the energy of the fundamental mode leads to an improvement of the beam quality. The standard way to determine beam quality is to measure the M^2-parameter (m-squared). In fact, beam rate of divergence from the Gaussian is measured. But, since self-cleaning is a nonlinear redistribution of energy carried by a large number of fiber modes, this approach is not entirely correct, and the mode decomposition of the output beam seems to be a much more informative method.

Mode decomposition is a beam analysis technique that measures the amplitudes and relative phases of the modes that the beam consists of. Existing decomposition methods are based on genetic algorithms [3], adaptive optics [4], or phase modulation [5]. The last option can be realized using a spatial light modulator (SLM). An SLM is a device that superimposes a certain form of spatial modulation (amplitude, phase, or amplitude and phase simultaneously) on the beam, and usually controlled by a computer. Existing works on mode decomposition included the analysis of the output beam from MM fibers with small number of guided modes. Our goal was to make the method suitable for GRIN fibers with a large number of modes.

The experimental setup is shown in Figure 1. Using the property of orthonormalization of fiber modes, the Jacobi-Anger expansion and the Fourier transform theorems, phase masks were formed in a such way that the center of the first diffraction order contains information about the mode amplitude or its relative phase (in relation to some mode, usually fundamental) [5]. In this work, a numerical simulation of the decomposition process for a randomly generated beam was made. The result is that the amplitudes and phases were measured with an accuracy of 10^{-7}, and the reconstructed beam was almost indistinguishable from the original one. The sampling was added in order to compare the results for 10-bit and 8-bit modulators numerically. Calculations have shown that the difference in sampling did not significantly affect the accuracy of measuring the amplitudes (~ 10^{-4}). In the case of measuring the phases, the difference is more significant, but still not critical (accuracy 10^{-3} for 10 bits, and 10^{-3} for 8 bits).

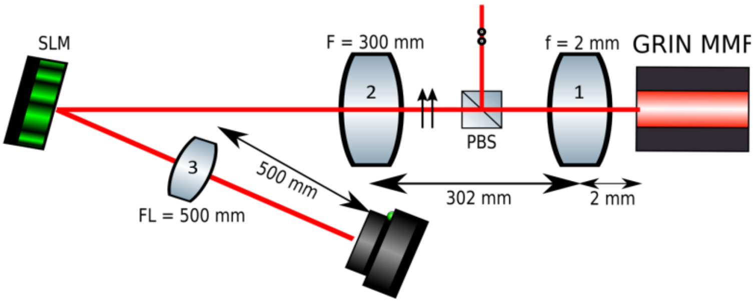

Fig. 1. Experimental setup. Lenses 1 and 2 transfer the near field distribution (from the output of the fiber) to the modulator. Lens 3 performs the Fourier transform from the modulated field (forms the far field image).

The influence of the phase mask resolution on the decomposition results was checked. We compared masks with a fundamental mode radius of 120, 90, 60 and 30 pixels. It was found that with decreasing resolution, an especially strong increase in the error occurs at a mode radius of 30 pixels (Fig. 2 (a, b)). In this case, the shape of the reconstructed beam differs slightly from the original one (Fig. 2 (c)).

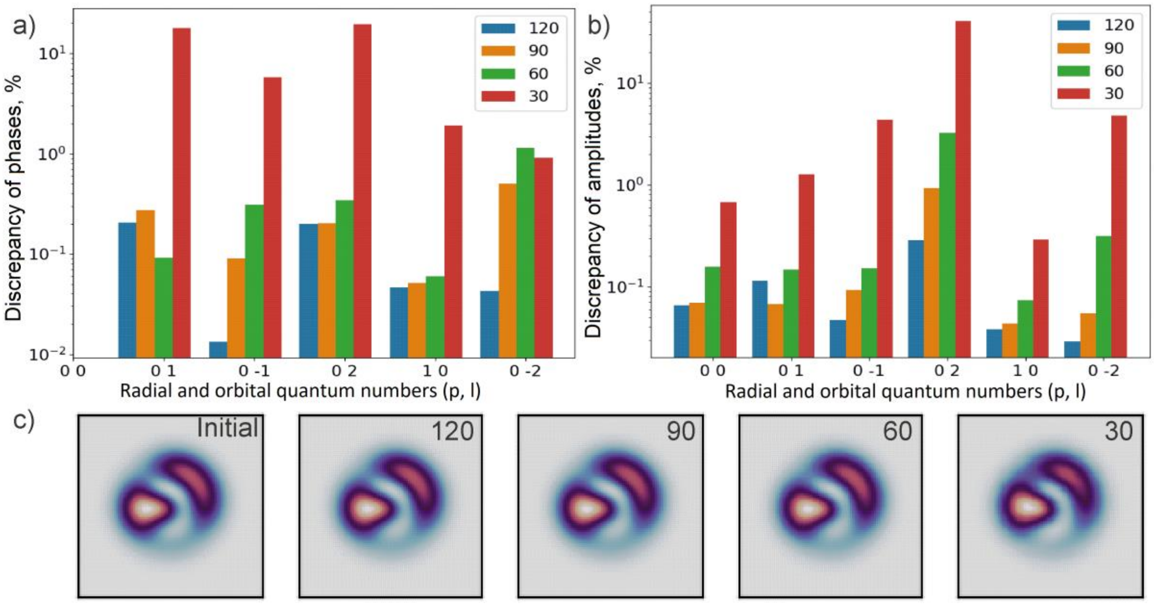

Рис. 2. a) Discrepancy of phases (logarithmic scale), calculated in the process of the decomposition simulation; b) The discrepancy of the amplitudes (logarithmic scale), calculated in the process of the decomposition simulation; c) From left to right - the original beam; a beam reconstructed as a result of decomposition with a fundamental mode size of 120 pixels; 90 pixels; 60 pixels; 30 pixels;

This work was supported by the Ministry of Science and Higher Education of the Russian Federation (14.Y26.31.0017).

References

[1] K. Krupa, A. Tonello, et al. *Nat. Photonics* **11**, 237-241 (2017).
[2] G. Lopez-Galmiche, Z. S. Eznaveh, et al. *Opt. Lett.* **41**, 2553 (2016).
[3] L. Li, J. Leng, et al. *Opt. Express* **25**, 19680 (2017).
[4] C. Schulze, D. Naidoo, et al. *Opt. Express* **20**, 19714 (2012).
[5] D. Flamm, D. Naidoo, et al. *Opt. Letters* **37**, 2478 (2012).

Raman laser based on a 7-core fiber with cross-coupling between the cores

A.V. Dostovalov[1,*], M.I. Skvortsov[1], A.A. Wolf[1], V.I. Labuntsov[1,2], O.N. Egorova[3], S.L. Semenov[4], S.A. Babin[1,2]

[1]*Institute of Automation and Electrometry of the SB RAS, Novosibirsk*
[2]*Novosibirsk State University, Novosibirsk*
[3]*Prokhorov General Physics Institute of the RAS, Moscow*
[4]*Dianov Fiber Optics Research Center, Prokhorov General Physics Institute of the RAS, Moscow*
**E-mail:* alexdost@gmail.com

Raman lasers based on multicore fibers (MCFs) with cross-coupling between the cores are promising high-power sources, since the power density in this type of lasers decreases as compared with single-core lasers, leading to a decrease in nonlinear effects inside the laser cavity. For example, in [1], a Raman fiber laser based on a polarization- maintaining (PM) twin-core fiber (TCF) with random distributed feedback was presented. In this case, a fiber loop mirror based on a 50/50 PM coupler at 1064 nm is used to form a half-open cavity. The linewidth of this laser was found to be about 5 times narrower than the linewidth of a random Raman laser in a similar configuration based on a single-core fiber. It was shown that the narrowing of the lasing line is due to weakening of nonlinear effects and spectral-selective properties of a TCF. The femtosecond point-by-point technique [2], which allows writing fiber Bragg gratings (FBGs) in selected cores with high positioning accuracy, was used in [3, 4] to form different cavity configurations of a Raman laser based on TCF. Thus, in [3], a scheme with point reflectors was demonstrated, where the laser cavity was formed by highly reflective FBG selectively inscribed in a single core and a right angle cleavage or a weakly reflecting FBG at the output end of the laser. In [4], a method of additional spectral filtering is presented due to the writing of two highly reflective FBGs in different cores at the cavity input, which are displaced relative to each other in the longitudinal direction, thereby forming a Michelson interferometer. Compared with [1], it was shown that the use of FBGs in TCF Raman laser cavity improve the stability of the laser power characteristics and provide the narrow linewidth.

In this work, we demonstrate a Raman fiber laser configuration based on a 7-core fiber (Fig.1a) and point reflectors consisting of highly reflective FBGs. Core-selective inscription of FBGs was carried out using the femtosecond point-by-point technique in the peripheral cores at the input and output of the laser cavity. The effective reflection coefficient of the FBG array for each side of the cavity is estimated to be ≈80%. To reduce the effect of nonresonant losses, single-mode fiber guiding the pump signal was spliced to the central core. The lasing threshold was reached at a pump power of ≈3 W, while the maximum lasing linewidth at an output power of ≈2.5 W was less than 350 pm (Fig. 1b).

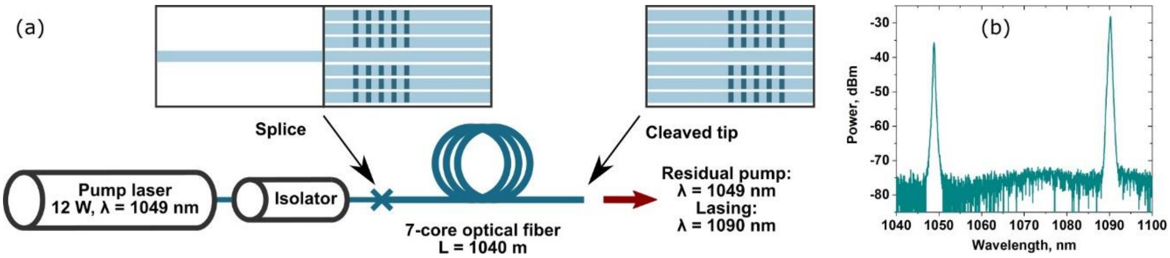

Figure: 1. (a) Experimental setup of a Raman fiber laser based on a 7-core fiber. (b) Spectrum of pump (≈ 1049 nm) and Stokes lasing (≈ 1090 nm)

Since highly reflective FBGs at the Stokes wavelength were inscribed only in the peripheral cores, the maximum Raman power was observed for the central core. Thus, the use of the femtosecond laser for writing FBGs in the selected cores makes it possible to set the spatial distribution of the transverse modes for a Raman fiber laser based on an MCF. An increase in the effective area of transverse modes, as well as the spectral-selective properties of MCF provide the possibility to create high-power Raman fiber lasers with a narrow linewidth.

In the report, we are going to discuss the specifics of the lasing regimes of this type of Raman fiber laser, as well as its spectral and power characteristics.

This work was supported by the Russian Foundation for Basic Research (project 20-32-70132).

References

[1] A. E. Budarnykh, I. A. Lobach et al, *Opt. Lett.* **43**, 567-570 (2018)
[2] A.V. Dostovalov, A.A. Wolf et al, *Opt. Exp.* **24**, 16232-16237 (2016)
[3] M.I. Skvortsov, S.R. Abdullina et al, *Quant. Elect.* **48**, 1089 (2018)
[4] M.I. Skvortsov, S.R. Abdullina et al, *Opt. Lett.* **44**, 295-298 (2019)

Prospects of generation of terahertz radiation in borate nonlinear crystals

N.A. Nikolaev[1] , A.A. Mamrashev[1,*], V.D. Antsygin[1], G.V. Lanskii[2], Yu.M. Andreev[2,3]

[1]*Institute of Automation and Electrometry SB RAS*
[2]*Institute of Monitoring of Climatic and Ecological Systems SB RAS*
[3]*Tomsk State University*
[*]*E-mail: mamrashev@iae.nsk.su*

Crystals of the borate family are widely used in various areas of nonlinear optics owing to their advantages such as relatively large effective nonlinear coefficient, wide spectral transparency range, high damage threshold, etc. [1]. Typical representatives of this family of crystals are barium beta-borate (β-BaB_2O_4, BBO), lithium triborate (LiB_3O_5, LBO), and bismuth triborate (BiB_3O_6, BIBO).

Recently, researchers started to show interest in using these materials in the terahertz (THz) spectral range. Terahertz optical properties (refractive index and absorption coefficient) of the crystals were measured at room and liquid nitrogen temperatures [2-4]. This work considers prospects of nonlinear conversion of fiber laser radiation (at the wavelengths of 1 μm and 1.5 μm) into terahertz radiation by the difference frequency generation (DFG). The most promising is the conversion into sub-THz (or millimeter) radiation due to the longer coherence length and low absorption of the phonon modes. This range is relevant for the new generation of telecommunication systems, including 6G. As an example, Fig. 1 shows the calculated collinear phase matching curves for the DFG process in BBO crystal and the comparison of its absorption coefficient with other borates in the THz region.

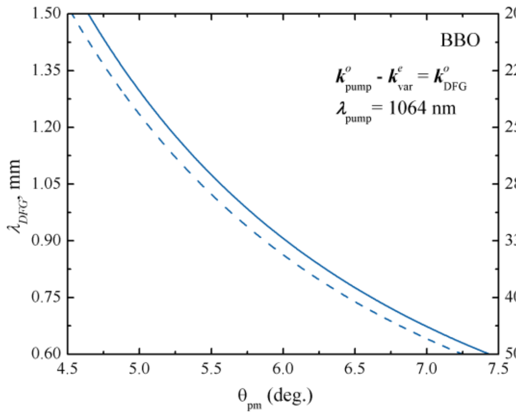

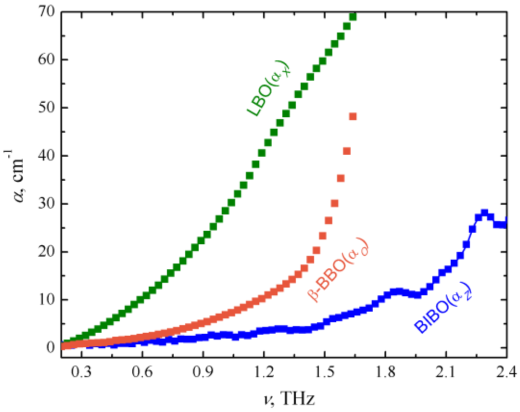

Fig. 1. DFG phase matching curves in BBO crystal pumped at the wavelength of 1.064 μm at the temperatures of 300 K (solid line) and 77 K (dashed line), left. Absorption spectra of borate crystals in the THz spectral range, right.

References

[1] C. Chen, T. Sasaki et al. *Nonlinear optical borate crystals, principles and applications*, 1st ed., Wiley-VCH, 2012, 387 p.
[2] N. A. Nikolaev, Yu. M Andreev et al., Journal of Physics: Conference Series, **951**, 012003 (2018)
[3] N. A. Nikolaev, Yu. M Andreev et al., Journal of Physics: Conference Series, **951**, 012005 (2018)
[4] Y. Li, J. Huang et al., Results in Physics, **16**, 102815 (2020)

Application potential of nonlinear ferroelectric crystals $KTiOPO_4$, $KTiOAsO_4$, and $KNbO_3$ in the millimeter waves

N. A. Nikolaev[1,*], A. A. Mamrashev[1], G. V. Lanskii[2], V. D. Antsygin[1], Yu. M. Andreev[2,3]

[1] *Institute of Automation and Electrometry SB RAS, Novosibirsk, Russia;*
[2] *Institute of Monitoring of Climatic and Ecological Systems SB RAS, Tomsk, Russia;*
[3] *Tomsk State University, Tomsk, Russia*
[*] *E-mail: Nazar@iae.nsk.su*

Today's progress in radio and radio-photonic technologies shows the growth of carrier frequencies of optical and wireless transmission channels up to hundreds of gigahertz. Many experts note that this trend will lead to an excess of channel capacity of more than 100 Gbps in recent years [1]. Realization of these expectations requires the development of millimeter-waves (100-300 GHz) and terahertz (0.3-10 THz) technologies and techniques where a search for new materials and study of their properties is important. Not only new dielectric materials for substrates and waveguides are required but also nonlinear-optical materials serving as efficient optical-to-THz and THz-to-optical converters are needed. Since "classical" electronic devices have limited performance in the designated ranges a new approach based on the optical-to-optical conversion of laser radiation into the millimeter-waves range was proposed.

Ferroelectrics like lithium niobate $LiNbO_3$ [2] and titanyl potassium phosphate $KTiOPO_4$ [3] are shown to be efficient optical-THz converters. In the case of integrated photonics devices, ferroelectrics allow designing waveguides and periodic structures by poling. Such structures show a sufficient increase in the efficiency of laser frequencies downconversion [4] and upconversion [5]. Recent studies show an efficient detection of terahertz waves using two-stage upconversion in a lithium niobate crystal [6]. Moreover, according to the old works of Yu. V. Shaldin [7] the nonlinear components of the dielectric tensor responsible for the conversion processes within the millimeter-wave range are 4 orders of magnitude higher than the values of the components in the optical range. Thus, ferroelectrics are positioned as potentially promising nonlinear media for millimeter-wave and terahertz photonics, including radio-photonics.

Here we present the dielectric properties of three common nonlinear ferroelectric crystals $KTiOPO_4$, $KTiOAsO_4$, and $KNbO_3$ in the millimeter-wave range. The dispersion of the measured refractive index is approximated in the form of Sellmeier equations. Collinear phase matching for fiber lasers frequencies (wavelengths in the vicinity of 1 μm and 1.5 μm) down-conversion into the millimeter-wave range was estimated. Additionally, phase-matching curves of the second harmonic generation process within the millimeter-wave range are presented.

References

[1] J. Federici and L. Moeller. J. Appl. Phys. **107**, 111101 (2010).
[2] Huang, Shu-Wei, et al. Optics Letters **38.5**, 796-798 (2013).
[3] Wu, Ming-Hsiung, et al. Optica **6.6**, 723-730 (2019).
[4] Jankowski, Marc, et al. Optica **7.1**, 40-46 (2020).
[5] Ma, Fei, et al. JOSA B **35.9**, 2096-2101 (2018).
[6] Sakai, Hikaru, Kodo Kawase, and Kosuke Murate. Optics Letters **45.14**, 3905-3908 (2020).

Mode coupling coefficients of curved few-mode optical fiber

D.E. Praporshchikov*, K.A. Volkov, A.V. Bourdine, V.A. Burdin

Povozhskiy State University of Telecommunications and Informatics

**E-mail: dep82@mail.ru*

Few-mode optical fibers are one of the upcoming trends of fiber optic development. Main objective is overcoming the "non-linear Shannon limit" [1-7]. Signal distortions during transmission over such fiber are primarily due to the combined action of differential mode delay and mode coupling. The latter in turn result from irregularities in the optical fiber, randomly distributing along the length of the optical cable. The most typical irregularities of optical fiber of the delivery length of the optical cable are macro and micro bends. Therefore, the working purpose is calculation the mode coupling coefficients at the bending of a few-mode optical fiber with a bending radius significantly larger than the fiber core diameter.

The calculation of mode coupling coefficients was executed for a multimode optical fiber with a truncated parabolic refractive index profile. It is shown on Fig. 1. Well-known Gaussian approximation method and a stratification method were used as a mathematical apparatus. The curved lightguide was replaced by a straight optical fiber with an equivalent refractive index profile. The dependencies of the mode coupling coefficients of the principal mode LP_{01} with the modes LP_{11}, LP_{02}, LP_{12} and LP_{03} on the bending radius were obtained as a result of the calculations and shown on Fig. 2.

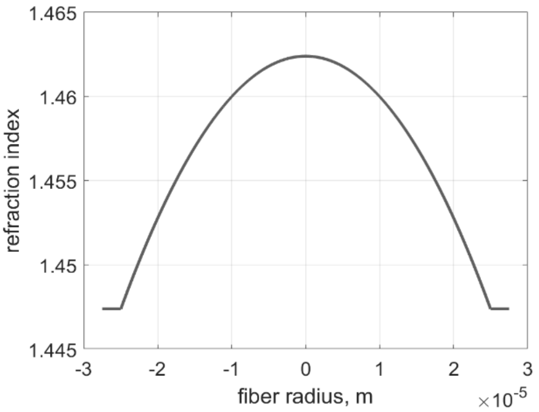

Fig. 1. Refractive index profile of the researched optical fiber under investigation.

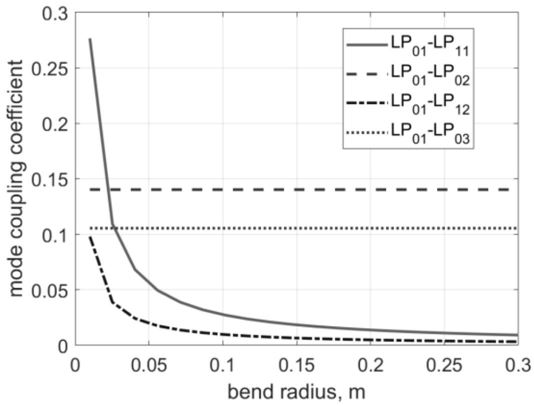

Fig. 2. Dependencies of mode coupling coefficients on bending radius of optical fiber.

The calculations showed that the mode coupling of different azimuthal orders increases sharply with a decrease on the bending radius. At the same time, the mode coupling of same azimuthal order practically does not depend on the fiber bending radius. There is no mode coupling of different azimuthal order for a perfectly straight optical fiber, but even the weak curvature of the optical fiber leads to its occurrence.

Reference

[1] P.P. Mitra, J.B. Stark, *Nature* **411**, 1027-1030 (2001)
[2] J.M. Kahn, P.H. Keang, *Nature* **411**, 1007-1010 (2001)

[3] R.J. Essiambre, G.J. Foschini, G. Kramer et al, *Physical review letters* **101(16)**, 163901-1-4 (2008)

[4] R.J. Essiambre, G.J. Foschini, P.J. Winzer et al, https://www.researchgate.net/publication/241159582_Capacity_Limits_of_Fiber-Optic_Communication_Systems

[5] A.D. Ellis, J. Zhao, D. Cotter, *Journal of lightwave technology* **28(4)**, 423-433 (2010)

[6] R.J. Essiambre, G. Kramer, P.J. Winzer et al, *Journal of Lightwave Technology* **28(4)**, 662-701 (2010)

[7] A. Amphawan, *Optical Engineering* **50(10)**, 102001-1-102001-6 (2011)

Switching between single- and dual-wavelength generation in passively mode-locked Nd: YAG waveguide laser

M.V. Ponarina*, A.G. Okhrimchuk, P.A. Obraztsov

Prokhorov General Physics Institute of RAS, Moscow, Russia

**E-mail: ponarinamariya@gmail.com*

Dual-wavelength lasers are interesting for various applications, such as optical communication, laser location, generation of THz radiation [1]. One of the methods for producing a laser with two wavelengths is the use of crystals with several nearby emitting transitions. Nd:YAG crystal is one of such crystal and the most widely used active medium due to its excellent optical and mechanical properties.

We present a compact diode-pumped Nd:YAG solid-state laser with novel waveguide architecture. The diameter of a waveguide created in an active crystal by direct recording with a femtosecond laser beam [2] is 20 μm. Passive mode-locking is carried out by a graphene-based saturable absorber deposited on the output mirror of the cavity [3]. Precise tuning of the intracavity interferometer formed between the active medium and the output mirror makes it possible to control the spectral and temporal parameters of the output radiation [4]. The laser operation of single- (Fig. 1 (a) and dual-wavelength (Fig. 1 (b) generation, as well as the possibility of switching between them by using a precision change of the cavity length, is demonstrated.

In addition, we demonstrate the possibility of controlled switching between the generation regimes of a waveguide Nd:YAG laser by changing the polarization of the pump radiation. When horizontal polarization of the pump radiation is used, the laser operation is close to the stable passive mode-locking. When vertical polarization of pump radiation is used, the output power is higher than with horizontal polarization, but mode-locking is not observed.

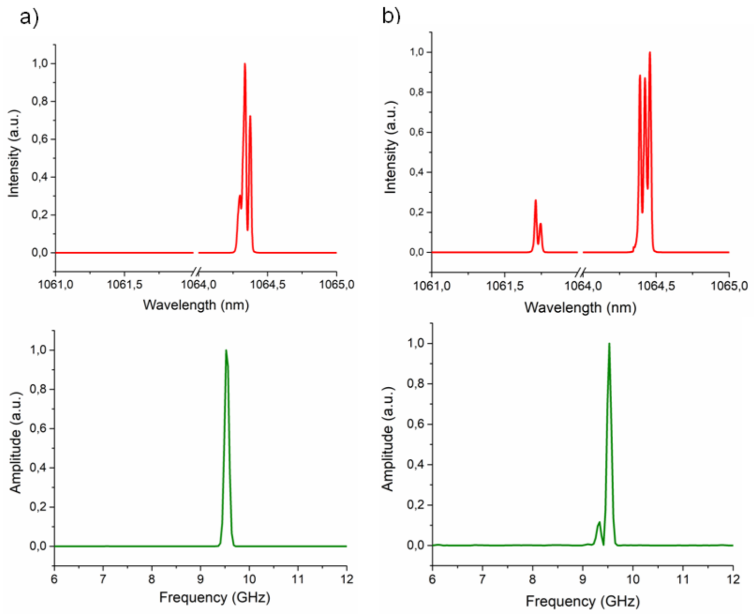

Fig.1. Optical and radio frequency spectra obtained at single- (a) and dual-wavelength (b) generation of a waveguide Nd:YAG laser.

By combining the advantages of each linear component of the pump polarization and controlling the value of intracavity losses, a passive mode-locking with a pulse repetition rate of 9.5 GHz was obtained at a wavelength of 1064 nm.

The work of M.V. Ponarina was funded by RFBR, project No. 19-32-90215. P.A. Obraztsov expresses his gratitude to the Russian Science Foundation (Grant No. 19-72-00175).

References

[1] B.M. Walsh, Laser Phys. 20, 622–634 (2010)
[2] A. Okhrimchuk, V. Mezentsev, et al, Opt. Express, 20 (4), 3832–3843 (2012)
[3] A. Okhrimchuk, P. Obraztsov, Sci Rep 5, 11172 (2015)
[4] M. V. Ponarina, A. G. Okhrimchuk, et al, Quantum Electron, 49 (4), 365–370 (2019)

Fiber lasers applications: telecommunications, sensors, biomedicine, material processing and modification

Nonlinearity mitigation in polarization multiplexed fiber-optic transmission system based on fully-connected neural networks

S.A. Bogdanov[1,*], O.S. Sidelnikov[1], M.P. Fedoruk[1,2], S.K. Turitsyn[1,3]

[1]*Novosibirsk State University, Novosibirsk,*
[2]*Institute of Computational Technologies SB RAS, Novosibirsk,*
[3]*Aston Institute of Photonic Technologies, Aston University, Birmingham,*
[*]*E-mail: s.bogdanov@g.nsu.ru*

A growth of fiber-optic communication systems capacity by increasing the signal power (increasing signal-to-noise ratio in linear systems) is limited due to the nonlinear properties of optical fiber. Polarization-division multiplexing (PDM), which doubles the data transmission rate by using both polarizations, leads to additional nonlinear distortions caused by interactions between different polarizations. Machine learning approaches are powerful tools for digital signal processing in fiber-optic communications [1,2]. In this work we propose to use the fully-connected feed-forward neural networks (NNs) for nonlinearity mitigation at the receiver side of fiber-optic communication systems with polarization-division multiplexing. NNs of different architectures were studied and the comparison of their effectiveness was performed.

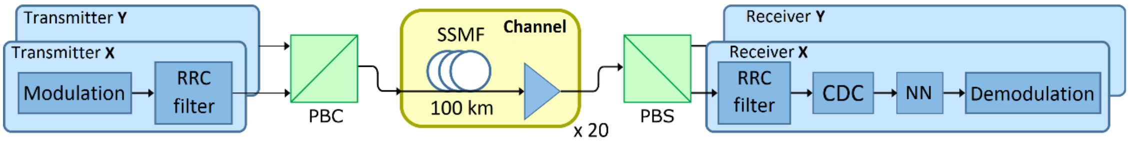

Fig. 1. Communication line scheme.

The scheme of the considered fiber-optic communication system is depicted in figure 1. Every transmitter generates 16-QAM signals with symbol rate R_s = 32 GBaud. The pulses are shaped using RRC filter with roll-off factor of 0.1. Then, signals from both transmitters are combined to one PDM-signal that is fed to the channel. The communication link consists of 20 spans of 100 km standard single mode fiber and erbium doped fiber amplifiers with NF = 4.5 dB after each span. At the receiver separated signal polarizations pass through a matched filter and, then, the ideal compensation of chromatic dispersion is performed. After this, the signal is downsampled to 1 sample per symbol and NN for nonlinear effects compensation is applied. Then, signal demodulation is performed and the bit error rate is calculated.

A neural network for 16-QAM symbols classification is used at the receiver. For every symbol processing the real and imaginary parts of N previous and N following symbols of both polarizations are fed to the input of NN. So, the input layer consists of $2 \cdot 2 \cdot (2 \cdot N+1)$ neurons. NN also has two hidden layers with a variable number of neurons and nonlinear activation function (tanh). Output layer consists of 16 neurons that is related to the number of points for the 16-QAM constellation. To train NN the Adam optimizer and TensorFlow are used.

In figure 2a results of two NN implementation at the communication system receiver are shown: first, the data is transmitted using one polarization state and, second, the data is transmitted using two polarizations but only one of them is fed to NN input (blue and green curve correspondingly). In the both cases for every symbol its 10 previous and 10 following neighbors were taken into account, and NN had 64 neurons on each hidden layer. Next, for two polarizations system the symbols from the both polarizations are used to predict symbols from the one of the polarizations (red dots). We can see that applying a NN with 64 neurons on hidden layers is ineffective because such simple networks are not able to process large numbers of symbols. But increasing the number of neurons in hidden layers lets to improve the effectiveness of using symbols from the second polarization.

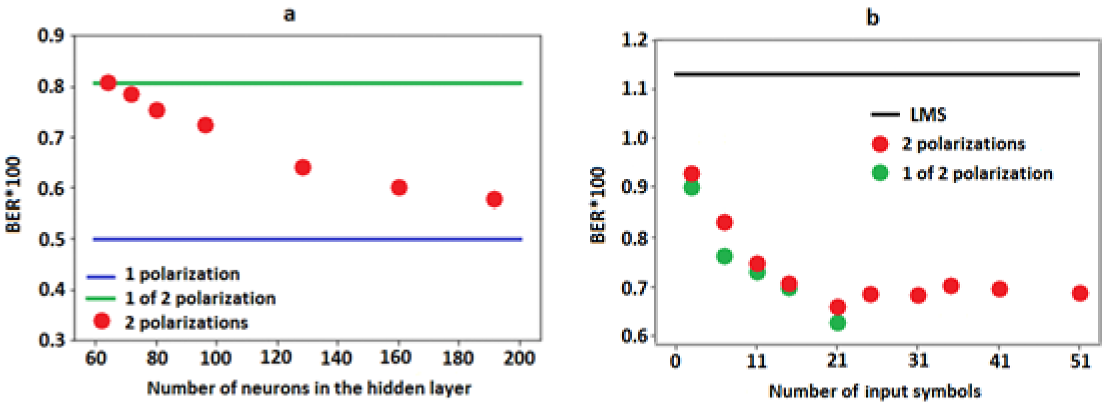

Fig. 2. Efficiency of accounting for the second polarization in dependence on number neuron in the hidden layer (a). The result of applying NN for prediction one and two polarizations (b).

Figure 2b depicts a result of data processing from both polarizations by the NN with 192 neurons in each hidden layer in dependence on the number of input symbols from each polarization. In the figure the result of a linear compensation scheme based on adaptive filters (Least Mean Square - LMS), that compensate for the nonlinear phase shift, is presented as a benchmark. In this case NN predicts data either from only one polarization or from both (green and red dots correspondingly). We see some degradation of data processing performance for two polarizations and this can be explained by the classification into 256 classes.

The work of O.S. Sidelnikov was supported by grant of the President of the Russian Federation (MK-915.2020.9). The work of S.A. Bogdanov was supported by the state funding program FSUS-2020-0034.

References

[1] O.S. Sidelnikov, et al, *Opt.Express.* **26**, 32765-32776 (2018).
[2] C. Häger, et al, *Proc. OFC*, W3A.4 (2018).

Optical regeneration of a telecommunication signal with amplitude modulation

E. Kuprikov[1], **A. Kokhanovskiy**[1], **O. Sidelnikov**[1], **S. Turitsyn**[1,2]

[1]*Novosibirsk State University, 1, Pirogova str., Novosibirsk*
[2]*Aston Institute of Photonic Technologies, Aston University, Birmingham*
[*]*E-mail: e.kuprikov@g.nsu.ru*

Fiber lines with a high data rate (100 Gbps) over single-mode fiber over short distances are in wide demand in data centers for the implementation of the IEEE 802.3bs 400 Gbps protocol [1]. To achieve these data rates, it is necessary to compensate for optical signal distortions caused by chromatic dispersion, nonlinear effects, and their combination. However, not all existing solutions used in backbone communication lines can be implemented in data processing centers. The main requirements for fiber systems used in data centers are low cost, ease of implementation, and efficient energy performance. Therefore, it is desirable to avoid complex digital signal processing circuits to compensate for these effects, which can lead to additional power consumption and signal delay. In this work, we propose an optical regressor scheme that allows the restoration of an optical signal prior to direct detection. Such optic methods have the potential to be energy efficient and have a wide frequency bandwidth.

Figure 1 shows a diagram of a 27 km fiber link with an optical regressor. As the modulation format of the optical signal, a 4-level amplitude-pulse modulation with a transmission rate of 14 Giga-baud was used. After passing through the communication line and the optical regressor, the signal is detected by a photodetector. Average signal power ranged from 0 to 4 dBm.

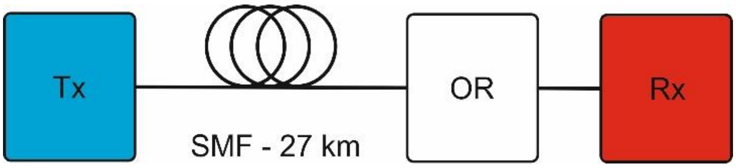

Fig. 1. Communication line diagram with optical regressor

Figure 2 shows a schematic of the proposed optical signal processing method, which consists of 3 fiber couplers and 3 fiber combiners.

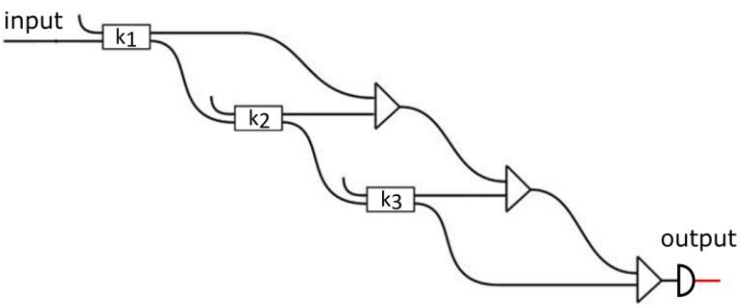

Fig. 2. Optical regressor circuit

The number of taps and the length of the fiber line between adjacent taps are hyperparameters of the proposed device and are selected for a given signal transmission rate and length of the fiber-optic communication line. For each set of hyperparameters, the split ratios α of the taps are determined by the backpropagation method. The backpropagation method finds a set of values of the division coefficients of the taps k, which provides the minimum root-mean-square error Err between the detected signal and the original signal without distortion.

$$Err = \frac{1}{N}\sum_{i=0}^{N}\left|D\big(F(u(i),k)\big) - D(\hat{Y}(i))\right|^2 \to min,$$

where u – is the signal at the output from the optical communication line, F – is the device transformation function, which depends on the set of dividing factors of the couplers k, D – is the detector function, Y – is the signal before transmission over the optical communication line, i – is the number of the transmitted symbol from 0 to N.

To demonstrate the operation of the optical regressor, we used numerical simulation of the propagation of an optical signal along an optical fiber by solving the nonlinear Schrödinger equation, which describes the evolution of the envelope of the optical signal A (z, t):

$$\frac{\partial A}{\partial z} = -\frac{\alpha}{2}A - i\frac{\beta_2}{2}\frac{\partial^2 A}{\partial t^2} + i\gamma|A|^2 A.$$

This equation was solved numerically using the symmetric Fourier splitting into physical processes with the following parameters: linear loss α = 0.2 dB / km, fiber nonlinearity γ = 1.4 1 / (W km), chromatic dispersion β2 = -25 ps2 / km, length wavelength λ = 1550 nm, number of counts per period q = 16. Figure 3 shows the eye-diagrams of the signal after detection for the case when the proposed scheme was used (a) and for the case of direct detection (b). The average signal power was 0 dBm. In the process of determining the circuit parameters, we received the following device architecture: 4 couplers with a distance of 0.9116 mm between them and coefficients of 0.99, 0.45, 0.08 and 0.25, respectively. The bit error rate (BER) without using the proposed method is 0.00415, and after applying 0.00026. For a power of 4 dBm, the BER without using the proposed method was 0.0042 and after applying 0.00038. The tap ratios are 0.95, 0.4, 0.09 and 0.66, respectively.

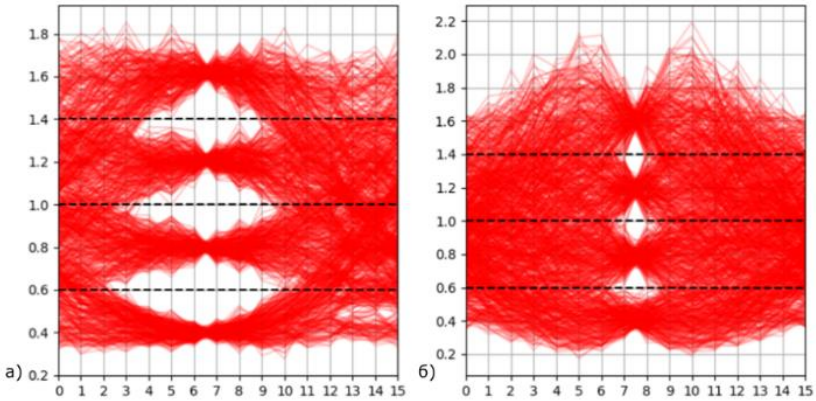

Fig. 3. Eye-diagrams of the recorded signal a) after passing through the device b) with direct detection after passing through the communication line.

This work was supported by the Russian Science Foundation (project No. 17-72- 30006).

Reference

[1] "IEEE Standard for Ethernet, Standard 802.3bs", 2017.
[2] G.P. Agrawal, Nonlinear fiber optics, 4th ed. Academic press, 2007, 539 c.

High-speed, multichannel, variable dispersion compensation link for suppression of nonlinear distortion

E.G. Shapiro, D.A. Shapiro

Institute of Automation and Electrometry, Novosibirsk
Novosibirsk State University, Novosibirsk

**E-mail: shapiro@iae.nsk.su*

Multichannel information transmission, high transmission rate in a separate channel, and high-order coding formats improve fiber communication lines. The signal distortion's main factors are amplifier noise and nonlinear effects accompanying signal propagation through the communication line. This paper considers a combination of methods for suppressing nonlinear distortions in a communication line with zero average dispersion: the large chirping of the input pulses and variable dispersion compensation. We show that the simultaneous use of these methods significantly improves the signal quality in multichannel information transmission.

We performed a numerical calculation of signal propagation in the framework of nonlinear coupled Schrödinger equations [1] for three channels. The communication line consists of 10 sections of the type

SMF(100 км) + EDFA + $DC(i)$.

Here SMF is a standard single-mode fiber, EDFA is an erbium amplifier that fully compensated for the signal attenuation in the fiber section, $DC(i)$, the i-th compensator. We assume that the compensation is based on Bragg grating's low loss and neglect the polarization dispersion. Let us denote by d_i the amount of chromatic dispersion that the $DC(i)$ device compensates. The d_i values form an arithmetic progression with a step Δd. The sum of d_i is -17000 ps/nm, i.e. fully compensates for the 10 SMF spans' accumulated dispersion. Thus, in contrast to work [2], this design does not require a post-compensation of accumulated chromatic dispersion. The modulation format is 8QAM. Here, we use two amplitude values (0.043 $W^{1/2}$ and 0.086 $W^{1/2}$) and four-phase values for each amplitude. The information is encoded with Gaussian pulses of the form $a_n(\tau) = B_n \exp[-(\tau^2 - iC\tau^2)/2T_0^2]$, where B_n is the amplitude of the bit with number n, C is the chirp parameter, T_0 = 6 ps is the pulse width, the bit-length is 25 ps. The channels are spaced by interval 100 GHz.

Below are the constellation diagrams for the central channel at the receiver after processing to separate the channels and reduce the amplifiers' noise. Fig. 1 shows a graph for Δd = 0 and zero initial chirp. Fig. 2 shows a graph for Δd = 288.89 ps / nm of zero chirp C = 0. Fig. 3 shows a graph for Δd = 222.22 ps/nm and C = 5. We see that in the last case the symbols are most distinguishable; the achieved bit error rate is 6.8×10^{-3}.

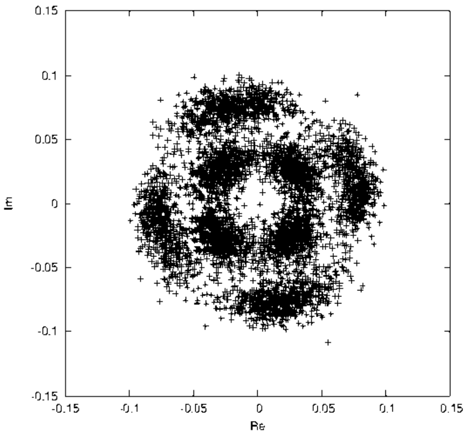

Fig. 1

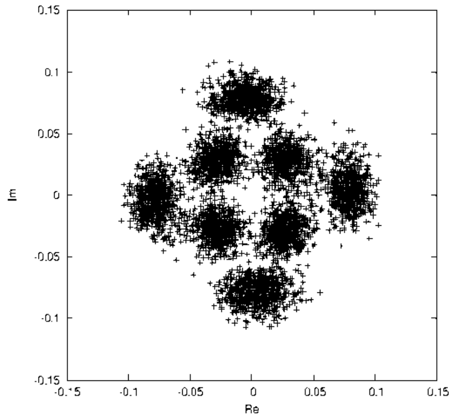

Fig. 2

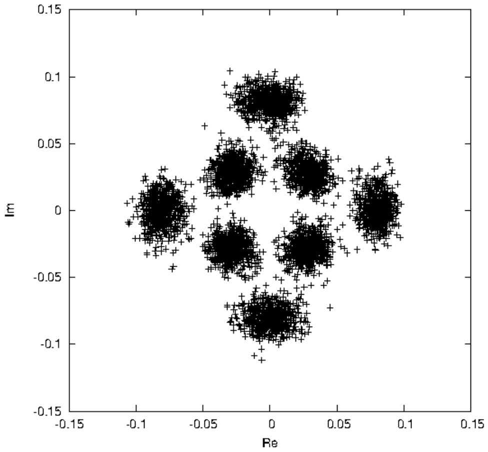

Fig. 3

Because of the strong chirp, the channels overlap the frequency domain. However, the amplitudes of Fourier components remain small, and then the interchannel interference is linear. The chirp, along with the variable dispersion compensation, also reduces the intersymbol interference in each channel.

This work is supported by the Ministry of Science and Higher Education of the Russian Federation, State. Reg. No. AAAAA17-117062110026-3.

References

[1] G. P. Agrawal, *Nonlinear fiber optics*, Amsterdam, Elsevier, 2007
[2] E. G. Shapiro, D. A. Shapiro, *Quant. Electr.*, **50**(2) 184–186 (2020).

Acoustic diagnostics of optical fibers strength in the cable

V.A. Andreev[1], A.V. Burdin[1,2], V.A. Burdn[1,*], M.V. Dashkov[1]

[1]*Povozhskiy State University of Telecommunications and Informatics*
[2]*JSC "Scientific Production Association State Optical Institute Named after Vavilov S.I."*
[*]*E-mail*: burdin@psati.ru

At present one of the most actual problems for communication networks is the service life prediction for installed optical cables. This is explained by the fact that the operating time of the optical cables on the communication lines built in the 90s of the last century exceeded or close to the declared by cable manufacturers guarantee service life of 25-30 years. According to the generally accepted recommendations, the service life of the optical cable is estimated by the services life of the optical fibers [1]. This is justified since others structural elements in optical cable are used to protect optical fibers from external factors. To predict the service life of an optical fiber with a specified probability the well-known formulas are using, which define that target estimation determined by the relation of the applied to optical fiber load and its strength [1, 2]. Distribution of stresses in optical fibers of installed cable line can be measured by reflectometric methods. Optical fiber stresses due to tensile loads are determined from the results of measurements using BOTDR, and the bending stresses of optical fibers are estimated by the results of measurements of the distributions of optical fibers bends along cable line [3]. There are no recommendations for methods of non-destructive testing of the optical fibers strength in the cable.

For a long time, methods of non-destructive testing of products made from various materials based on acoustic emission were widely used [4]. Such methods based on measurement of acoustic emission signals of tested sample under the mechanical loading, and subsequent determination of the sample strength and/or localization of the defect according to the characteristics of the acoustic emission signal and applied mechanical load. To measure the acoustic signal emission and load control special sensors should be installed. Such solution was applied for evaluation of the strength of optical fiber bundles [5].

Over the past three decades distributed fiber-optic acoustic sensors (DAS – Distributed Fiber Sensor), which are characterized by resistance to electromagnetic interference, high sensitivity and large bandwidth, are widely used in various applications [6, 7]. In such systems the highly sensitive sensor is an optical fiber. Taking into account the characteristics of DAS, the possibilities of using these systems for measuring acoustic emission of an optical fiber itself were considered. A novel method for non-destructive testing of optical fiber strength in cable based on the acoustic emission method proposed in this paper. Distinctive features of this method: the mechanical load in the optical fiber is created due to the vibro-acoustic influence on the cable, and for measurement of the acoustic signal emission and control of the influencing vibro-acoustic signal the tested optical fiber is used. Conceptual scheme for one of the realization of the proposed method is shown on Fig. 1. Here 1 and 2 are the tested and reference optical fibers, respectively, 3 is a source of vibro-acoustic influence, 5 is the optical switch, 4 is a measuring system.

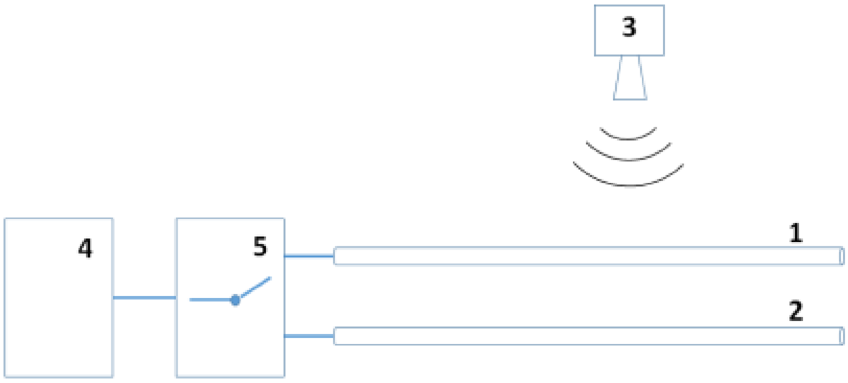

Fig.1. Conceptual scheme of the proposed method

In report the theoretical substantiation of the proposed method and the results of its experimental testing will be represented. The results of measurements of the influencing acoustic signal, acoustic emission signal and the results of optical fibers strength calculation for samples of optical cables which are in maintenance since 1996, 1998, 2011 and 2017 were represented. These estimates were compared with the estimates of the strength for same fibers obtained by the method of destructive control. The method of two-point bending was used [8]. Results of approbation demonstrate the possible application of the proposed method.

References

[1] ITU-T G-series Recommendations – Supplement 59, Guidance on optical fibre and cable reliability, 21 (2018).
[2] IEC TR 62048:2014 Optical fibres – Reliability – Power law theory, 66 (2014).
[3] I. Sankawa, Y. Koyamada et al., IEICE Transactions on Communications **E76-B(4)**, 402-409 (1993).
[4] V.N. Ivanov, Territory NDT **1**, 44-51 (2019).
[5] A. Cowking, A. Attou et al. J. Mater. Sci. **26**, 1301–1310 (1991).
[6] Y. Wu, J. Gan et al., IEEE Photonics Journal **7(6)**, 6803810 (2015).
[7] Y. Muanenda, Hindawi Journal of Sensors **23(3897873)**, 1-16 (2018).
[8] GOST R MEK 60793-1-33-2014

Compact narrow-linewidth lasers for distributed fiber optic sensors

D.R. Kharasov[1,2*], E.A. Fomiryakov[1,3], O.E. Naniy[1,3], S. P. Nikitin[1], V.N. Treshchikov[1]

[1]*T8 Sensor Ltd., Moscow*
[2]*Moscow Institute of Physics and Technology, Dolgoprudny*
[3]*Lomonosov Moscow State University, Physical department, Moscow*
[*] *E-mail: kharasov@phystech.ru*

Highly stable narrow-linewidth single frequency lasers are widely used both in scientific research and in multiple applications such as fiber-optic communications, distributed fiber optic sensing (including coherent reflectometry [1-3]), radio over fiber technology, optical interferometry etc. In addition to the low level of phase and amplitude noises of laser radiation, most of these applications also require compactness, portability, easy and low cost production combined with various methods of phase noise reduction: laser diode coupled with an external whispering gallery modes (WGM) optical cavity [4, 5] (e.g. OE Waves lasers), a laser diode with external planar Bragg grating (BR) [6] (e.g. RIO “Orion” laser) and a single-frequency DFB fiber laser (e.g. EFL-SF-1550 laser manufactured by Inversion Fiber, LLC).

Earlier [7] linewidths and frequency drifts were measured in a variety of lasers by using the method of optical heterodyning. In this work, the previous results are supplemented with measurements made using the self-heterodyning method employing a 100 km optical delay line [8, 9], which allows measurements of white and flicker frequency noise levels [10] without a reference laser.

The experimental results incorporating measurements of frequency Allan deviation have been also confirmed by numerical analysis of the interferometer output signal based on white and flicker noises model [11] as shown in Fig.1.

The processed experimental data are summarized in Table 1. Among the tested lasers, the OE Waves laser has demonstrated the lowest phase noise, however, the use of this type of lasers is difficult in presence of strong external vibrations that can violate the mode coupling of the laser to the WGM cavity. The laser manufactured Inversion Fiber, LLC has a very narrow line (less than 100 Hz), but at the same time its flicker noise level is an order of magnitude higher than that of the WGM lasers. The RIO Orion laser has at least an order of magnitude larger linewidth (~ 2 kHz), and approximately the same flicker noise level than those of the OE Waves and Inversion-Fiber lasers. The main advantage of the RIO Orion laser is its low sensitivity to external vibrations and temperature changes [5], which makes it possible to use it in optical sensors for actual field applications. Since the frequency flicker noise in lasers is usually associated with the technical factors, the development of methods for suppressing frequency flicker noise [12–14] is an important practical problem.

In summary, this paper presents self-heterodyning measurements of phase noise levels made with a number of different compact lasers specified by low levels of phase noise and suitable for a wide range of practically important applications.

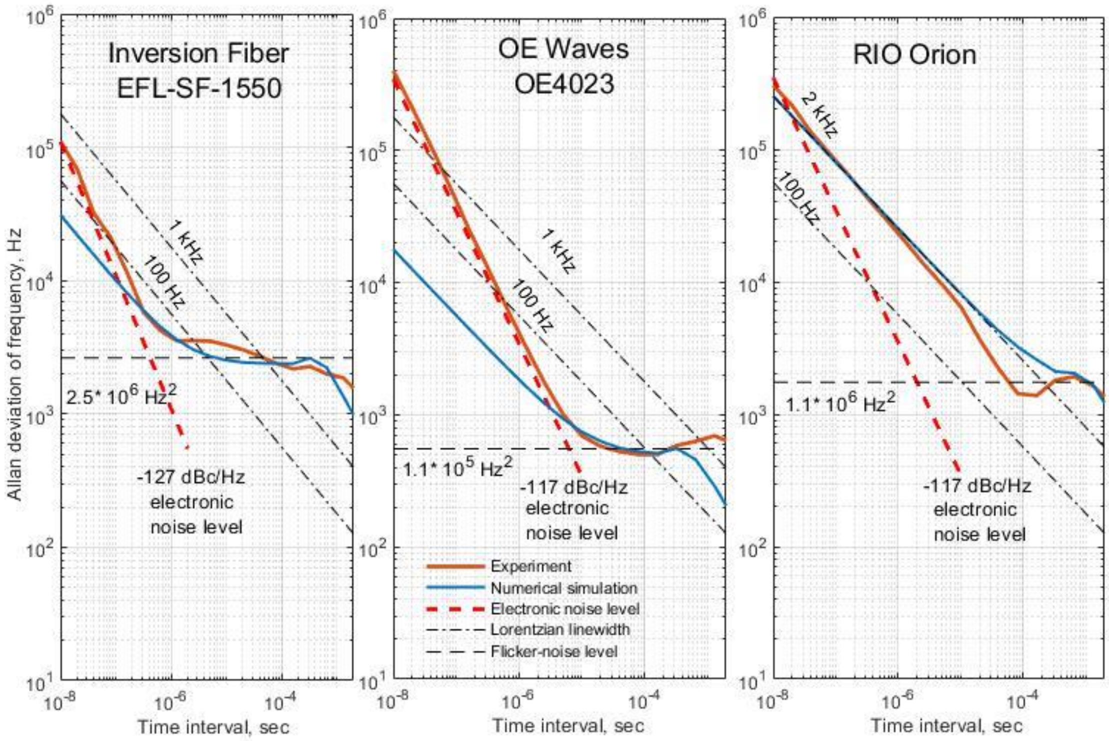

Fig.1 Experimentally measured and numerically simulated Allan deviation dependencies of the beat note frequency of tested lasers at the output of a path-mismatched Mach-Zehnder interferometer with a delay line of 100 km

Table 1. Lasers parameters measurement results

Laser	Linewidth narrowing method	Instant linewidth, kHz	Flicker-noise level, Hz^2	Frequency linear drift[7], MHz/s
OE Waves OE4023	WGM-resonator	< 0,1	1,1 10^5	< 1
RIO Orion	Planar BG	2	1,1 10^6	-
Inversion Fiber	Active fiber with inscribed BG	< 0,1	2,5 10^6	< 0,25

References

[1] S.V. Shatalin, V. N. Treschikov & A. J. Rogers, Applied optics, 37(24), 5600-5604 (1998).
[2] S.P. Nikitin, A.I. Kuzmenkov et al, Laser Physics, 28(8), 085107 (2018).
[3] S.P. Nikitin, P.I. Ulanovskiy et al, Laser Physics, 26(10), 105106 (2016).
[4] W. Liang et al., Nature communications 6.1, 1-6 (2015).
[5] N. M. Kondratiev et al., Optics Express 25.23 (2017): 28167-28178.
[6] M. Alalusi et al., Fiber Optic Sensors and Applications VI. International Society for Optics and Photonics (2009).
[7] S.P. Nikitin, E.A. Fomiryakov et al, J. Lightwave Technology 38, 1446-1453 (2020).
[8] L. Richter et al., IEEE Journal of Quantum Electronics 22.11, 2070-2074 (1986).
[9] L. B. Mercer, J. Lightwave Technology 9.4, 485-493 (1991).
[10] F. Riehle, Frequency standards: basics and applications. – John Wiley & Sons, 2006.
[11] J. N. Kasdin, Proceedings of the IEEE 83.5, 802-827 (1995).
[12] Drever, R. W. P., et al. Applied Physics B 31.2, 97-105 (1983)
[13] M. Poulin et al. Laser Resonators and Beam Control XII. Vol. 7579. International Society for Optics and Photonics (2010).
[14] E. Kirilov et al. Applied Physics B 119.2, 233-240 (2015).

FBG-sensors interrogation with coherent optical frequency-domain reflectometer based on self-sweeping fiber laser

A.Yu. Tkachenko*, N.N. Smolyaninov, M.I. Skvortsov, I.A. Lobach, S.I. Kablukov

Institute of automation and electrometry SB RAS, Novosibirsk

**E-mail: alinka.tkacenko@yandex.ru*

Optical reflectometry is a key technology for distributed measurements of physical quantities along optical lines using dependencies of scattered in an optical fiber radiation parameters (e.g., the polarization, intensity, and optical frequency) on the physical parameters of external actions (the temperature or strain) [1]. Time- and frequency-domain reflectometry are distinguished from each other according to their principles of operation. The principle of coherent optical reflectometry in the frequency-domain (optical frequency-domain reflectometry, OFDR, for short) operation is based on spectral analysis of an interference signal produced by mixing of probe and scattered radiation. This analysis can be carried out with continuous wave (CW) tunable probe radiation. In this case, spatial coordinates of reflectors located along the tested line are proportional to the frequency coordinates of maxima in a Fourier spectrum of the interference signal measured during the tuning of the probe radiation.

Implementation of a self-sweeping fiber laser as the key element of the OFDR is proposed in [2]. In this type of laser, the optical frequency tunes due to internal processes in the laser active fiber without using any actively tuned elements. One important feature of this laser is generation of a sequence of coherent microsecond pulses with spectral width of less than 1 MHz and with strict discreteness of the optical frequency tuning. The possibility of attaining a spatial sampling of ~200 μm and reflectance sensitivity as high as –85 dB/mm at a test line length of ~9 m was demonstrated in [2]. In this paper we present the first results of implementation of the OFDR based on a self-sweeping fiber laser for sensor applications.

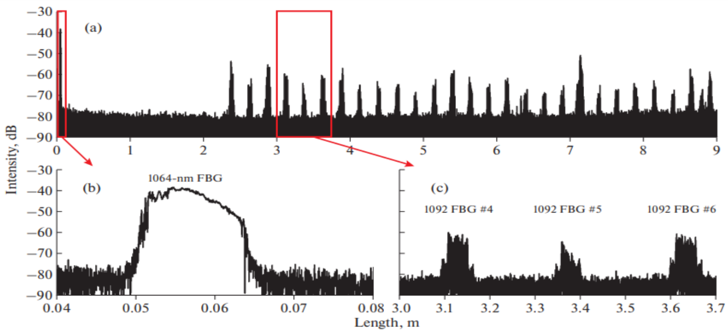

Fig.1. A reflectogram of the sensing line in different scales.

The optical scheme of the OFDR is based on a Mach–Zehnder interferometer formed by three couplers. One of the interferometer arms contained a FBG array sensor. The FBG array consisted of a set of 28 FBGs with reflection peak maxima centered approximately at the same wavelength of 1092 nm and one FBG at wavelength of ~1064 nm. Only in the later case reflection spectrum of the FBG falls into the tuning range of the self-sweeping laser. For this reason, we will further divide all FBGs into the resonant FBG (at 1064 nm) and the non resonant FBGs (at 1092 nm). Owing to the linear relationship between the optical frequency and the pulse number, the spectral dependence of the normalized amplitude of the interference signal can be obtained based on the relative pulse number [2]. A reflectogram, i.e., the longitudinal distribution of reflectors along the fiber sensing line, was obtained by applying the fast Fourier transform to the dependence of the normalized interference signal on the optical frequency (Fig.1). One can see that the reflectogram consists of numerous peaks and each peak corresponds to its own FBG. Figure 1a shows that the amplitude of the reflection signal from the resonant FBG is higher as compared with nonresonant ones.

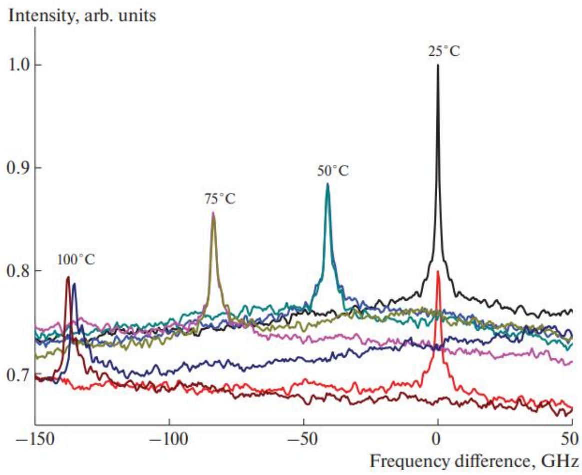

Fig. 2. Correlation functions for reflection spectra of a non-resonant FBG at room temperature (25°C) and when heated.

To demonstrate applicability of the system for sensing, one of the non-resonant FBGs is placed into a thermostat with temperature control from room to 100°C. A correlation function of the FBG reflection spectra at room temperature (25°C) and in the heated state is analyzed in the experiments. An offset of the correlation peak maximum can originate both from the heating and from fluctuations of starting optical frequency of the sweeping laser. To eliminate the latter contribution, the offset was taken into account by considering similar correlation peak of a reference FBG kept at room temperature. Fig. 2 shows the offset of the narrow correlation peak towards lower frequencies during heating of a nonresonant FBG. The offset of the correlation peak is related to temperature according to the linear law with a slope of 1.83 GHz/°C (0.73 nm/100°C).

This work was carried out as a part of the state assignment of the IA&E SB RAS (No. AAAA-A19-119112990054-4).

References

[1] A.H. Hartog, An Introduction to Distributed Optical Fibre Sensors *CRC Press* (2018)
[2] A.Yu. Tkachenko, I.A. Lobach, S.I. Kablukov, *Quantum Electronics*, **49(12)**, 1121-1126, (2019)

Acoustic sensor based on few-mode optical fibers

M.V. Dashkov

Povozhskiy State University of Telecommunications and Informatics

E-mail: mvd.srttc@gmail.com

The application of few-mode optical fibers as a sensing element was considered in a number of works [1-3]. In this paper the results of a study of an acoustic impact sensor based on the basis of an optical fiber, operating in a few-mode regime, are represented.

An experimental setup for studying acoustic effects on the parameters of light propagating in a few-mode fiber is shown on Fig. 1. A laser diode (LD) with a center wavelength of 980 nm and an output power of 5 mW was used as a radiation source. A polarization controller (PC) was used to control the state of polarization. The mode controller (MC) was used to control the higher order mode excitation. In experimental setup Corning SMF-28e+® optical fiber, total length of 5.9 km, was used as a sensor. The acoustic impact was applied on the short section of the optical fiber at a distance of 4.9 km. A p-i-n photodiode with a transimpedance amplifier (PD/TIA) is used for detection.

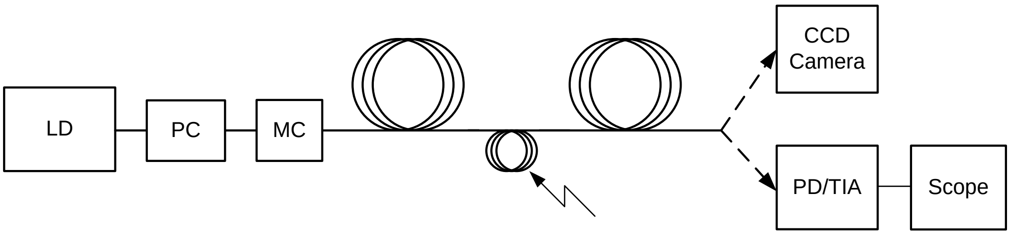

Fig. 1. Experimental setup

As a result of theoretical calculations, it was determined that when using a radiation source with a wavelength of 980 nm, the optical fiber supports the propagation of two modes LP_{01} and LP_{11}. A digital CCD camera was used to experimentally study the mode composition in the optical fiber. In Fig. 2 the distributions of the optical field obtained at various settings of the mode controller are shown.

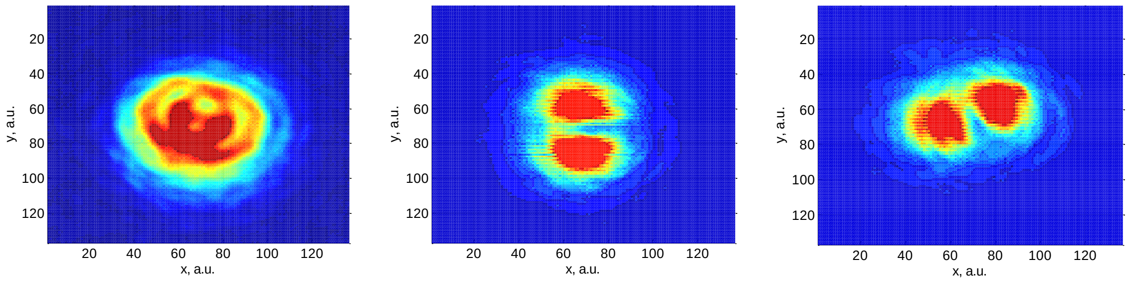

a) b) c)

Fig. 2. Optical field distributions at different settings of the mode controller: a) total field; b) LP11a; c) LP11b

The study of acoustic effects was carried out with various configurations of the sensor element and its orientation in relation to the acoustic field. A speaker with a diaphragm diameter of 40 cm was used as a source of acoustic impact. The following configurations were investigated: a coil of 4 turns of an optical fiber with a diameter of 50 cm with vertical orientation; coil of 4 turns of optical fiber with a diameter of 50 cm with horizontal orientation; a straight section of the fiber with a length of 40 cm, located above the speaker diaphragm.

For acoustic isolation and prevention of parasitic influences, the interrogation system and a sensitive element with a speaker were placed in different rooms. A sinusoidal signal with a frequency in the range of 500 - 10000 Hz was supplied to the speaker, while providing an acoustic exposure level of 60-70 dBa for the range 800 - 2400 kHz. Examples of measurement results for a frequency of 1.7 kHz are shown in Fig. 3.

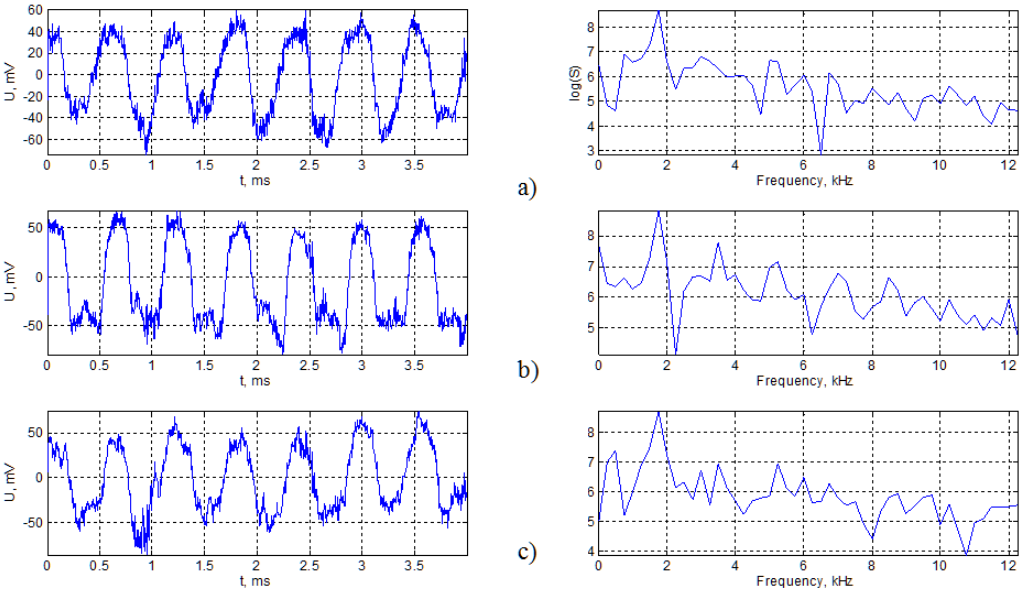

Fig. 3. Detected signal and spectral characteristics: a) fiber coil, horizontal; b) fiber coil, vertical; c) straight fiber section

Thus, the ability to identify the impact and determine its characteristics was demonstrated. It was noted that the amplitude of the detected signal largely depends on the settings of the mode controller and the polarization controller.

References

[1] M.R. Layton, J.A. Bucaro, *Applied Optics* **18 (5)**, 666-670 (1979)
[2] A. Kumar, N.K. Goel, R.K. Varshney, *J. Lightwave Technology*, **19 (3)**, 358-362 (2001)
[3] O.I. Kotov, G.B. Liokumovich, S.I. Markov, *Proc. SPIE* **5381**, 91-102 (2004)

Direct femtosecond-laser projection lithography on perovskites for advanced nanophotonic applications

A. Kuchmizhak[1,2,*], **A. Zhizhchenko**[1,2], **S. Makarov**[3]

[1]Institute for Automation and Control Processes, 5 Radio St., Vladivostok
[2]Far Eastern Federal University, 8 Sukhanova St., Vladivostok
[3]ITMO University, 49 Kronverksky Pr., St. Petersburg
[*]E-mail: alex.iacp.dvo@mail.ru

Nanophotonics based on resonant nanostructures and metasurfaces made of halide perovskites have become a prospective direction for efficient light manipulation at subwavelength scale in advanced photonic designs. One of the main challenges in this field is the lack of large-scale low-cost technique for subwavelength perovskite structures fabrication preserving highly efficient luminescence. We demonstrate novel approach for 3D micropatterning of perovskite films via direct femtosecond laser projection lithography. Whereas majority of previous works used laser processing only for rough cutting/scribing of perovskite materials at microscale level, here by using advanced laser beam engineering and delicate multi-pulse processing we showed capability of flexible non-destructive 3D processing of perovskites at sub-diffraction resolution down to 250 nm [1]. Additionally, for the first time in literature, we provide valuable theoretical insight into ablation mechanism of halide-perovskite material with ultrashort laser radiation [2]. The elaborated optimized laser processing regime allowed to control 3D surface morphology preserving optoelectronic properties of the irradiated perovskite material, thus opening pathway for high-performing inexpensive and large-scale fabrication of nanostructures and surface textures suitable for advanced light-emitting, surface coloring and information encryption applications (Fig. 1).

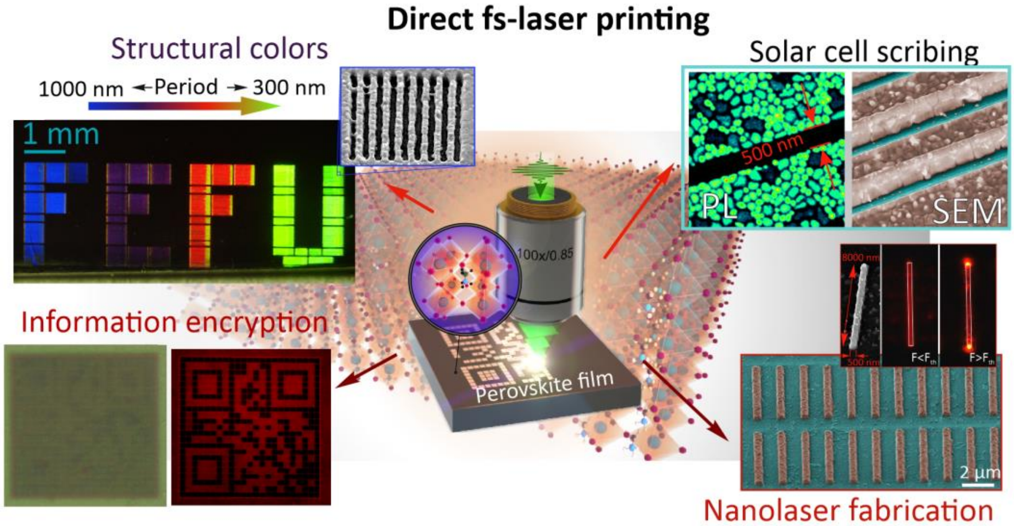

Fig.1. Scheme showing diverse applications of nanostructures made of halide perovskites via direct femtosecond laser projection lithography.

This work was supported by the Russian Science Foundation (grant no. 19-19-00177)

Литература

[1] A. Zhizhchenko, S. Syubaev, et al, *ACS Nano* **13**, 4140 (2019)
[2] A.Y. Zhizhchenko, P. Tonkaev et al, *Small* **16**, 2000410 (2020)

Laser Additive Manufacturing of Bioresorbable Magnesium Implants and Means of its Automation

Y.N. Kulchin, P.A. Nikiforov, A.I. Nikitin*, D.S. Pivovarov, D.S. Yatsko, V.A. Timchenko

Institute of Automation and Control Processes Far Eastern Branch of the Russian Academy of Sciences (IACP FEB RAS),

**E-mail: anikitin@iacp.dvo.ru*

Magnesium and its alloys belong to a class of degradable biomaterials with a mechanical strength similar to that of bone. Rapid creation of an individual implant from magnesium powder according to an electronic geometric model as a result of a laser additive process eliminates the need for an operation to remove it. However, the complexity of the laser fusion process when performing the part construction cycle due to the high chemical reactivity of magnesium, which creates the risk of ignition, does not allow yet practical application of this material in medicine: orthopedics, traumatology and pediatrics. In the course of fundamental scientific research, an interdisciplinary group of researchers of the Far Eastern Branch of the Russian Academy of Sciences studied the effect of many factors affecting the mechanical characteristics and chemical properties of layer-by-layer samples created from magnesium powder MPF-4 [1–3] in the LPDED ("laser powder-based directed energy deposition") process of additive manufacturing.

The analysis of 3D modeling and 3D printing applications in surgery [4] and the results of our own research [5] made it possible to develop an algorithm for the transition from the initial information contained in computed tomography files to the program code that specifies the additive process of forming the physical shape of the bone implant by fusion metal powder material when exposed to laser energy.

The process of stage-by-stage formation of a conceptual prototype of a bone implant from magnesium powder MPF-4 is schematically shown in Figure 1.

To automate the design stage of an additive technological process for the synthesis of an implant according to its model, the concept of a decision support software for LPDED additive manufacturing processes based on an ontological approach is proposed [6].

The results of the research are accumulated in the databases of the knowledge portal of technological processes (operations) of the additive manufacturing of metal products (parts) using laser technological equipment. This portal, which is based on the concept [6], was created on the IACPaaS cloud platform [7,8] and is intended for development of optimal (according to the quality criterion of the additive manufacturing process) technological modes suitable for practical use.

The research work aimed at creating a program for the synthesis of parts of a given shape in the process of laser additive manufacturing was both scientific and practical, since the results obtained can be used in medicine, in particular, in surgery in the manufacture of bioresorbable magnesium individual implants for bone osteosynthesis.

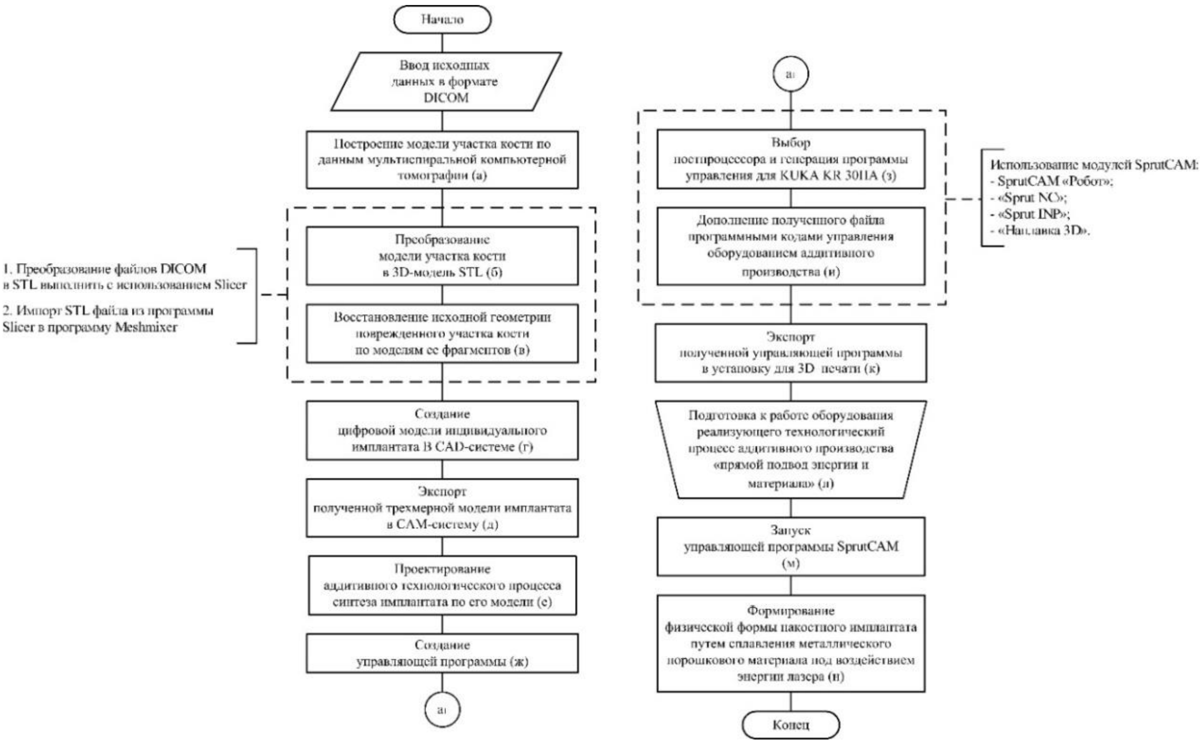

Fig. 1. Diagram of the process of forming an extra-bone implant according to a virtual model for the process of additive manufacturing "laser powder-based directed energy deposition".

The databases of the knowledge portal will be useful in the process of training laser equipment operators, and their formalized representation will provide the possibility of using this information by decision support software systems.

The work was partially supported by Russian Foundation for Basic Research, project no. 20-01-00449.

References

[1] Y.N. Kulchin, A.I. Nikitin et al, International Multi-Conference on Industrial Engineering and Modern technologies (FarEastCon2019) **992**, 780-785 (2019).

[2] V.I. Sergienko, A.S. Gnedenkov et al, 29th International Ocean and Polar Engineering Conference, ISOPE 2019 Honolulu; USA. I-19-284 ISOPE Conference Paper (2019).

[3] S.V. Gnedenkov, S.L. Sinebryukhov et al, Journal of Alloys and Compounds **808**, 151629 (2019).

[4] A.N. Nikolaenko, Medline.ru **19(2)**, 20-44 (2018).

[5] Sinebryukhov S.L., Gnedenkov S.V., Y. N. Kulchin et al, Asia-Pacific Conference on Fundamental Problems of Opto- and Microelectronics 2017 **11024**, (2017).

[6] V.V. Gribova, V.A. Timchenko, Ontology of Designing **10(2)**, 176-189 (2020).

[7] V.V. Gribova, A.S. Kleschev, et al, Software & Systems. **31(3)** 527-536 (2018). (in Russian)

[8] Gribova Valeria, Kleschev Alexander et al, Open Semantic Technology for Intelligent Systems. **3**, 21-24 (2019).

Laser Underwater Cleaning of Hulls of Sea Vessels

Y.N. Kulchin*, A.I. Nikitin, E.P. Subbotin

Institute of Automation and Control Processes Far Eastern Branch of the Russian Academy of Sciences (IACP FEB RAS),

**E-mail: kulchin@iacp.dvo.ru*

The natural phenomenon of biological fouling of the surfaces of ship hulls in the tropical waters of the World Ocean occurs rather quickly and has a negative effect on the hydrodynamic parameters. Considering its scale, huge resources are spent annually in the world to combat the problem of marine fouling [1].

Analysis of existing research on issues related to the search for optimal technical solutions for the operational and environmentally safe underwater cleaning of marine vessels from fouling showed that currently there are no industrial technologies and devices that allow fast, accurate restoration of the hydrodynamics of the hulls of ocean-going ships [1,2].

In Institute of Automation and Control Processes (IACP) FEB RAS it was proposed to use laser energy to clean ship hulls from biological fouling directly in the marine environment without docking [3].

The results of the research carried out on the processes of interaction of laser radiation with biofouling and anti-fouling coatings of the underwater part of the surface of the hulls of sea-going ships showed that the most effective spectral range for ablative cleaning of the surface of ships from biofouling is 1100 - 1500 nm.

This makes it possible to use a compact and energy-efficient technological fiber laser as part of robotic underwater complexes [4].

During the development of the "Device for laser underwater cleaning of the surface of objects from biofouling", special attention was paid to the search for technological solutions in which a focused laser beam, being in an underwater air-gas bubble, removes material objects of biological origin at a depth of 20 meters.

The optical scanning system is equipped with a “flat slit nozzle” that protects the laser beam and optical components from water due to the formation of a gas bubble.

In fig. 1 shows the appearance of the manufactured arrangement of a flat slit nozzle installed on the 2D-scanning system "IPGP Mid-Power Scanner".

Fig. 1. External view of the manufactured model of a flat slit nozzle connected to the 2D-scanning system "IPGP Mid-Power Scanner"

"Device for laser underwater cleaning of the surface of objects from biofouling" is equipped with a robot-carrier of the laser optical scanning system (Fig. 2).

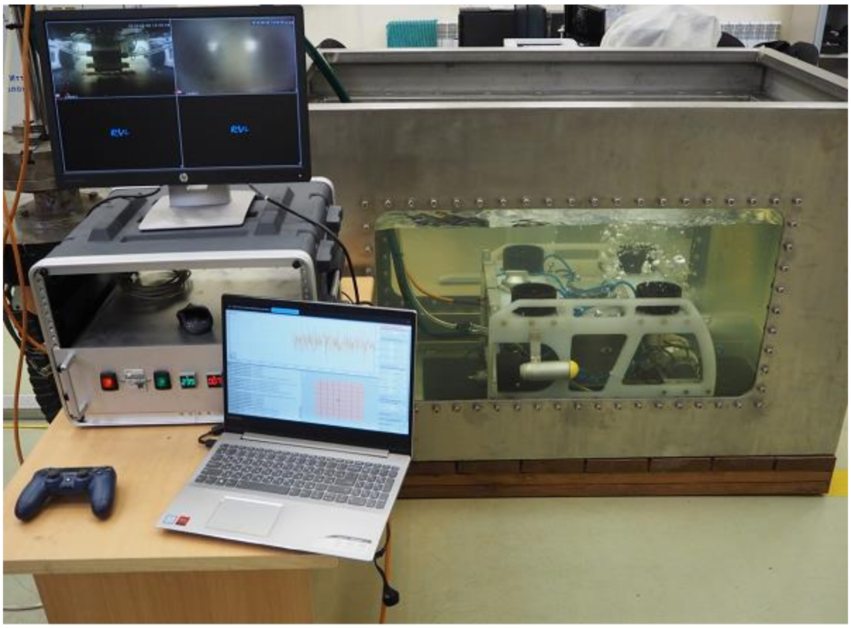

Fig. 2. External view of the manufactured "Model of the device for laser underwater cleaning of the surface of objects from biofouling"

An analysis of the results of preliminary studies showed that with an appropriate choice of the spectrum and power of laser radiation, the ship's hull can be cleaned without damaging the paint, and the cleaning speed is at least 15 m^2 / h, with an average cost of \$ 0.25 / m^2.

References

[1] Yu.N. Kulchin, A.Yu. Zviagintsev et al, Vestnik of the Far East Branch of the Russian Academy of Sciences **6**, 96-103 (2015)
[2] A.A. Begun, A.Yu. Zviagintsev et al, Assessing the influence of laser radiation on the species composition of marine biofouling community on the experimental steel plates Water: chemistry and ecology: **10**, 33-46 (2016) (in Russian)
[3] I.G. Zhevtun, E.P. Subbotin, et al, *Corrosion: materials, protection* **4**, 34-40 (2018)
[4] Yu.N. Kulchin, S.S. Voznesensky, et al, Quantum Electronics **50** (5), 475 – 488 (2020).

Application of neural network to find the discrete spectrum of the direct Zakharov-Shabat problem

E.V. Sedov[1,*], **I.S. Chekhovskoy**[1,2]

[1] *Novosibirsk State University, Novosibirsk,*
[2] *Federal Research Center for Information and Computational Technologies, Novosibirsk*
* *E-mail:* e.sedov@g.nsu.ru

Optical telecommunications are currently actively developing. However, the constant increase in the amount of traffic transmitted in the near future will exceed the potential of the communication lines based on current developments. Therefore, many scientific groups are actively exploring new promising ways to increase the capacity of communication lines. In particular, it has recently been proposed to use the Nonlinear Fourier Transform (NFT) for data transmission [1]. Direct NFT for the nonlinear Schrödinger (NLS) equation is the computation of the nonlinear spectrum of an optical signal (solving the direct Zakharov-Shabat problem). The nonlinear spectrum consists of discrete and continuous parts. The set of discrete eigenvalues (d.e.) corresponds to the soliton part of the signal. This representation evolves in a trivial way as the signal propagates. At any value of the evolutionary variable, the signal can be fully restored using the inverse NFT. Data transmission using NFT allows taking into account the influence of nonlinear effects in the propagation of an optical signal along the fiber.

The main difficulty in the widespread adoption of NFT is the lack of fast and accurate numerical methods. At the moment, a large number of methods have been proposed for determining the nonlinear spectrum, and significant progress has been made in reducing the complexity of algorithms and increasing their accuracy. However, there are problems with the robustness of computational algorithms when applied to complex signals. It is also difficult to compute NFT in real time for complex waveforms, which limits the possible implementation of the NFT at the hardware level in modern communication lines.

A promising area of research is the application of machine learning, in particular neural networks. In the past decade, great progress has been made in the development of machine learning methods for solving algorithmically complex problems such as, for example, image recognition and classification. The main steps in this are training the model based on a set of some data and applying the model for prediction. The first stage takes a long time to complete. However, the application of the trained model is usually much faster, which makes it possible to implement systems based on machine learning methods on various devices with low performance. Machine learning has also been proposed to be used in NFT-based data transmission systems at the post-processing stage [2]. In our work, we propose to implement a more radical approach and calculate the NFT using neural networks.

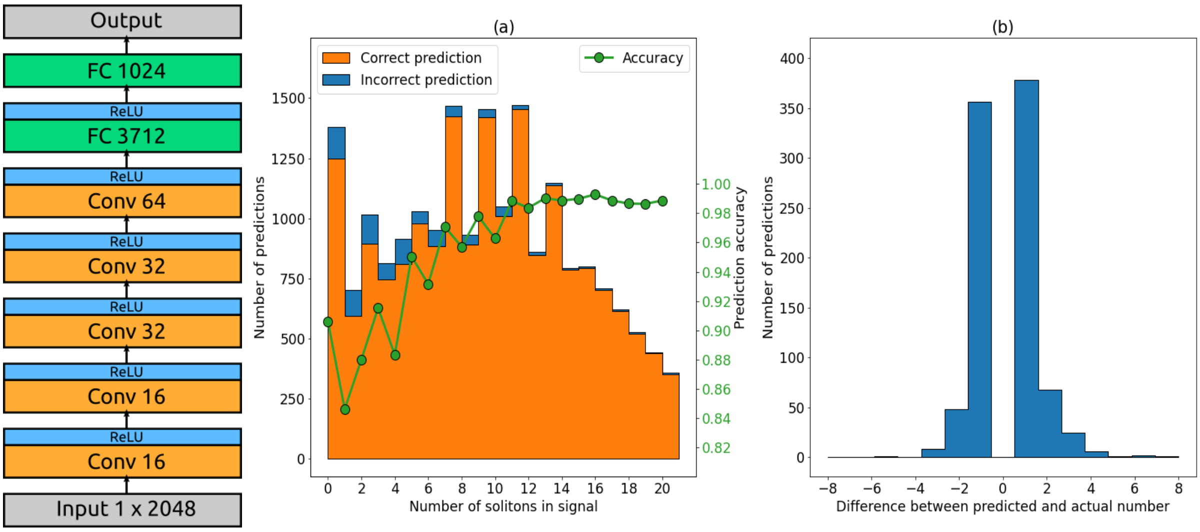

Fig. 1. Neural network architecture and its prediction accuracy.

In this work, we use a neural network to predict the number of d.e. in the nonlinear spectrum of telecommunication signals. Discrete eigenvalues reflect the internal structure of the signal. Knowledge of the internal structure of a signal makes it possible to study its properties and features of propagation in an optical fiber. For our research, we chose the WDM format, which is widely used in optical communication. The signal was generated from a random data set encoded in one of the modulation formats: QPSK, 16-QAM, 64-QAM, 1024-QAM. A simplified version of the VGG-16 network, which is used in image recognition tasks, was chosen as the basis for the network architecture. At the input, the network receives a complex signal consisting of 1024 points. This signal is converted into a vector with 2048 elements, in which the real and imaginary parts of each point of the initial complex signal are sequentially arrayed. Then the signal is processed by several convolutional layers with activation functions and fully connected layers. The network output is the number of solitons in the signal. The number of trained parameters in the network was 3834145.

In total, there were 174847 generated signals in the training set, which contain from 0 to 20 solitons, inclusive. For each signal, this number has been calculated in advance by other methods. The network accuracy was calculated using a validation set of 19427 signals. The network was trained for 300 epochs, the final prediction accuracy for validation was 95.39%. In this case, the maximum error of the network predictions - the difference between the real number of solitons in the signal and the predicted one - was 8. Most of the erroneous results are in the range [-2; 2]. The network works best for signals where the number of solitons is more than 10. For such cases, the accuracy is better than 98%. The worst were the signals with only one soliton - for them the accuracy was 84%. The results obtained show that neural networks have great potential for implementing various stages of NFT.

The work was supported by grant of the President of the Russian Federation (MK-677.2020.9). The work of E. V. Sedov was supported by the state funding program FSUS-2020-0034.

References

[1] S. K. Turitsyn, J. E. Prilepsky et al, *Optica*, **4**, 307–322 (2017)
[2] O. Kotlyar, M. Pankratova et al, *Opt. Lett.*, **45**, 3462 (2020)

Quantum optical technologies for information processing and communications

A.K. Fedorov

Russian Quantum Center
Moscow Institute of Physics and Technology
E-mail: akf@rqc.ru

Today quantum technologies are one of the most rapidly developed areas. Quantum technologies open new possibilities for various fields. Thanks to their unusual properties quantum systems can be considered as a basis for a new generation of high-performance computing devices (quantum computers), methods of information protection (with the use of quantum cryptography), and highly accurate measurement devices (quantum sensors and quantum metrology devices).

Recent progress is related to the development and implementation of quantum optical technologies for information processing and communications. In particular, an active field is the development of quantum key distribution devices, which use the transmission of individual quantum states of light for distributing confidential keys. In this report, a review of recent experiments on quantum key distribution in urban condition will be presented [1,2].

Quantum optical technologies are actively discussed in the context of quantum computing. First, they can be considered as a way to control quantum systems that are used ultracold atoms and ions. Second, this a computation platform. In the report, we will present an analysis of recent successes in the development of quantum computing devices, which use quantum optical technologies as the method for experimental control [3]. In particular, we will present preliminary results, which are obtained in the framework of the project on the development of a quantum computing device on the basis of ions.

This research is supported by grant MK-923.2019.2.

Литература

[1] A.V. Duplinskiy, E.O. Kiktenko et al, J. Russ. Laser Res. **39**, 113 (2018).
[2] E.O. Kiktenko, N.O. Pozhar et al, Quant. Sci. Technol. 3, 035004 (2018).
[3] E.O. Kiktenko, A.S. Nikolaeva et al, Phys. Rev. A 101, 022304 (2020).

MIMO application to detection nonreflecting events on reflectograms of optical fibers of cable lines

E.S. Zaitseva[1,*], A.V. Bourdine[1,2,3], V.A. Burdin[1]
[1]*Povozhskiy State University of Telecommunications and Informatics*
[2]*JSC "Scientific Production Association State Optical Institute Named after Vavilov S.I."*
[3]*LLC «LinkIn Tech»*
[*]*E-mail:* zaytzewa@inbox.ru

One of the problems with processing the optical fiber traces of cable line sections is the detection of nonreflecting events – fusion splices, irregularities, associated with optical cable bends [1 - 6]. The task of searching for such events on traces arises in the case of restoring the line documentation, detecting unauthorized access, fiber bending in a cable with an unacceptably small radius. Some methods are known for detecting and localizing nonreflecting irregularities of optical fibers in a cable [1 - 2, 7 - 14]. In particular, the application of the methods of the wavelet analysis for these purposes is considered [7, 12 - 13]. On the one hand, the application of these methods requires the usage of special equipment, and, on the other hand, their capabilities are limited by some threshold values of the signal/noise ratio. It is possible to significantly increase the probability and accuracy of target detection with a significant decrease in signal/noise ratio due to the use of MIMO (Multiple Input, Multiple Output) technology in radar systems [15 - 17]. This technique involves transmitting space-divided probing signals, receiving backscattering signals and co-processing received signals. Application of MIMO technology for detecting and localizing nonreflecting events in optical fibers of cable line of fiber optic link segment offered in paper [14].

Events, displayed on optical fiber traces in one place of the cable line (fusion splices in optical closure, additional losses due to the cable bending), are of the same nature, differing only in the degree of variation in the backscattering characteristic of the fiber. This suggests that co-processing of backscattering characteristics of optical fiber group of cable line will increase the probability of detecting nonreflecting events. This raises the question of the effectiveness of using MIMO technology to searching and detecting nonreflecting events on traces of optical fiber group of cable line.

Reference

[1] Anderson D.R., Johnson L., Bell F.G // Elsevier, London, 437 (2004)
[2] Listvin A.V., Listvin V.N. Reflectometry of optical fibers//LESARart, 150 (2005)
[3] Understanding OTDRs//*Anritsu* **1**, 56 (2011)
[4] Peters J.Measurements in New Optical Cables. // Sterlite Technologies, Application Notes, (2012)
[5] Bayandin D.V., Bochkova S.D., *Mezhdunarodnyi studencheskii nauchnyi vestnik* **5**, (2018)
[6] Evchenko E.V., *Alleya nauki* **8(24)**, 1-13 (2018)
[7] Manonina I.V. // *T-Comm* **10**, 61-66 (2013)
[8] Lee, W., Myong, S. I., Lee, J. C., & Lee, S, *Optics Express* **22(1)**, 325 (2014)
[9] Cen, M., Moeyaert, V., Mégret, P., & Wuilpart, M., *Optics Express* **22(8)**, (2014)
[10] Shubin V. V. // Patent RU 2506701 C1, 9 (2014)
[11] Amaral G. C., Baldivieso A., Garcia J. D. et al, A, *Journal of Lightwave Technology* 35**(10)**, 2025 (2017)
[12] Rudnev G.S., Shpilevoy A.A., Burmistrov V.I. et al. //*Vestnik Baltiyskogo federalnogo universiteta im. I. Kanta. Ser. Fiziko-matematicheskie I tehnicheskie nauki* **2**, 72-80 (2018)
[13] Bourdine A.V., Burdin V.A., Delmukhametov O.R. et al., *II Vserossiyskaya konferenciya «Opticheskaya reflektometriya – 2018»*, 55-57 (2018)
[14] Bourdine A. V., Delmukhametov O.R., Zheludkov M. A. et al //Patent RU 2698962C2, 25 (2019)
[15] Li J., Stoica P. MIMO Radar Signal Processing// Wiley-IEEE Press, 448 (2009)

[16] Chernyak V.S., *Uspehi sovremennoy radioelektroniki* **2**, 5-20 (2011)
[17] Zhukov M.N., Tatarskiy B. G., *Informacionno-izmeritelnie b upravlyauschie sistemi* **9(1)**, 36-45 (2011)
[18] Fernández M.P., Rossini L.A.B., Pascual J.P. et al., *Optics Express* **26(21)**, 27127-27140 (2018).

Laser optics and components: fibers, fiber and hybrid resonator elements, diffraction and integrated optics

Laser Diode Module of High Energy Brightness with Fiber Optic Output LMD-50

D.A. Avtaikin, E.V. Borisov, V.A. Velikanov, I.V. Galushka, A. V. Kuznechikhin, G.T. Mikaelyan, V.A. Panarin, S. N. Sokolov*, T.D. Tokareva

RME Inject, LLC, Saratov,
**E-mail: s.sokolov@nppinject.ru*

The results of the development of a high-energy diode laser module with a fiber-optic output for pumping fiber lasers are presented.

The last decade has seen rapid progress in materials, designs, and manufacturing technologies for diode lasers. The global output of diode lasers of types consistently exceeds 40% (6.9846 billion USD) of the production of lasers of all types in 2019. [1]. High-power diode lasers are most widely used in the market for laser processing plants for material processing, pumping systems for fiber and solid-state lasers. In this regard, the creation of high-power, highly efficient diode laser modules is a priority task. A laser diode module LMD-50 was developed RME Inject, LLC and its production started. In the process of developing this module, the topology and manufacturing technology of an active element - a laser diode (LD) and a precision assembly of the module - were created. An optical scheme for outputting radiation from the module case was designed and optical micro-lens elements were manufactured to achieve a laser output power of 50 W in a continuous mode in the core of an optical fiber with a diameter of 105 μm and a numerical aperture of 0.22. The overall dimensions of the module case are: 78 (L) x28 (W) x13.5 (H) mm. The external view of the module is shown in the photo Fig. 1.

Fig. 1. External view of the laser diode module LMD-50.

The main parameters of the LD module are shown in Table 1 below.

Table 1

Parameter	Units	Min.	Nom.	Max.
CW Laser Output Power	W	44	50	54
Central Laser Wavelength	nm	973	976	979
Laser spectrum half-width (FWHM)	nm	4	5	6
Temperature shift of laser wavelength	nm/°C		0,35	
Operating Current Shift of the Laser Wavelength	нм/A		0,9	
Efficiency	%		46	
Operating Current	A		12	
Threshold Current	A		0,6	
Operating Voltage	V		9	
Differential Efficiency	W/A		6,5	
Fiber Outer Protective Coating Diameter	μ	Teflon (ETFE)	900	

An analysis of the designs of LD modules with fiber optic output produced by foreign companies: Jenoptik, DILAS / Coherent, II-VI, Lumentum, Suzhou Everbright Photonics, Jilin Province Changguang Rays Laser Technology, BWT Beijing, showed that only DILAS / Coherent is produced LD module with the same rated output power of 50 W, suitable for a number of applications. The LMD-50 module has a laser wavelength of 976 +/- 3 nm, which is optimal for pumping fiber lasers. In terms of the main technical parameters, a LD module of high energy brightness with a fiber-optic output LMD-50 corresponds to a foreign analogue. Materials made in Russia were used in the design of the LMD-50 LD module, therefore, the use of modules in new domestic developments of fiber lasers and laser devices eliminates the need for imports, dependence on a monopoly supplier, and opens up new opportunities for creating domestic fiber lasers.

The laser diode module is intended for use as a source of high-power optical radiation and has good prospects for use in equipment for widespread use in systems for diode pumping of fiber lasers; laser micromachining of materials; medical devices and scientific research.

References

[1] Annual Laser Market Review & Forecast 2020: Laser markets navigate turbulent times, Jan 28th, 2020; Electronic resource: URL: https://www.laserfocusworld.com/lasers-sources/article/14073907/laser-markets-navigate-turbulent-times
(date of access: 07/10/2020).

Two-wave Ring Nonlinear Fibre Microcavity Spatio-Temporal Dynamics Modelling

V.A. Razukov*, L.A. Melnikov

Yuri Gagarin State Technical University of Saratov, Russia
**E-mail: razukov.vad@gmail.com*

It is obvious that the ability to predict the electromagnetic field behavior in the microcavities has a heavy practical value. Since such cavities operate in highly nonlinear regimes, it is possible to investigate their dynamics only by employing the numerical modeling methods, with the models used being adequate enough to describe the ongoing process, but at the same not being time costly. Modal approach is the main one [1], when the field inside of the microcavity is expanded along the longitudinal modes, and equations for the time dependant complex amplitudes of those modes are written. The result would be a set of tens or even hundreds of common boundary nonlinear equations, and solving them on a computer is a non-trivial task. For example, the nonlinearity causes sums of all the possible modes products to appear in the equations, and the calculation will take significant temporal and machine resources to be carried out. Moreover, to calculate the temporal profile of the field it is necessary to add all the fields of every mode, what also takes a lot of time, if there are large numbers of such modes. These are all examples of a spectral expand method. An alternative way to approach the problem of the field dynamics inside of a microcavity would be a differences scheme, built upon the transport equations [2], successfully used to simulate Raman and SBS lasers. This work is devoted to the further improvement of this numerical model [2], and analysis of the results, achieved when using this method.

The equations describing the pulse propagation inside of a microcavity are given as follows:

$$2i\left(\frac{\partial F}{\partial t}+v\frac{\partial F}{\partial z}\right)+D\frac{\partial^2 F}{\partial z^2}+2\chi(|F|^2+2|B|^2)F=0,$$

$$2i\left(\frac{\partial B}{\partial t}-v\frac{\partial B}{\partial z}\right)+D\frac{\partial^2 B}{\partial z^2}+2\chi(2|F|^2+|B|^2)B=0.$$

Boundary conditions are: $F(0)=\sqrt{1-R}\sqrt{1-r}F(L)+\sqrt{R}\sqrt{A}\sqrt{1-r}+\sqrt{r}B(0);\ B(L)=\sqrt{1-R}\sqrt{1-r}B(0)-\sqrt{r}(1-r)F(L)+\sqrt{Rr}\sqrt{1-R}\sqrt{A}.$

Here F and B – are fields of the waves, propagating clock and counterclockwise respectively, $D<0$ – GVD coefficient, v – group velocity, χ – phase cross and self-modulation coefficient, R – coupler reflection coefficient, r – intra-cavity mirror reflection coefficient, A – continuous pump intensity, L – cavity length.

In our model we consider the dispersion and nonlinearity of the microcavity, coupler and a mirror, situated in a random spot inside of the fiber. Beside the aforementioned effects there could also be modulation instability. To solve the problem we use an effective second order difference scheme “Cabaret” [3]. The figure shows an example of the model being used to calculate the effects of the nonreciprocal phase shift caused, for example, by the fibre rotation, and Rayleigh scattering on the random impurities in the cavity medium [4].

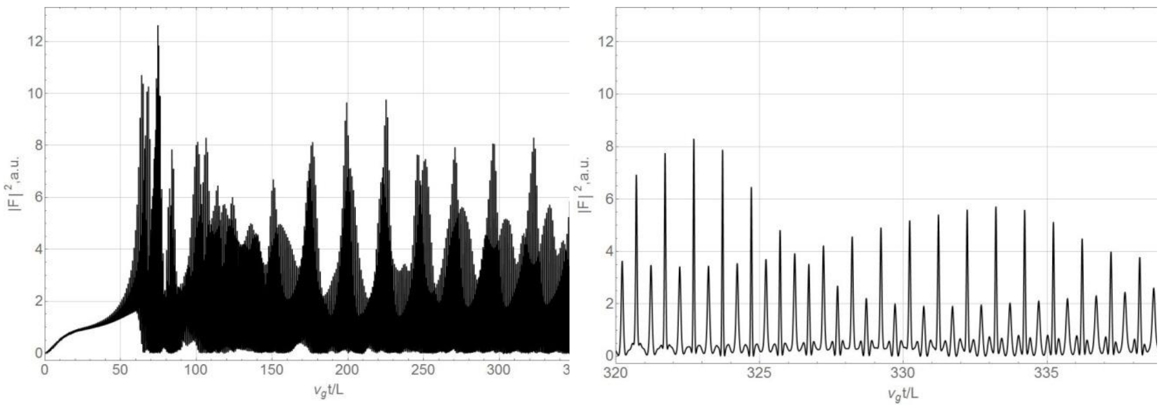

Fig. 1. Optical frequency comb formation. Strong background phase noise is visible. Modulation coefficient χ = *0,25*. Wave linear interface coefficient *r* = *0.001*. Losses ratio *0.0001*.

Summarizing we can conclude that using the implicit-explicit "Cabaret" scheme we can with ease consider for the necessary nonlinear effects in the system under investigation. It is nearly impossible when using the modal method since the number of the equations is several times greater with every new effect introduced, with the respective growth in the necessary time to compute the results.

References

[1] T. Herr, V. Brasch et al, *Nature Photonics*, **8**, 145–152 (2014).

[2] V. A. Razukov and L. A. Melnikov, *Saratov Fall Meeting 2015: Third International Symposium on Optics and Biophotonics and Seventh Finnish-Russian Photonics and Laser Symposium (PALS)*, **9917**, 788 – 792 (2016)

[3] G. V.M. and S. A.A., Matem. Mod. **10**, 86–100 (1998).

[4] V. Razukov and L. Melnikov, Izvestiya of Saratov University. New series. Series: Physics **20**, 64–71 (2020).

Two-beam interferometer based on a quartz beam-splitting unit with a fixed photodetector and simulated rotational tuning

S.L. Mikerin and V.D. Ugozhaev*
Institute of Automation & Electometry, SB RAS
**E-mail:vdu@iae.nsk.su*

Two-beam interferometers with the possibility of varying the period of the recorded diffraction gratings are in wide demand in various fields of holography and photonics. They are in demand, for example, for studying the properties of photopolymer materials and holograms recorded in them [1], for recording arrays of distributed Bragg gratings (FBGs) in optical fibers as sensors of the physical state of the fiber [2] and for other applications. In [3], an interferometer based on a beam-splitting cube (BSC) with two mirrors and a photodetector (PD), fixed relative to the BSC is described. In the interferometer, the stabilization of the position of the interference pattern (IP) while the angle of convergence of partial light beams (PB) is varied is provided by mutually coordinated linear and angular displacements of the movable mirror (MM) directing the light beam to the BSC. Such interferometers can be combined into systems for recording two-dimensional gratings with an independent setting of the period in each dimension [4]. However, for recording extended FBGs (10–15 mm), an interferometer based on a beam-splitting unit (BSU) seems to be more suitable [5], since in it the path length of light beams in BSU material is more than 3 times shorter than in BSC of the corresponding dimensions. The purpose of this report is to analyze the period tuning in a quartz glass BSU-based interferometer with stabilization of the IP position, provided by matching the linear and angular displacements of the initial light beam (IB) at the entrance to the BSU by means of a rotation simulation mechanism [3].

Fig. 1 shows the optical scheme of the interferometer under study, and the path of light beams is displayed by their axes. The interferometer, which includes BSU *1* and two mirrors *3.1* and *3.2*, is optically coupled with PD *4*, which is at a distance L_{ph} from the end of C_2C_3. BSU consists of two identical plates of quartz glass with a length M and a thickness of $A \approx 0.15M$, tightly joined by their working surfaces, with a dividing mirror (DM) *2* between them. The mirrors are installed symmetrically to the DM plane at a distance H from each other at an angle ξ (in Fig. 1 $\xi > 0$). IB *7* with diameter D is directed to the entrance surface C_1C_2 at a distance Q from the C_1 edge at an angle of incidence θ by MM *5* and then splits by DM into two PB *8.1* and *8.2*. After reflection from mirrors the axes of these beams intersect at the point O at the angle of convergence 2α at a distance $L \approx L_{ph}$ from the end C_2C_3: $\alpha = 90° + 2\xi - \theta$.

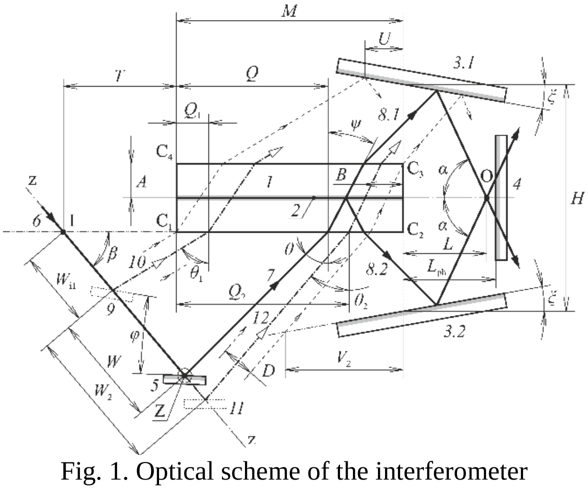

Fig. 1. Optical scheme of the interferometer

The current MM position is given by coordinates W and φ. MM is moved along the input beam *6* from the initial position *9* ($W_1 = 0$, $\varphi_1 = 0$) to the final position *11* (W_2,

φ_2), corresponding to the lower *10* (Q_1, θ_1) and upper *12* (Q_2, θ_2) boundary positions of IB. The latter are caused by touching IB edge C_1 and touching PB edges C_2, C_3. In turn, the pairs of IB coordinates (Q_1, θ_1) and (Q_2, θ_2) satisfy the condition $L \approx L_{fix}$ = const, supported in the entire interval between them. Such movement of IB is determined by the formula:

$$Q = M - 2A\,\mathrm{tg}\,\psi - \left[H\sin(\theta-\xi)\cos\xi - A\sin\theta - L_{fix}\cos(\theta-2\xi)\right]/\cos\theta, \qquad (1)$$

where $\mathrm{tg}\,\psi = \sin\theta/\sqrt{n^2-\sin^2\theta}$, n — refractive index of the BSU material. The boundary positions can be found numerically according to the above-mentioned touching conditions: $Q_1 = D/(\cos\theta_1)$, $Q_2 = M - 2A\,\mathrm{tg}\,\psi_2 - D/(\cos\theta_2)$ and set the corresponding boundary values of the angle α: α_1 and α_2, as well as the width of the tuning range of this angle: $\Delta\alpha = \alpha_2 - \alpha_1$. The dependence $Q(\theta)$,obtained from (1), is close to linear for a wide set of combinations of the parameters H and L_{fix}, which opens up the possibility of using the lever mechanism in [3] as a mechanism for coordinating linear and angular displacements of MM. The $Q(\theta)$ dependence was analyzed taking into account vignetting by the BSU working surfaces (parameter G) and/or by the mirror on the input surface side (parameters U, V, and V_2). The parameters G and V for the current IB position are determined similarly to the parameters U and V_2 (see Fig. 1). This restriction is possible in the case of $H \approx M$ and $L_{fix} < M$ at least for $\xi < 0$.

Fig. 2 shows the delimitation of the range of parameters $h = H/M$ and $l_{fix} = L_{fix}/M$ by the criterion of the presence or absence of vignetting in the studied interferometer at $\xi = -15°$. Above curve *1* there is an area free of vignetting; below curve *2*, the light beams overlap partially or completely in the entire tuning range limited by the touching conditions. Between curves *1* and *2*, the tuning ranges are partially limited by vignetting. Curves *3* and *4* are extrapolations of the corresponding curves *1* and *2* to the edges of the studied area; *5* — $h = 1.175$; *6* — $l_{fix} = 0.24$. For example, for recording FBGs with $\lambda_Б = 1…2$ microns in a quartz fiber with $n = 1.5$, it is possible to implement an interferometer characterized by pairs of parameters (h; l_{fix}): (1.0; 1.25), (1.0; 1.75), (1.25; 2.5). The rotation imitation mechanism is analyzed similarly to [3].

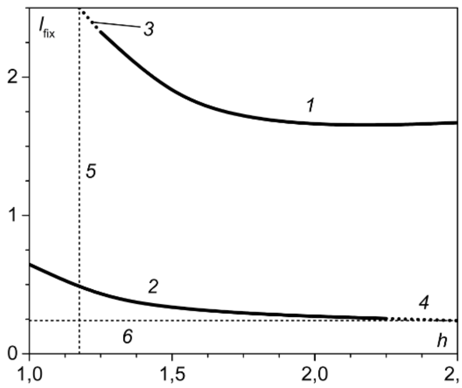

Fig. 2. Regions of vignetting

References

[1] V.V. Shelkovnikov, E.V. Vasil'ev etc., *Optics and Spectroscopy* **99**, Iss. 5 806–815 (2005) - DOI: 10.1134/1.2135860

[2] J. Habel, T. Boilard, Y. Messadeq, F. Trépanier, M. Bernier, *Advanced Photonics Congress* (BGPP, IPR, NP, Networks, NOMA, Sensors, SOF, SPPCom) OSA, BM3A.4 (2010)

[3] S.L. Mikerin, V.D. Ugozhaev, *Applied photonics* **5**, Iss. 3, 218-237 (2018) - DOI: 10.15593/2411-4367/2018.3.07

[4] S.L. Mikerin, V.D. Ugozhaev, *Intern. Conf. "SibOptica-2018"*: Proc. in 2 v. – Novosibirsk : SSUGT, V. **1**, 101–107 (2018)

[5] V.D. Ugozhaev, *Optoelectronics, Instrumentation and Data Processing* **54**, Iss. 4, 375-384. (2018) - DOI: 10.3103/S875669901804009X

Whispering gallery modes on the surface of an optical fiber reflecting from its end

D.V. Kudashkin*, I.D. Vatnik, D.V. Churkin

Novosibirsk State University, Novosibirsk

*E-mail: d.kudashkin@g.nsu.ru

Whispering gallery modes (WGMs) excited on the surface of cylindrical fiber microcavities, and in particular on the surface of an optical fiber, can have a nonzero propagation velocity along the cavity axis, which depends on the variation of the effective radius [1]. The speed of propagation of modes can be controlled by varying the radius of the fiber. Also, the mode propagation speed depends on the difference between the resonant wavelength of the microcavity and the wavelength at which the mode propagates [2]. On the basis of such resonators, devices can be created for generating optical combs, delay lines, optomechanical switches, etc.

An actual task is to find new ways of controlling the axial propagation of modes. One such method would be to use fiber geometry such as a fiber end. When radiation in the whispering gallery mode is incident on the fiber end, the angle between the direction of propagation of the axial WGM and the cleave interface is small (in the ray approximation). Since the refractive index of the silica cladding of the optical fiber is higher than the refractive index of air, total internal reflection can occur at the fiber end. In our work, we studied this WGM reflection process and determined the reflection coefficient.

For this purpose, laser pulses of 0.5 ns duration with wavelengths close to the resonant wavelength with zero axial wave vector were launched into the microcavity made of standard optical fiber. The microcavity end was made by cleaving the fiber with a diamond knife. Radiation was introduced into the resonator through a tapered microfiber. The taper waist is perpendicular to the microcavity. A second taper was used for scanning along the axis of the resonator to probe space-time dynamics of the radiation intensity $I(z, t)$.

Under pulsed excitation, the original wave packet is divided into several pulses propagating along the cladding with different group velocities: in Fig. 1a, at least two separate pulses can be distinguished: the first has such a high group velocity that the time resolution of the oscilloscope is insufficient to see its reflection. It seems that this part of the pulse instantly appears everywhere in the resonator. The other part of the excitation propagates with a finite velocity from the exciting taper located at the point $z = -3200$ μm in the direction of the end, and then is reflected from the fiber cleavage at the point $z = 0$ and moves back from the cleavage.

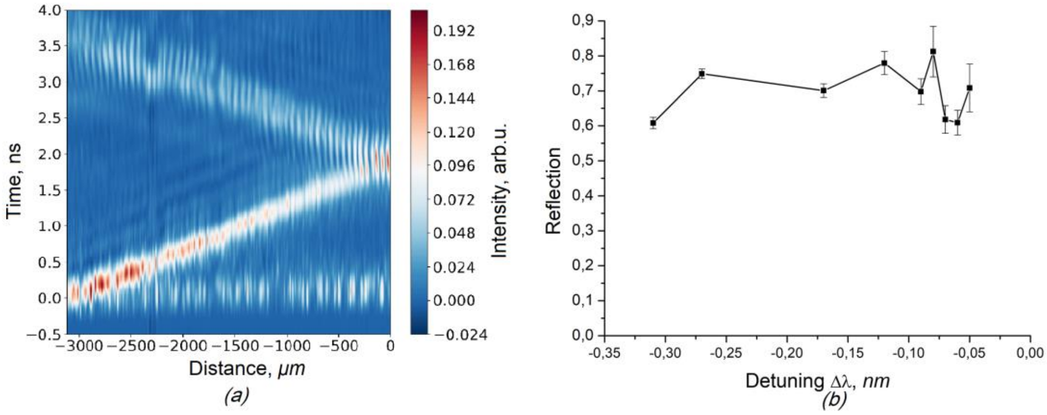

Fig. 1. (a) Spatio-temporal dynamics of a WGM with mode splitting after reflection. (b) Calculated reflection R at the fiber end face as a function of wavelength detuning.

Figure 1b shows a graph of the dependence of the reflection coefficient on $\Delta\lambda$ - the detuning of the pulse wavelength from the resonant wavelength of the mode. The coefficient was calculated as the ratio of the total intensity of the incident and reflected modes. For the sample under study, the reflection coefficient is about 70%. The independence of the reflection coefficient R on $\Delta\lambda$ provides additional information about the reflection process. First, it proves that propagation loss does not affect reflection estimates. Indeed, one might expect that the linear propagation loss should strongly depend on the wavelength - large detunings and large group velocities make the optical path of the mode shorter. This should reduce the net loss and its contribution to the reflectance estimated by our method. Conversely, the independence of the obtained reflectivity from the detuning signals that the effect of losses is negligible. Second, since different $\Delta\lambda$ imply different angles of incidence of the WGM beam to the fiber end, the independence of R on the angle is in good agreement with the assumption that total internal reflection occurs.

The results obtained can be used in devices based on axial WGM resonators to control the properties of modes.

This work was supported by the Russian Science Foundation (18-72-10053).

References

[1] Sumetsky, M. and Fini, J. M., "Surface nanoscale axial photonics", Opt. Express **19**(27), 26470 (2011).

[2] Dmitry Kudashkin, Ilya Vatnik, et al., "Dynamics of the whispering gallery modes at the surface of the optical fiber near its facet", Proc. SPIE. **11355**, Micro-Structured and Specialty Optical Fibres VI

Contents

Nonlinear conversion of fiber laser radiation: SRS, SBS, parametric generation, harmonics generation, generation of THz radiation	
Y. Feng. Wavelength-agile fiber amplifiers for quantum technology.	
A.A. Fotiadi, V.V. Spirin, J.L. Bueno-Escobedo, P. Mégret, D.A. Korobko, I.O. Zolotovskii. Stabilizing Brillouin Fiber Lasers.	
V.L. Kalashnikov, S. Wabnitz. Spatiotemporal Mode-Locking in a Fiber Laser.	
M.D. Gervaziev, D.S. Kharenko, I. Zhdanov, V.A. Gonta, E.V. Podivilov, S.A. Babin, S. Wabnitz. Mode decomposition of laser beam propagated in a multimode fiber in the Kerr self-cleaning regime	
A.V. Dostovalov, M.I. Skvortsov, A.A. Wolf, V.I. Labuntsov, O.N. Egorova, S.L. Semenov, S.A. Babin. Raman laser based on a 7-core fiber with cross-coupling between the cores	
N.A. Nikolaev, A.A. Mamrashev, V.D. Antsygin, G.V. Lanskii, Yu.M. Andreev, Prospects of generation of terahertz radiation in borate nonlinear crystals	
N.A. Nikolaev, A.A. Mamrashev, G.V. Lanskii, V.D. Antsygin, Yu.M. Andreev. Application potential of nonlinear ferroelectric crystals KTiOPO4, KTiOAsO4, and KNbO3 in the millimeter waves	
D.E. Praporshchikov, K.A. Volkov, A.V. Bourdine, V.A. Burdin, Mode coupling coefficients of curved few-mode optical fiber	
M.V. Ponarina, A.G. Okhrimchuk, P.A. Obraztsov. Switching between single- and dual-wavelength generation in passively mode-locked Nd: YAG waveguide laser	

Russian Fiber Lasers

2020